

2018

Assessment Of Upper Cretaceous Strata For Offshore CO₂ Storage: Southeastern United States

Khaled F. Almutairi
University of South Carolina

Follow this and additional works at: <https://scholarcommons.sc.edu/etd>

 Part of the [Geology Commons](#)

Recommended Citation

Almutairi, K. F. (2018). *Assessment Of Upper Cretaceous Strata For Offshore CO₂ Storage: Southeastern United States*. (Doctoral dissertation). Retrieved from <https://scholarcommons.sc.edu/etd/4811>

This Open Access Dissertation is brought to you by Scholar Commons. It has been accepted for inclusion in Theses and Dissertations by an authorized administrator of Scholar Commons. For more information, please contact dillarda@mailbox.sc.edu.

ASSESSMENT OF UPPER CRETACEOUS STRATA FOR OFFSHORE
CO₂ STORAGE: SOUTHEASTERN UNITED STATES

by

Khaled F. Almutairi

Bachelor of Science
King Saud University, 2002

Master of Science
King Saud University, 2007

Submitted in Partial Fulfillment of the Requirements

For the Degree of Doctor of Philosophy in

Geological Sciences

College of Arts and Sciences

University of South Carolina

2018

Accepted by:

Camelia Knapp, Major Professor

James Kellogg, Committee Member

James Knapp, Committee Member

Duke Brantley, Committee Member

Cheryl L. Addy, Vice Provost and Dean of the Graduate School

© Copyright by Khaled F. Almutairi, 2018
All Rights Reserved.

DEDICATION

First, I dedicate me dissertation to my great parents and my family members for their love and support throughout my life. Also, I dedicate my work to my sincere friends, environment protectors and geoscience researchers. I would also like to dedicate this work to everyone helps me specially my dissertation's committee, Camelia Knapp, James Knapp, James Kellogg and Duke Brantley.

ACKNOWLEDGEMENTS

This work was supported by the U.S. Department of Energy, National Energy Technology Laboratory, through Cooperative Agreement DE-FE0026086, CFDA 81.089, with the Southern States Energy Board. Cost share and research support are provided by the Project Partners and an Advisory Committee. Seismic reflection and well data were provided by the Bureau of Ocean Energy Management (BOEM) and United States Geological Survey (USGS) data base. Special thanks for Schlumberger for providing free licenses of *Petrel software* and special thanks to CGG GeoSoftware for providing free licenses of *HampsonRussell software*. This work could not have taken place without their software contribution. I would like to thank King Abdulaziz City for Science and Technology (KACST) at Saudi Arabia, for full scholarship. Many thanks to School of the Earth, Ocean and Environment, College of Art and Sciences at University of South Carolina.

ABSTRACT

This is the first assessment of Upper Cretaceous strata for offshore CO₂ storage resources in the southeastern United States outer continental shelf. This research focuses on Upper Cretaceous geological units using legacy industry 2-D seismic reflection and well data. It provides an integrated description and reliable subsurface evaluation of Upper Cretaceous potential storage reservoirs. In addition, it provides a detailed evaluation on how rock porosities and permeabilities are distributed across the Upper Cretaceous strata restricted to the South Georgia Embayment (SGE). Structure and thickness (isochore) maps were generated for the main potential reservoirs and seals on a regional and local scale. This assessment is the first application of multiple seismic inversion techniques in SEG. It provides a reliable and reputable workflow of Model-Based inversion which gives an improved image to discriminate lithology and predict porosity. This workflow can be applied to future CO₂ storage resource assessment studies elsewhere. The inversion results indicated that distinct porosity and permeability regimes are present and distributed in Upper Cretaceous within the SGE. The impedance and porosity relationships show well founded and reliable correlation. This relationship reveals low impedance coincident to the high porosity intervals which are proposed as potential reservoir intervals for CO₂ storage. In addition, it shows that the Upper Cretaceous strata have two main potential reservoirs in the lower part. These are overlain by a thick impermeable interval, mostly shale which has high impedance, low porosity, and low permeability, which extends within the SGE. Since porosity distribution is estimated using different methods, it follows the trends of seismic

signature and structures of Upper Cretaceous strata. The extracted values of porosity, ranging from 15 to 36 %, and permeability, ranging from 1 to 100 mD, are close to the measured values from the well core data at the Upper Cretaceous strata interval.

Five reservoirs and seals were recognized as potential storage units. Two reservoirs are particularly considered as the main CO₂ storage units with quality and integrity capable to meet the CO₂ storage requirements by the U.S. Department of Energy. They consist of limestone deposits with significant interbedded sandstones, shales and dolomites, and are sealed by thick shales interbedded with limestone. The porosity ranges from 20 to 30 % and the permeability ranges from 1 to 447 mD. Regional CO₂ storage capacity is estimated to be approximately 32 GT in Upper Cretaceous units. The local storage capacity for the two significant reservoirs in the SGE contribute ~ 9 GT of that amount.

TABLE OF CONTENTS

Dedication	iii
Acknowledgements	iv
Abstract	v
List of Tables	viii
List of Figures	ix
Chapter 1: Introduction and Motivation	1
Chapter 2: Assessment of Upper Cretaceous Strata for Offshore CO ₂ Storage: Southeastern United States	16
Chapter 3: Acoustic Impedance Inversions for Offshore CO ₂ storage: South Georgia Embayment	41
Chapter 4: Discussions and Conclusions	81
References	90
Appendix A: Copyright Permission	95

LIST OF TABLES

Table 1.1 Wells used for seismic-well tie and formation evaluation.....	15
Table 2.1 Stratigraphic nomenclature of rock formations identified onshore along the U.S. southeastern coast	24
Table 3.1 Wells used for acoustic impedance inversions and formation evaluations	48
Table 4.1 CO ₂ storage capacity estimation in GT using different storage efficiency factor for the saline reservoir	88
Table 4.2 Summary of prospective reservoirs and seals for CO ₂ sequestration in Upper Cretaceous strata of the Southeast Georgia Embayment	89

LIST OF FIGURES

Figure 1.1 [A] Location map showing the main regional geologic provinces within the offshore areas considered for potential storage of CO ₂ , [B] Schematic geologic cross section <i>T-T'</i> of the Southeast Georgia Embayment and Blake Plateau	12
Figure 1.2 Location of areas considered for potential geologic storage of CO ₂ generated in North and South Carolina.	13
Figure 1.3 Location map of legacy Atlantic Margin industry seismic reflection data, with a total length of more than 100,000 miles. Red circle indicates location of high-density seismic survey within Southeast Georgia Basin	14
Figure 2.1 Flowchart outlining seismic data calibration and interpretation workflow	22
Figure 2.2 Seismic-well tie for COST GE-1 well.....	23
Figure 2.3 Analysis of seismic sections: [Top] Two seismic sections that were tied with different wells; [Bottom] Paleontological tops and picking the top and base of Upper Cretaceous at the COST GE-1 well	28
Figure 2.4 Examples of the interval velocity interpolation within the Southeast Georgia Embayment using the advanced Velocity Model; (Left): between the top of Upper Cretaceous and Turonian surface; (Right): between the Turonian surface and the base of Upper Cretaceous.....	29
Figure 2.5 Regional 2D structure maps (in feet) for: [A] top of Upper Cretaceous [Maastrichtian], [B] Turonian and [C] base of Upper Cretaceous [Albian]	30
Figure 2.6 Regional thickness maps [isochore, in feet]: for [A] entire Upper Cretaceous section, [B] Maastrichtian to Turonian, and [C] Turonian to base of Upper Cretaceous ..	31
Figure 2.7 Structure maps, in feet, for [A] top of Upper Cretaceous [Late Maastrichtian], [B] Turonian, and [C] base of Upper Cretaceous [Albian].....	32
Figure 2.8 Thickness maps [isochore] in feet for [A] prospective seal and [B] potential reservoir within the offshore of Southeast Georgia Basin	33
Figure 2.9 Logs for different wells: [A] calculated porosity logs at COST GE-1 and Exxon 564-1 wells, [B] gamma ray versus calculated porosity in one track, in the next track, shows density versus neutron log	34

Figure 2.10 lithology logs (gamma and SP) and the porosity logs (sonic, density, neutron) and porosity and permeability that calculated from core, for the COST GE-1, Exxon 564-1 and Transco 1005-1 wells respectively35

Figure 2.11 Relationship between porosities and permeabilities versus depth for the COST GE-1 well: [A] values measured on conventional and sidewall cores; [B] core porosities plotted against core permeabilities for the entire well; [C] plotting interval velocity, porosity, permeability, and densities that calculated from the cores, for Upper Cretaceous section38

Figure 2.12 Logs of gamma ray, self-Potential, sonic, density, neutron as well as porosities and the permeabilities that calculated from the core data. Also, lithology description with a geological model for the main two potentials reservoirs and seals at the Upper Cretaceous Section.....39

Figure 3.1 [A] location map showing the main regional geologic provinces within the offshore areas considered for potential storage of CO₂; [B] stratigraphic columns and lithology description at COST GE-1 and Transco 1005-1 wells, located at Southeast Georgia embayment47

Figure 3.2 Location map of seismic survey and exploratory wells within Southeast Georgia Embayment (SGE). Seismic lines used in the acoustic inversion analysis are bold.....49

Figure 3.3 Flowchart outlining the seismic inversion workflow to extract the acoustic impedance50

Figure 3.4 Extract statistical wavelets. [A] using seismic line # 7021A, and [B] using the 1005-1 well53

Figure 3.5 Seismic well correlation, achieved by matching events on the synthetic with the same events on seismic trace at the Transco 1005-1 well54

Figure 3.6 [A] Initial model for the acoustic impedance, [B] post stack seismic inversion analysis results at the COST GE-1 well.....58

Figure 3.7 Comparison results of different post stack inversion that cover the Upper cretaceous strata using seismic line # 7021A and the Transco 1005-1 well. [A] Bandlimited inversion, [B] Colored Inversion, [C] Linear Programming Sparse Spike, and [D] Maximum Likelihood Sparse Spike.....59

Figure 3.8 Calculated porosity logs at COST GE-1, Exxon 564-1 and Transco 1005-1 wells.....60

Figure 3.9 Extrapolated porosity using inversion property builder at the well GE-1.....62

Figure 3.10 Acoustic impedance at the Transco 1005-1 well.....63

Figure 3.11 3D view of the acoustic impedance and the extrapolated porosity, using seismic lines # 7053A across the COST GE-1 well65

Figure 3.12 Zooming in for the acoustic impedance and the extrapolated porosity66

Figure 3.13 Acoustic impedance relationship with calculated porosity at an interested zone [3,150-7,600] ft of the COST GE-1 well where the correlation coefficient is (0.75); [B] is the acoustic impedance and measured porosity relationship for the entire well, where the correlation coefficient is (0.62).....68

Figure 3.14 Acoustic impedance versus calculated porosities from density and neutron logs at three different depth intervals at the Transco 1005-1 well, where the best correlation coefficient achieved is 0.6847 at the interval between 4,046 to 6,000 ft.....69

Figure 3.15 Extracted Porosity from the acoustic impedance at the GE-1 well using the linear regression relationship where the correlation coefficient is 0.75.....71

Figure 3.16 Extracted porosity from the acoustic impedance at three different intervals at the Transco 1005-1 well which discriminates two strata within the potential reservoir intervals at Upper Cretaceous72

Figure 3.17 Porosity and permeability relationship at the COST GE-1 well: [A] values measured on conventional and sidewall cores as a function of depth; [B] cross plotting core porosities versus core permeabilities for the entire well; [C] permeability distribution using the core's porosities and permeability relationship73

Figure 3.18 [A] Acoustic impedance, [B] extracted porosity and [C] lithology description with a geological model for the main two potentials reservoirs and seals at the Upper Cretaceous strata at South Georgia Embayment.....77

CHAPTER 1

INTRODUCTION AND MOTIVATION

1.1 Introduction and Objectives

With more than 80% of the world's energy derived from fossil fuel, and considering that the U.S. Environmental Protection Agency estimates that about 40 percent of the anthropogenic CO₂ emissions in the U.S. are generated in the southeast, the lack of an offshore CO₂ assessment constitutes a major gap in understanding the prospective regional storage resource. The contribution is about 1,444 million metric tons of CO₂ (Litynski et al., 2008). Offshore geological repositories have received relatively little attention as potential CO₂ storage sites, despite having a number of important advantages over onshore sites (Franklin, 2009). Subsurface geologic storage of carbon dioxide (CO₂) can play a major role in offsetting greenhouse gas emissions in a manner that is safe, economical, and acceptable to the public. Due to legal advantages and apparently vast resource capacity, offshore storage offers an attractive alternative to onshore storage. Although the storage capacity of offshore reservoirs is expected to be vast, no comprehensive assessment of the offshore storage resource in the southeastern United States has been performed.

In an analysis of a 10,000 mi² area of offshore Alabama and the western Florida Panhandle, studies suggested that about 170 GT of CO₂ could be stored in the Miocene Sandstone and that at least 30 GT could be stored in deeper Cretaceous formations Hills

and Pashin (2010). To date, only limited studies have been conducted. Smyth et al. (2008) considered storage options in the Carolinas and recognized that significant storage potential exists along the length of the Atlantic continental shelf (ACS), although the potential storage resource was not quantified. Two potential CO₂ sinks are present in geologic strata below the Atlantic seafloor, in Upper and Lower Cretaceous (Figure 1.1) and the estimated capacities are about 16 Gt and up to 175 Gt, respectively (Smyth et al., 2008; Vidas et al., 2012). However, this research is part of the Southeast Offshore Storage Resource Assessment (SOSRA) research project funded by Department of Energy (DOE), U.S., for assessment of offshore CO₂ storage resources. The project study areas are the offshores of North Carolina, South Carolina, Georgia and Florida (Figure 1.3). Since the project is divided based on the age of the geological units, this research focuses only on development of offshore prospective storage resource assessment of subsurface saline formations, especially Upper Cretaceous section of the Mid and South Atlantic offshore regions.

For CO₂ sequestration and storage, supercritical conditions are required. At depths of 2,625 ft (800 m) or greater, CO₂ can be sequestered underground as a supercritical fluid. Supercritical CO₂ means that the CO₂ is at its thermodynamic critical point, which includes a temperature exceeding 88.30F (31.10C) and a pressure exceeding of 72.9 atmospheres. At such high values, the CO₂ has hybrid properties of both a gas and liquid (NETL, 2015). Since the liquid, or supercritical CO₂, at reservoir conditions (with good porosity and permeability) occupies a much smaller volume than the gaseous state at atmospheric conditions, this provides the possibility of more effective exploitation of underground storage space and improves storage security (IEA, 2007; 2008). At sufficient depths, CO₂ is more like a liquid than a gas and the CO₂ density ranges from 50 to 80 % of the density

of water, and is close to the density of some crude oils. In this case, since the CO₂ is less dense than saline water, the buoyant forces will drive CO₂ upwards within the geologic formations and accumulates within a porous reservoir when a cap seal is reached, i.e. an impermeable layer and enclosed trap (NETL, 2013).

In the study area, the CO₂ geological storage options are deep saline formations which are found within the Upper and Lower Cretaceous sections. Geological criteria are needed to qualify the Upper Cretaceous section for CO₂ storage. The criteria include: 1) high porosity [more than 20% is preferable, and not less than 10%], 2) good permeability, such as ~200 millidarcy (mD), 3) a trapping mechanism, an overlying caprock, or seal, is very important to prevent vertical migration into overlying freshwater aquifers, however, stratigraphic trapping through lateral facies changes may be of greater interest in this study area than in other basins along the Atlantic offshore margin (Scholle, 1979), 4) cap-rock efficacy includes lateral continuity, no faults, and capillary entry pressure, 5) the Cap-rock thickness [100 m is perfect but not less than 20 m], 6) reservoir properties which include reservoir, seal, areal extent, depth, net reservoir thickness greater than 50 m, and 7) pressure, temperature, salinity, uniform stratigraphy, and seal integrity (Chadwick et al., 2008; Eiken et al., 2011).

1.2 Geological Setting of the Southeast Atlantic Offshore

The geology of the offshore area of the Southeastern United States is complex (Poag, 1978), therefore, a brief description of the Atlantic Continental Shelf is included here. Following the latest collisional event of Laurentia and Gondwana at the end of the Paleozoic (Alleghenian), continental rifting began in the Early Mesozoic as part of the breakup of the supercontinent Pangea. Locally, this involved tectonic subsidence in

restricted extensional basins, followed by thermal subsidence along the Eastern North American margin that still continues today (Dillon and Popenoe, 1988). The thermal subsidence probably ended before the Cretaceous but certainly before the Coastal Plain sediments. Generally speaking, stratigraphic sequences on this passive margin are characterized by extensive lateral continuity and relatively minor structural disruption. The oldest post-rift sediments, above a regional unconformity known as the “post rift unconformity”, are of Jurassic age and are the product of rapid clastic sedimentation from erosion followed by a period of evaporite deposition and subsequent initiation of widespread, shallow water carbonate deposition with some terrigenous input (Dillon and Popenoe, 1988). Geophysical and stratigraphic studies suggest that the Jurassic section is at least 4.6 miles thick in the basins, and thickens seawards (Dillon et al., 1979). The Cretaceous section is characterized by more clastic sedimentation in the north and more carbonate deposition in the south, forming a large carbonate platform over the Blake Plateau and offshore Florida. In Upper Cretaceous, the Suwanee Strait provided clastic sedimentation to the Blake Plateau creating a distinct facies change to the neighboring offshore Florida and Bahamas carbonate platforms (Pinet and Popenoe, 1985). Strong paleo-currents controlled the sedimentation in large portions of the offshore region from the Upper Cretaceous to the Cenozoic. The Suwanee Strait eventually evolved into today’s Gulf Stream providing strong erosive power that eroded most of the Paleogene sediments on the Blake Plateau and prevented deposition off the Florida-Hatteras slope where it continues to the north along the shelf edge (Pinet and Popenoe, 1985). The major sedimentary deposits from north to south include the Carolina Trough, the Southeast

Georgia Embayment, and the Blake Plateau Basin, which range in sediment column thicknesses from 10,000 to 23,000 ft (Maher and Applin, 1971).

1.2.1 Carolina Trough

The Carolina Trough is a long, narrow sedimentary basin located at the edge of the Atlantic Continental Shelf directly east off the coast of the Carolinas (Figure 1.1). The trough is roughly linear and positioned in a SW-NE trend parallel to the Eastern North American coastline. The Carolina Trough formed from initiation of rifting during the Triassic-Jurassic periods. During this time, evaporites were deposited in the trough, followed by a clastic deposition at the end of the Jurassic through the Cretaceous. This gave rise to salt diapirism as the salt beds mobilized and deformed the overlying sediments. The salt dome deformations are visible on the ocean floor, and are placed at a depth of 9,800 ft under water (Book, 1982). The deformations are characterized by major faults centered on the dome structures. Throughout the Cenozoic, the Gulf Stream eroded many of the sediments from the area; however, around a total of 7.5 miles of sediments is believed to have been accumulated in the Carolina Trough (Book, 1982).

1.2.2 Southeast Georgia Embayment

The Southeast Georgia Embayment is a broad depression plunging eastward from the Atlantic Coastal Plain (Figure 1.1). It is a major structural feature of the Florida-Hatteras Shelf, but is considered a minor sedimentary geologic unit compared to the other sedimentary basins in the region. Based on cores recovered from the COST GE-1 well, Paleozoic rocks sit at a depth of 10,560 ft and are overlain by probable Jurassic non-marine clasts, dolomites, coal, and anhydrite. This sedimentary sequence continued throughout the Mesozoic, until carbonate sedimentation took over in the Cretaceous. Sedimentation in the

Southeast Georgia Embayment is still likely ongoing today (Dillon et al., 1975; Book, 1982).

1.2.3 Florida-Hatteras Slope

The Florida-Hatteras Slope is a prominent geological feature, but is not a “true” continental slope (Figure 1.1). This feature separates the North American Continental Shelf from the Blake Plateau and was formed by mainly erosive processes of the Suwanee Strait. This prevented deposition on the eastern margin of the shelf while coastal margin sedimentation was unaffected, resulting in a slope-like feature (Book, 1982).

1.2.4 Blake Plateau Basin

The Blake Plateau Basin (Figure 1.1) is a major sedimentary basin formed at the same time and by the same processes that resulted in formation of the Carolina Trough. The basin lies at depth ranging approximately from 2,000 to 3,300 ft, and its subsidence depth is much greater than the Carolina Trough. Blake Plateau has a complex geology and tectonic history (Poag, 1978). The Blake Plateau basin is separated into two parts, northern and southern, and is separated by an east to west trending fracture system terminating at the Blake Spur on the western margin of the plateau (Dillon et al., 1979). The southern portion of the plateau is characterized by increased subsidence relative to the northern portion, and is the product of new oceanic crust created during rifting. The seaward margin of the southern portion consists of reef development from the Cretaceous time. In contrast, the northern seaward margin was developed from erosional sedimentation (Book, 1982).

1.3 Potential Storage Units and Capacity

The study area could have multiple potential storage geologic units within the Cenozoic and Mesozoic, especially the Cretaceous; however, this research will focus on the upper Cretaceous section. In order to assess the potential CO₂ storage units offshore Atlantic, there are, however, some activities required to perform an initial geologic characterization:

- 1) Identification and characterization of main geologic provinces and potential CO₂ storage units within the study area,
- 2) Assessment of the stratigraphic framework, depositional setting, tectonic framework, geologic history, spatial extents, key formations, and the implications of these characteristics for carbon storage.
- 3) Preliminary assessments of porosity and permeability, spatial extents, presence of seals and traps, proximity to other potential storage units, and other site-specific factors.

The main factors that play a role in the entrapment of CO₂ are impermeable seals, porous reservoir rocks, and stratigraphic and/ or structural traps. At COST GE-1 well, the reports indicate that there are impermeable beds that could act as seals for CO₂ entrapment. The thick shales and calcareous shales between 3,600 and 5,700 ft (1,100-1,750 m), as well as thinner shales and anhydrite beds in the deeper parts, are the best potential seals. In the form of shales, seals are present throughout the COST GE-1 well section. In addition, anhydrite beds, which would act as seals, are present below about 6,000 ft (1,800 m) (Scholle, 1979). Although sandstones are present below 10,000 ft (3,050 m), they are tightly cemented and, in spite of some gas shows in GE-1, must be considered as non-reservoir units in offshore hydrocarbon exploration. Stratigraphic trapping through lateral

facies changes may be of greater interest in this area than in other basins along the Atlantic offshore margin (Scholle, 1979).

1.4 CO₂ Storage Depth

From literature survey, the most important considerations and/ or recommendations, and some global lessons learned about the CO₂ sequestration depths, are summarized below:

- At a depth more than 1,968 ft, (600 m), CO₂ can be stored in dense phase natural geologic formations, but depths below 2,625–3,280 ft (800-1,000 m), the ambient pressures and temperatures in the reservoir will usually result in CO₂ being in a liquid or supercritical state. The supercritical CO₂ at reservoir conditions occupies a much smaller volume than the gaseous state at atmospheric conditions, which provides potential for more efficient utilization of storage space and improves storage security (IEA, 2007).
- Storing CO₂ in the supercritical condition has main advantage that the required storage volume is substantially less than if the CO₂ were at “standard” (room) pressure conditions (NETL, 2015).
- The sedimentary basins with low temperature gradients, are more favorable for CO₂ storage because CO₂ attains higher density at shallower depths 2,297–3,280 ft (700–1,000 m) than in ‘warm’ sedimentary basins, characterized by high temperature gradients where dense-fluid conditions are reached at greater depths 3,280–4,922 ft (1,000–1,500 m). The depth of the storage formation (leading to increased drilling and compression costs for deeper formations) may also influence the selection of storage sites (Semere, 2007).

- Shallow depths, generally less than 2,625 ft (800 m) may add to the risk profile because (1) CO₂ could be in gas phase and (2) the injection zone may be closer to underground source of drinking water (USDW; NETL, 2013).
- To be adsorbed by coal, CO₂ does not need to be in the supercritical (dense phase) state. Therefore, CO₂ storage in coals can take place at shallower depths, at least 656 ft (200 m) deep than storage in oil and natural gas reservoirs and saline formations, at least 2,625 ft (800 m) depth (NETL, 2015).
- A laboratory CO₂ SINK located at Ketzin, Germany aims to characterize a CO₂ injection site using innovative monitoring technologies. The target reservoir is an aquifer at a depth of 1,969 ft (600 m), underlying a redundant gas storage interval. The plan to inject 0.03 Mt of CO₂ a year for up to 3 years will involve a detailed risk assessment and a communication plan with all stakeholders, including local authorities, residents and other parties (IEA, 2008).
- Related to the reservoir thickness, at In-Salah onshore gas project, Algeria, CO₂ injected down flank in ~ 66 ft (20 m) thick reservoir zone as on the gas fields, (Eiken et al., 2011).

The CO₂ storage potential for the offshore Atlantic margin is unexplored, but preliminary considerations suggest that CO₂ sequestration options are significant along the entire eastern seaboard. Sinks at Carolinas with potential for long-term storage of CO₂, are all deep saline reservoirs within host geologic strata (Figure 1.2; Smyth et al., 2008), and located in:

- 1- Offshore in strata approximately ~1 to 3 km below the Atlantic seafloor (Unit 90 and Unit 120 sinks); both of them are overlain by low-permeability seal layers.

- 2- South Georgia Basin and extending offshore 80 to 120 km,
- 3- Nearby states (Tuscaloosa, Mt. Simon, and Knox sinks).

Regarding to the Cretaceous unit, two potential CO₂ sinks are present in geologic strata below the Atlantic seafloor located between 25 and 175 km offshore from the Carolinas, unit 90 in Upper Cretaceous and unit 120 in Lower Cretaceous strata between approximately 1,640 – 9,843 ft (500 and 3,000 m) beneath the seafloor in water depths between 164 – 3,280 ft (50 and 1,000 m) (Figure 1.1). Both of these potential sinks are overlain by low-permeability seal layers, the shallowest of which lies between 656 ft (200 m) (landward) and 6,562 ft (2,000 m) seaward below the seafloor. In addition, the estimated capacities are about 16 Gt for the shallower (unit 90) and up to 175 Gt for the deeper (unit 120) for potential sub-seafloor sinks (Smyth et al., 2008; Vidas, et al., 2012).

1.5 Potential risks, Errors and Accuracy

Error and accuracy can play a significant role in the risk analysis and management. The following factors could effect a robust stratigraphic characterization and CO₂ storage assessment:

- ❖ The availability and quality of the seismic data and well logs.
- ❖ The clarity and continuity of the seismic reflections (key horizons).
- ❖ Mis-ties in seismic data set and seismic sections.
- ❖ Datum reference for different seismic datasets.
- ❖ Seal and reservoir identification and extend as well as their quality and integrity.
- ❖ Presence of the structural and/or stratigraphic traps.
- ❖ Identification of the faulted areas that may represent migration pathways for the CO₂.

1.6 Geophysical Data

Two-dimensional (2D) industry seismic reflection data were collected on the Atlantic Margin in the 1970's and 1980's as part of a phase of offshore petroleum exploration. The acquisition parameters, navigation references, and processing methodologies vary among the various seismic surveys. These seismic data are available through the Bureau of Ocean Energy Management (BOEM) and United States Geological Survey (USGS) databases. There are seven exploratory wells with a variety of geophysical logs in the south Atlantic area; (Figure 1.3). Three wells have the digital logs necessary to conduct integration with seismic data; the others have reports (Table 1.1). In addition, there is a report of the Atlantic Margin Coring (AMCOR) for shallow wells (maximum depth is 1,010 ft) drilled in 1976. All depth references in this dissertation are based on depth below the Kelly Bushing (KB).

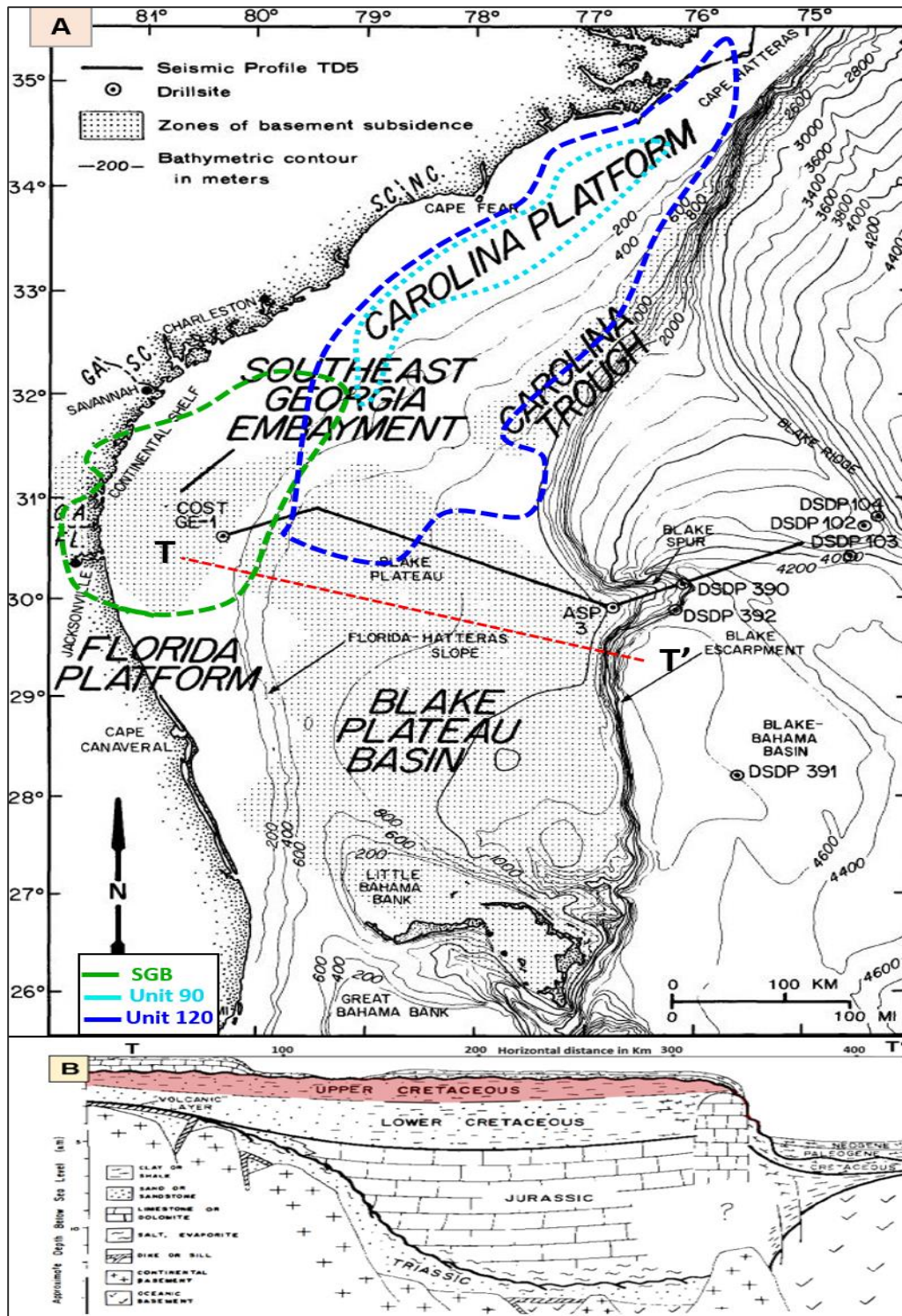


Figure 1.1: [A] Location map showing the main regional geologic provinces within the offshore areas considered for potential storage of CO₂, (modified after (Smyth et al., 2008), [B] Schematic geologic cross section T-T' of the Southeast Georgia Embayment and Blake Plateau, modified after (Poag, 1978; Dillon, et al., 1976).

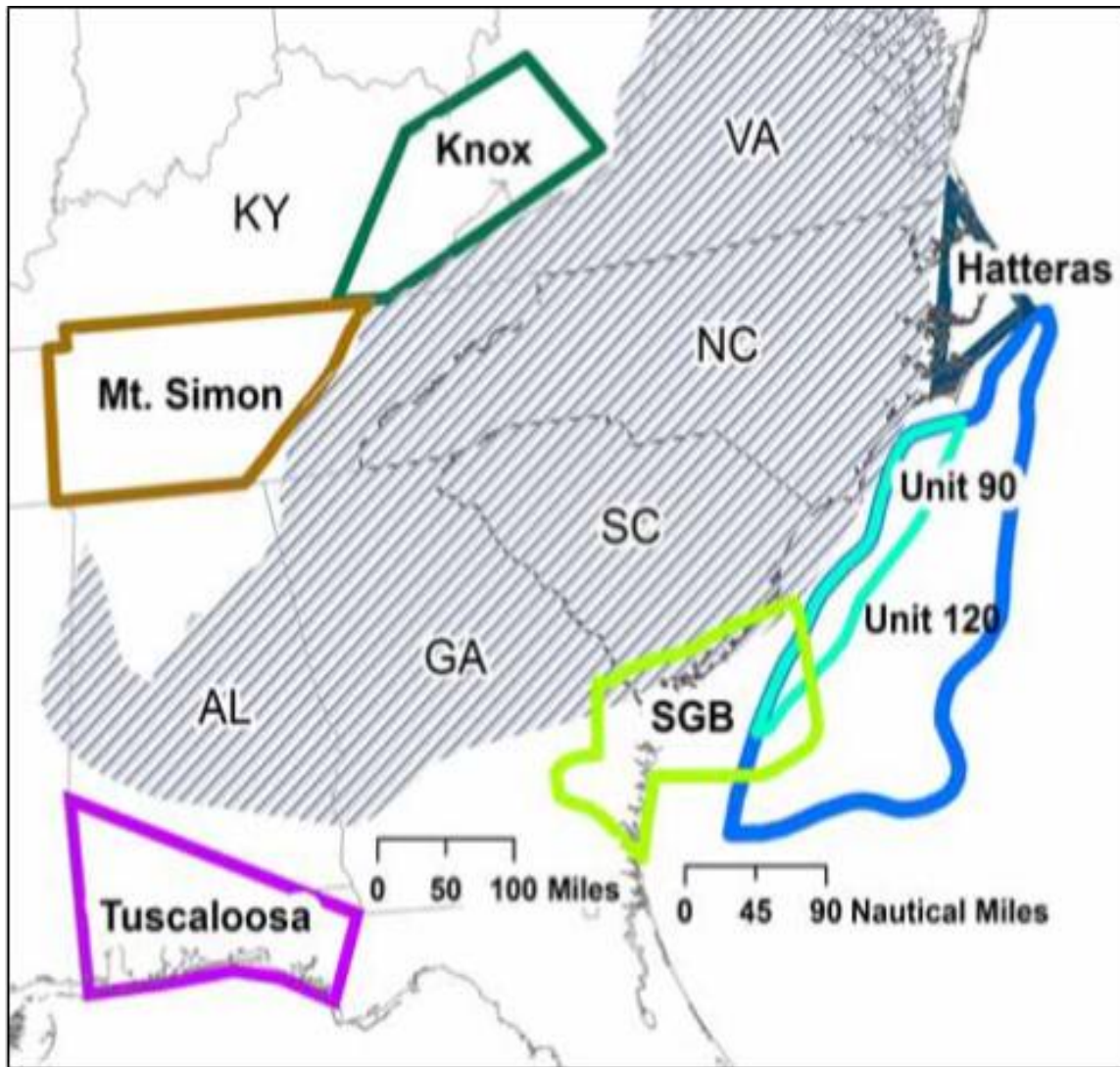


Figure 1.2: Location of areas considered for potential geologic storage of CO₂ generated in North and South Carolina. SGB = Cretaceous-age units in the South Georgia Basin (Smyth et al., 2008).

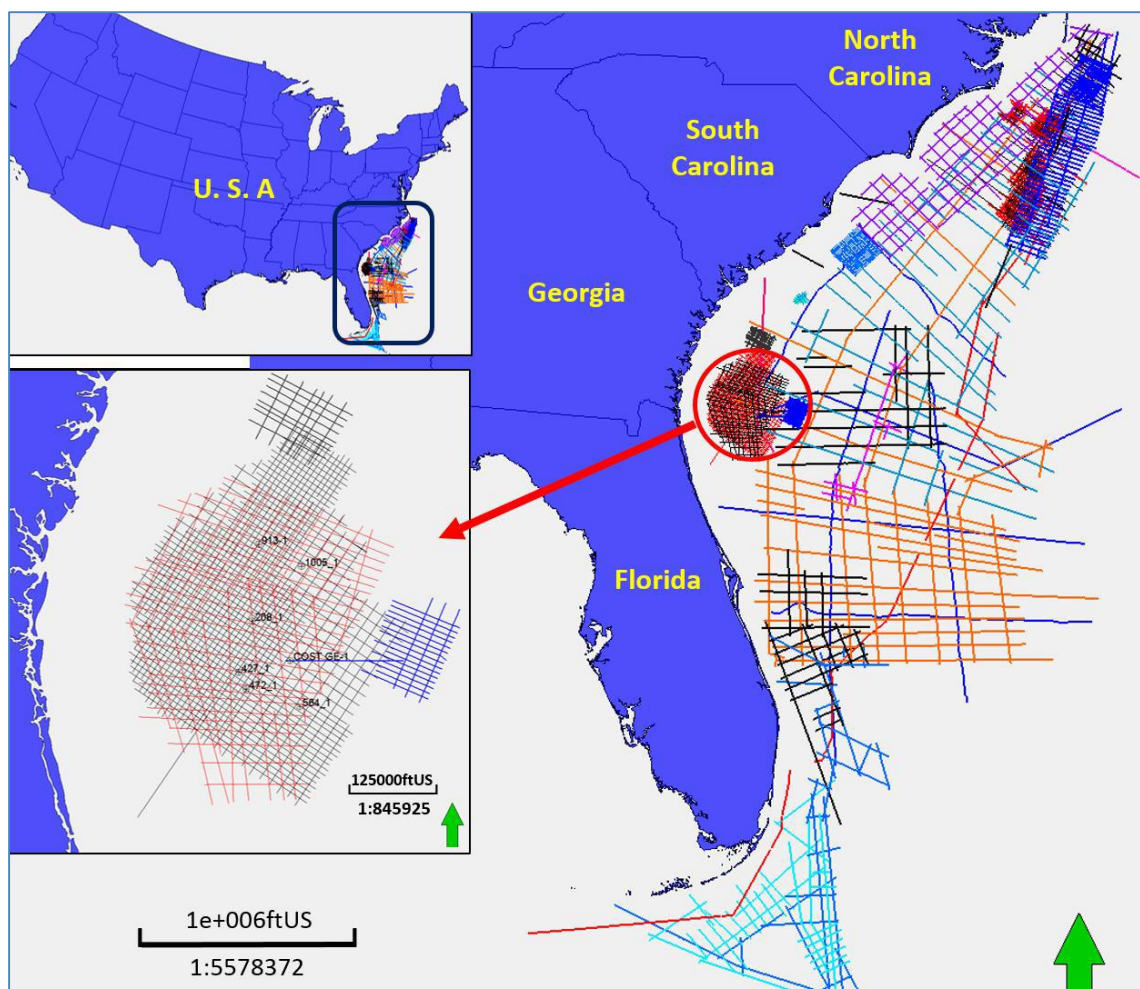


Figure 1.3: Location map of legacy Atlantic Margin industry seismic reflection data, with a total length of more than 100,000 miles. Red circle indicates location of high-density seismic survey within Southeast Georgia Basin.

Table 1.1 Wells used for seismic-well tie and formation evaluation.

Well name	Long. X	Lat. Y	Water Depth (ft)	KB (ft)	TD (ft)	TVD (ft)
COST GE-1	-80.2997	30.619	136	99	13254	13254
Transco 1005-1	-80.2439	30.9928	134	101	11635	11635
Exxon 564-1	-80.25583	30.43972	145	81	12863	12863
913-1	-80.4386	30.08808	109	104	7000	7000
208-1	-80.4706	30.7786	124	104	7754	7754
427-1	-80.53306	30.5761	98	119	7472	7472
472-1	-80.49833	30.5267	125	91	7758	7758

CHAPTER 2

ASSESSMENT OF UPPER CRETACEOUS STRATA FOR OFFSHORE CO₂ STORAGE: SOUTHEASTERN UNITED STATES

2.1 Objectives

The objectives of this research are to: 1) provide a consistent, integrated description, and a reliable subsurface evaluation of Upper Cretaceous section to predict potential for CO₂ geologic storage, 2) identify seismic reflectors and create maps to characterize the structure for Upper Cretaceous section, 3) understand the regional porosity and permeability regime, the quality of potential reservoirs and seals and the storage capacity of Upper Cretaceous section, 4) identify stratigraphic units containing reservoirs or sinks that might be suitable for effective, large-volume geologic storage of CO₂ in Upper Cretaceous age, and 5) evaluate the quality and lateral extent of the sealing rock and its ability to safely ensure the retention of the trapped CO₂ within the confined porous formation for hundreds of years. To achieve the research objectives, several hypotheses were proposed. These are 1) Upper Cretaceous formations have potential for at least 16 GT of CO₂ storage capacity, 2) Upper Cretaceous potential sink is overlain by a low-permeability seal layer, 3) distinct porosity and permeability regimes, which are influenced

¹ Khaled F. Almutairi, Camelia C. Knapp, James H. Knapp and Darrell A. Terry, (2017), "Assessment of Upper Cretaceous Strata for Offshore CO₂ Storage, Southeastern United States." *Modern Environmental Science and Engineering*, vol. 03, no. 08, 3 Aug. 2017, pp. 532–552

by depositional environments and lithologic composition are present and widely distributed in Upper Cretaceous, and 4) Upper Cretaceous units consist of moderately to highly compartmentalized stratigraphic systems which help increase the storage capacity. After assessing the study area for CO₂ sequestration, this research will attempt to answer additional research questions that are connected with the research objectives. These questions are: 1) do Upper Cretaceous geologic units have potential for significant CO₂ storage capacity? 2) what are the quality and spatial extent of the prospective reservoirs and seals? 3) how do reservoir and seal structures affect long-term CO₂ sequestration? 4) to what extent does the Upper Cretaceous sedimentary section extend offshore beneath the continental shelf? 5) does it have distinct porosity and permeability regimes? And how do these regimes impact CO₂ storage quality and capacity?

2.2 Methodology and Data Analysis

Seismic reflection data provide the basic structural control of the subsurface geology constrained by available exploration wells. For quality control, a series of data analysis techniques were applied in this study. A flowchart of the seismic data calibration with well control and further interpretation is provided in Figure 2.1. Seismic mis-tie analysis was performed and applied among the seismic lines used in this research. Well logs were used to derive a detailed assessment of the geologic formations penetrated by the boreholes and tie the interpreted geologic strata to key seismic horizons. This helped with the calibration and consistency of the seismic data interpretation. Wells with sonic and density logs were selected to calculate reflection coefficients. Wavelets were extracted from the seismic lines that intersected in the proximity of the wells and were used to generate synthetic seismograms. Check-shot surveys were used to verify the resulting

seismic-well ties. Geophysical well logs were used to identify rock types and determine fundamental storage parameters, including porosity and permeability. For seismic interpretation and geophysical log analysis, *Schlumberger's Petrel Software (2015)* was employed for stratigraphic and structural interpretation and for defining the storage geological windows of interest and the respective seals within the Upper Cretaceous unit. The seismic interpretation workflow includes picking significant horizons constrained by well control, creating main surfaces stratigraphy, and generating structural maps in time, and converting time to depth unit. Stratigraphic and structural cross sections as well as isochore, isolith, and structural contour maps provided the basis for geological characterization, and identification of prospective CO₂ sinks and reservoir seals (Figure 2.1). This characterization helps to define the areal extent and thickness of prospective storage formations.

2.2.1 Data Calibration and Normalization

To accomplish the research objectives, the data needed to be preprocessed to common specifications. The seismic datasets have different acquisition and processing parameters and were acquired over many years. The data sets have seismic mis-ties and variations in amplitude scaling. Therefore, two main steps were undertaken prior to interpretation including data calibration and amplitude normalization. These steps were necessary to account for the vintage and datum differences within the data. Figure 2.1 gives an overview of the data calibration and interpretation workflow.

2.2.2 Mis-Tie Analysis

Given different vintages and varying acquisition parameters, most seismic data sets have seismic mis-ties. The various data sets were acquired with different geographic

coordinate projections, different datums, and different processing flows. Analysis and removal of mis-ties from the seismic data is very important when an interpreted reflection does not close, or tie, when interpreting intersecting lines. Some solutions to the mis-tie issues include 1) application of amplitude normalization or scaling to unify the amplitude scale in the data sets, and 2) application of vertical mis-tie (absolute value) and phase mis-tie (absolute value) with constant correction.

2.2.3 Seismic Well-Tie

Seismic-well tie analysis has been conducted to compare well logs (measured in depth units), with seismic data (measured in time units). It is important to relate horizon tops identified in the wells with specific reflectors on the seismic sections in order to create the reservoir and seal structure maps to assess CO₂ potential storage. For quality control and verification of the check shot data, editing was applied to the sonic and the density logs to remove unwanted spicks before sonic calibration. For synthetic seismogram generation, several different wavelets were generated and assessed, especially the deterministic extended and the Ricker wavelets. Ricker wavelets were generated for several different central frequencies, the center frequency of 22.5Hz (USA phase) provides the best fit. The same sampling rate of 4 msec was used for all seismic data sets. Seismic-well tie analysis was applied using data from the COST GE-1, Exxon 564-1 and Transco 1005-1 wells. The COST GE-1 well data is shared to conduct multi seismic-well tie analysis using the neighboring seismic lines. Reflection coefficients (RC) were calculated using the calibrated sonic and density logs which were convolved with the selected wavelet to get the synthetic seismogram. Finally, the synthetic seismograms matched the seismic data achieving a good fit. The methods applied included 1) using key well tops to match peak –

peak or trough – trough, 2) using bulk shift to tie synthetic to seismic, or variable time shift to move and stretch two or more horizons, and 3) using the alignments points to make small adjustments between the synthetic and seismic data (Cubizolle et al., 2015); (Figure 2.2).

2.3 Structural Interpretation

2.3.1 Picking Horizons and Creating Surfaces

To achieve the research objectives, some factors were considered for selecting horizons in the Upper Cretaceous section. Porosity and permeability distribution versus depth are critical factors. Also, the lithology descriptions according to the cores and cuts, and well log interpretation were considered. The available control wells are clustered in the Southeast Georgia Embayment and not widely distributed along the Atlantic offshore. Although it was difficult to pick all horizons due to the reflectors pinch out caused by lateral facies changes (Scholle, 1979), the significant markers and the top and base of the Upper Cretaceous were picked within the Southeast Georgia Embayment, and then extrapolated at a larger regional scale. However, the tops were selected based on the paleontological data, depths versus geologic series or stage, from the COST GE-1 well (Amato, and Bebout, 1978; Figure 2.3). The corresponding geological formations to these horizons are illustrated in Table (2.1), (Poppe et al., 1995). The main units picked are 1) Maastrichtian top, which represents the top of Upper Cretaceous, 2) Turonian top and 3) Albian top, which represents the base of Upper Cretaceous. More detailed picking of horizons was conducted using the close loop approach which is based on selecting at least three adjacent seismic intersections as guides in order to close the picking loop and to make sure that the same reflectors are selected at the seismic intersections. Manual interpretation was used for picking horizons in some cases. In a few cases where the reflectors were

clearly continuous, the seeded 2D auto tracking feature in Petrel was used. Structure maps were generated and smoothed gently to remove any random noise or spikes. The maps' statistics and visual display were checked for quality control. However, the horizons picked in the Southeast Georgia Embayment have a high degree of confidence due to the high density of track lines, were diligently interpolated and extrapolated regionally along the offshore areas of Carolina Trough and Blake Plateau Basin.

2.3.2 Time Depth Conversion

Two methods were used to convert the interpreted structural maps from time to depth. Both methods give similar depths, when compared with the well data. The two methods are shown below; however, there is uncertainty with depth due to insufficient data.

a) A simple polynomial equation was used for plotting the relationship between the measured depth (ft) and TWT (ms) for the COST GE-1 well, where (x) and (R) represent the surface structure map (in msec) and the correlation coefficient for the linear regression, respectively (Johnston and Goncharov 2012). This polynomial equation gives an accurate depth for the interpreted surfaces at wells COST GE-1, Exxon 564-1 and Transco 1005-1 after converting the domains from time (ms) to depth (ft). Below is an example of a polynomial equation that was used, where the correlation coefficient is high ($R^2=0.9995$).

$$y = 0.00063x^2 + 3.9496x - 470.74$$

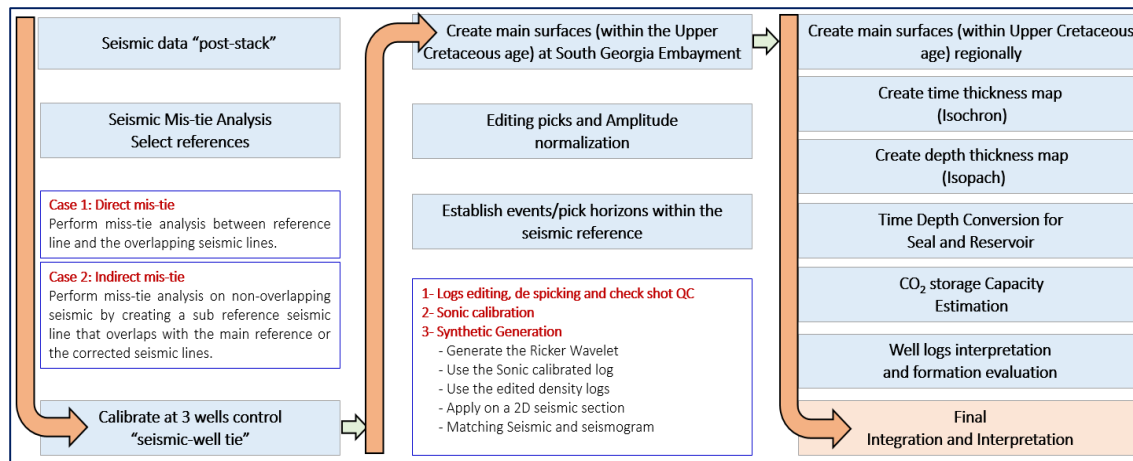


Figure 2.1: Flowchart outlining seismic data calibration and interpretation workflow.

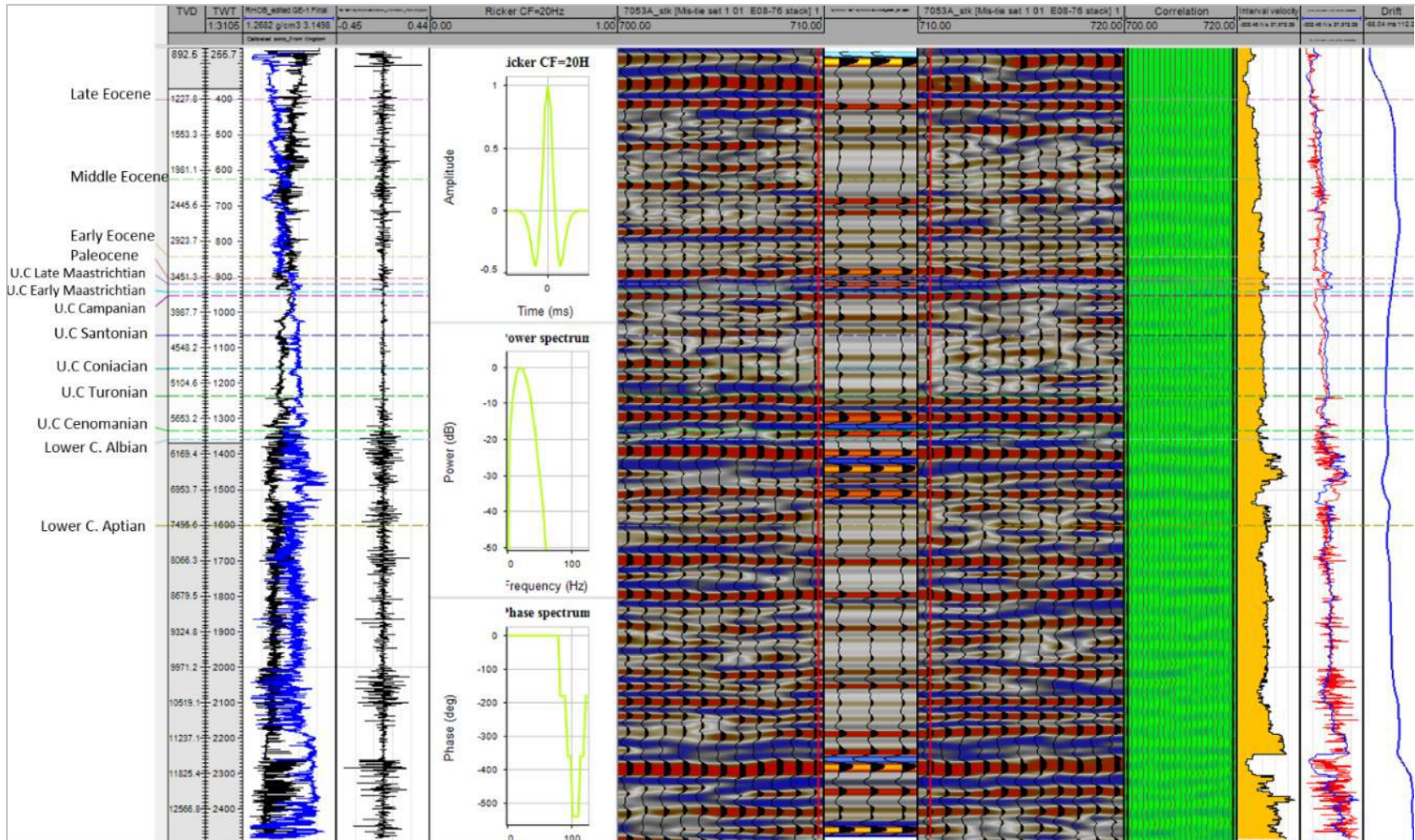


Figure 2.2: Seismic-well tie for COST GE-1 well.

Table 2.1 Stratigraphic nomenclature of rock formations identified onshore along the U.S. southeastern coast, from (Poppe et al., 1995).

Epoch	Stage / Age	South Carolina	Southeast Georgia	Florida
Upper Cretaceous	Maastrichtian	Peedee	Unnamed Marine Beds	Lawson Limestone
	Campanian	Black Creek Group		Pine Key
	Santonian	Middendorf	Middendorf	Atkinson
	Coniacian	Cape Fear		
	Turonian	Clubhouse	Atkinson	
	Cenomanian	Beech Hill		

b) To get a more accurate depth to the top of the reservoir, major velocity boundaries of the overburden layers are taken into consideration in order to build linear velocity models in a layer cake model from the surface down to the top of the reservoir. Schlumberger *Petrel 2015* offers an option to create an advanced velocity model. This velocity model is defined using input parameters such as tops, surfaces, time-depth relationship, and includes using two types of linear velocity functions.

Those velocity functions are $(V=V_0 + K*Z)$ and $(V=V_0 +K*(Z-Z_0))$, where V_0 derives at different locations (Schlumberger, 2016). The parameter K represents the linear velocity slope and describes the velocity increment with depth, which reflects the layer compaction. For each layer, the K value of the velocity law is the average of the K value derived at each well for the layer under consideration. A minimum error estimation of the compaction factor K is obtained and used derive a V_0 surface and any correction built into the velocity model is reflected in the V_0 surface. Due to the compaction being considered as a regional event, K remained constant. To create the velocity model, the time-depth relationship of the COST GE-1, Exxon 564-1 and Transco 1005-1 wells are used. The procedures included: 1) using cross plots of picked two-way travel times and the interval velocities from the check shot data for quality control in order to check the time-depth relationships, 2) calculating the interval velocity based on the well top depths, checking shot data and the interpreted surface times at the well top positions, and 3) using well tops to define the correction. However, the interpolated interval velocities range from 7,600 to 7,800 ft/sec along the top of Upper Cretaceous, and from 8,500 to 14,000 ft/sec along the Turonian surface (Figure 2.4).

2.3.3 Structure Maps

The regional extents of Upper Cretaceous formations have similarity. They are shallow towards the shoreline and dip gradually seaward beneath the offshore of Southeast Georgia Basin and continental shelf, and become deeper towards the continental slope. The top of Upper Cretaceous section varies from 1,000 ft to 6,000 ft depth, and it is encountered at a depth of 945 ft below MSL in well 6004B, (Hathaway et al., 1976). Such a depth is not suitable for CO₂ sequestration because the CO₂ would not reach supercritical conditions (NETL, 2015). However, the Turonian structure, which appears to be compartmentalized in several reservoirs, has a depth range from 2,500 ft (near the Carolinas), to approximately 9,000 ft (in the Carolina Trough). For the base of Upper Cretaceous surface, the depth ranges from 2,700 ft to 12,000 ft; (Figure 2.5).

Nevertheless, the regional thickness map of the entire Upper Cretaceous section indicates the presence of thick accumulated sediments in the Atlantic offshore, especially the Carolina Trough. The thickness range is approximately from 1,200 ft to more than 6,000 ft. This would represent a significant opportunity for CO₂ sequestration with large storage capacities since it has sequences of limestone and calcareous shales in the upper part, limestone and dolomites interbedded with sandstones in the middle, and shales with reasonable porosity and permeability values according to the cores and side-wall cuts in the lower part (Scholle, 1979). Sediments between the top of Upper Cretaceous and the Turonian surface, which are mostly calcareous shales with some limestone, arrange in thickness from 750 ft to more than 4,000 ft. Although it has up-dip within Carolina trough basin, it has potential to be the best regional seal. It has shale intervals sequences with low permeability less than 3 mD (Scholle, 1979). Similarly, sediments between the Turonian

surface and the base of Upper Cretaceous, have thicknesses from 250 ft to more than 2,500 ft, (Figure 2.6). It has potential for two compartmented reservoirs; (Figure 2.12). At the local scale in the Southeast Georgia Embayment, which has been extensively covered with seismic surveys and wells, the depth of the top of Upper Cretaceous section varies approximately from 3,000 ft to 4,500 ft; similarly, the Turonian surface, which would serve as a reservoir, has a depth range from 4,000 to 7,000 ft (Figure 2.7). Such depths and thicknesses are suitable for CO₂ sequestration. The sediment column between the top of Upper Cretaceous and Turonian surface, mostly shales with low permeability, would serve as a thick (800 to 2,600 ft) seal. Similarly, the difference in depth between the Turonian surface and the base of Upper Cretaceous has a thickness between 250 to 1,200 ft, (Figure 2.8). It represents the prospective reservoirs where high porosity and permeability exist; (Figure 2.12). All structure and thickness maps were created within specific boundaries (polygons), in which horizons were picked with high spatial density in order to get good lateral interpolation.

2.4 Well Log Interpretation

Well logs provide critical information on the geologic formations in the subsurface. The gamma-ray (GR) log tool measures the natural radioactivity in different rocks. Spontaneous Potential (SP) measures the potential difference versus depth between the voltage in the wellbore and an electrode on the surface (Asquith, 2004). Both GR and SP can be used to determine lithology and correlate stratigraphy and they have the same response to porous layers. For pure sandstones and carbonates, the gamma-ray values are generally less than 90 API due to very low radioactive material. Spontaneous Potential also has low values.

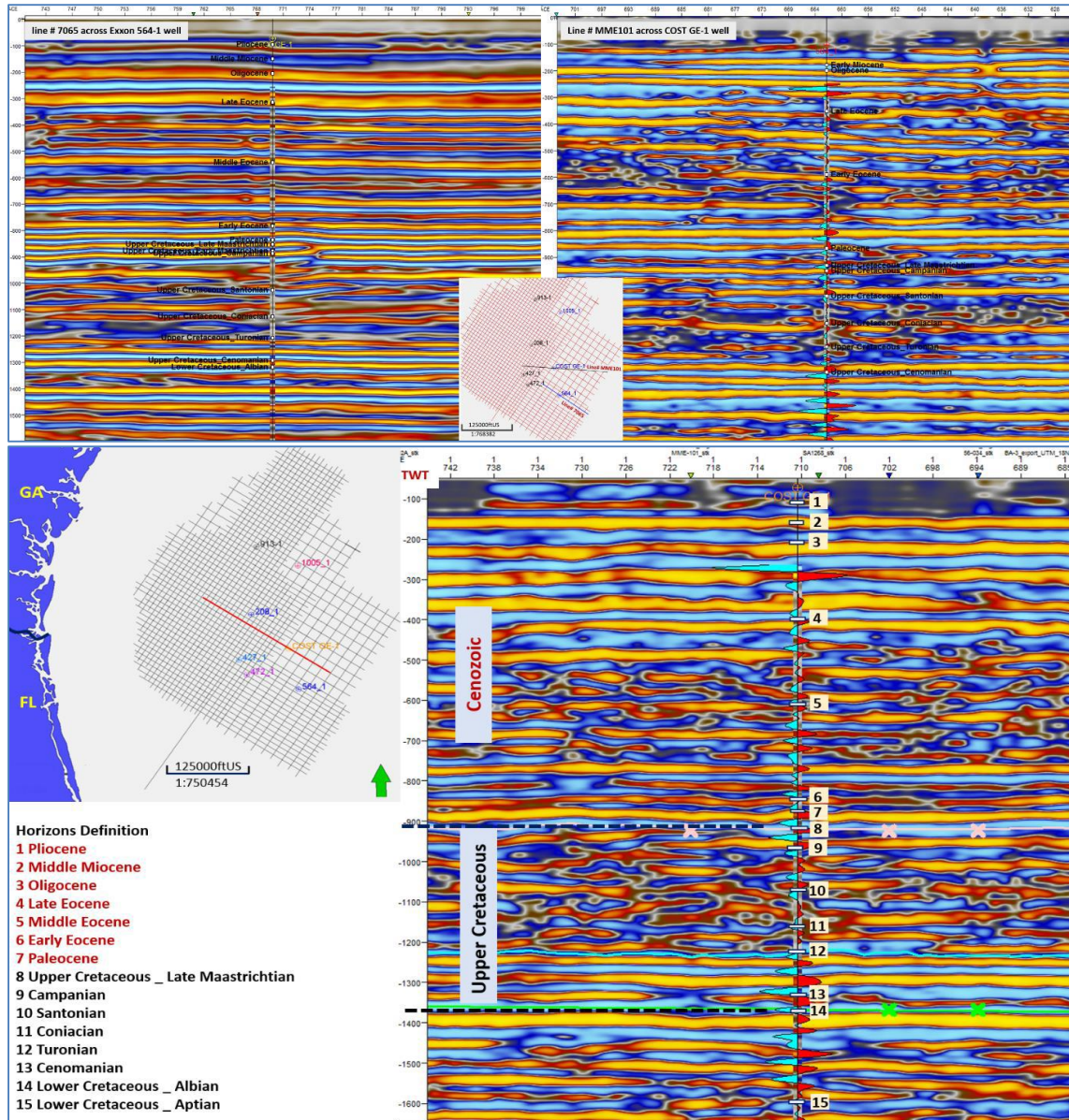


Figure 2.3: Analysis of seismic sections: [Top] Two seismic sections that were tied with different wells; [Bottom] Paleontological tops and picking the top and base of Upper Cretaceous at the COST GE-1 well.

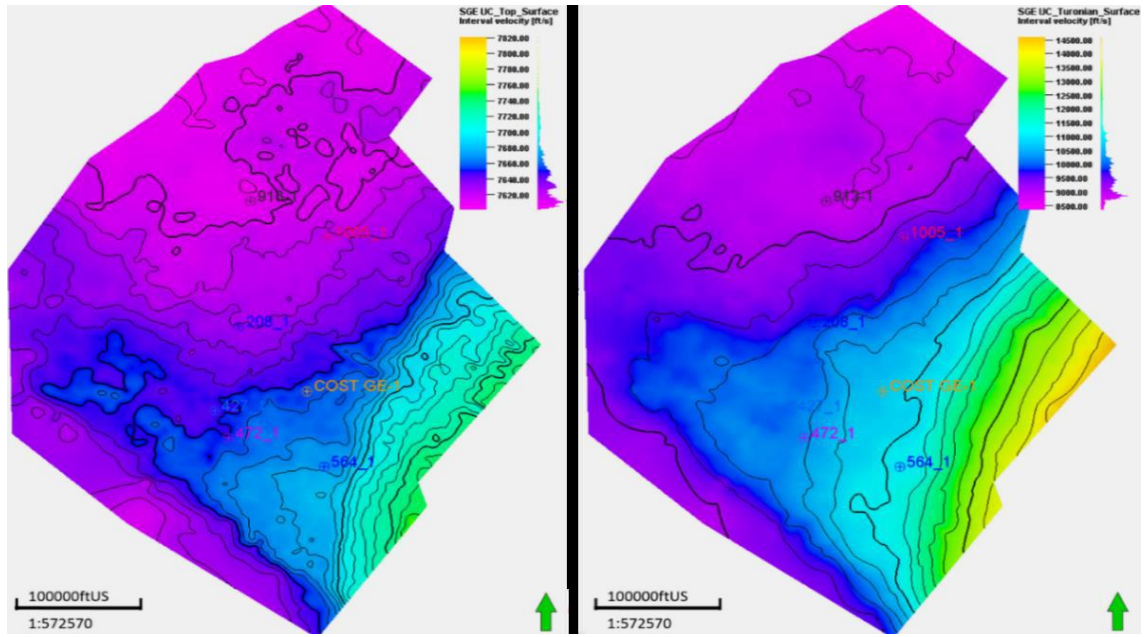


Figure 2.4: Examples of the interval velocity interpolation within the Southeast Georgia Embayment using the advanced Velocity Model; (Left): between the top of Upper Cretaceous and Turonian surface; (Right): between the Turonian surface and the base of Upper Cretaceous.

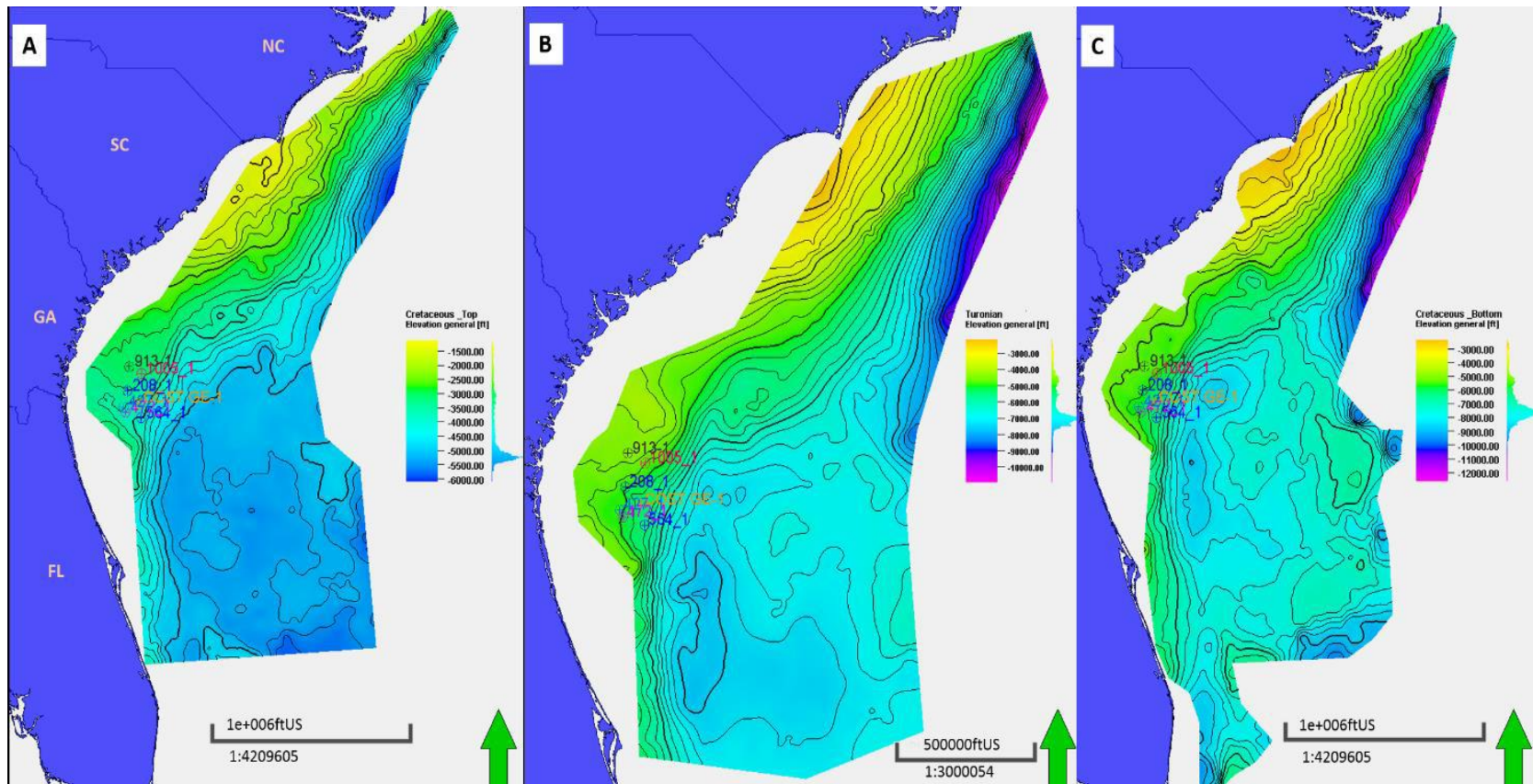


Figure 2.5: Regional 2D structure maps (in feet) for: [A] top of Upper Cretaceous [Maastrichtian], [B] Turonian and [C] base of Upper Cretaceous [Albian].

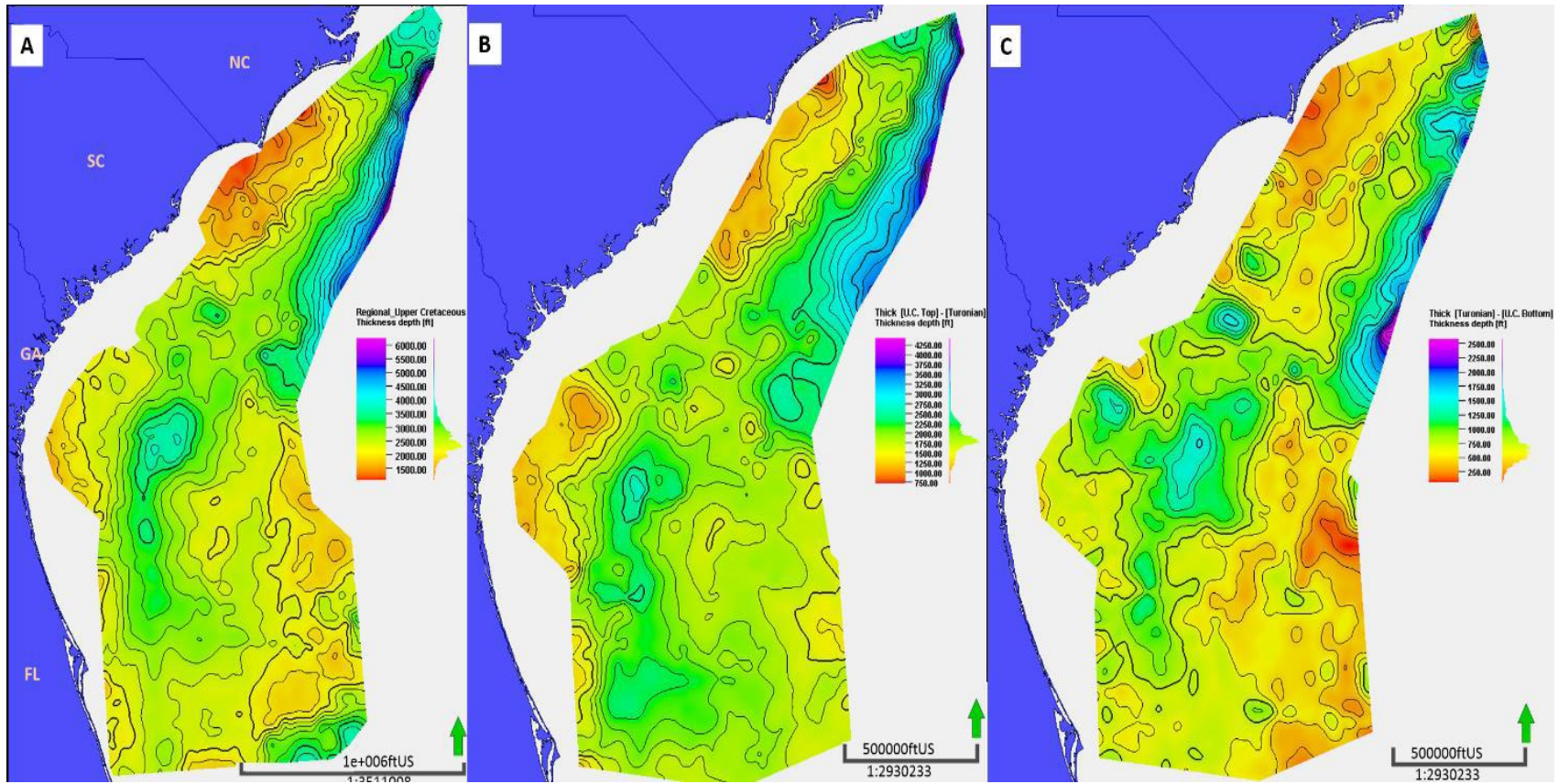


Figure 2.6: Regional thickness maps [isochore, in feet]: for [A] entire Upper Cretaceous section, [B] Maastrichtian to Turonian, and [C] Turonian to base of Upper Cretaceous.

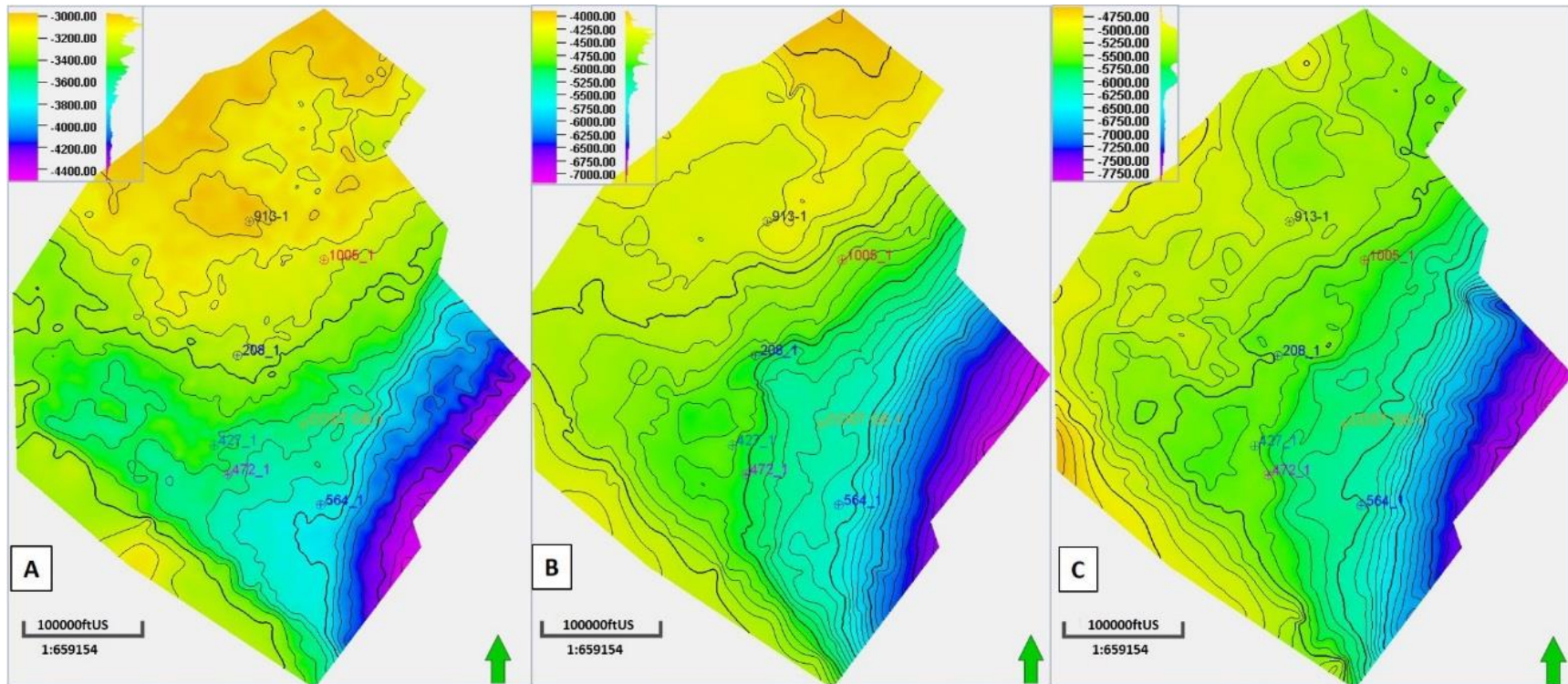


Figure 2.7: Structure maps, in feet, for [A] top of Upper Cretaceous [Late Maastrichtian], [B] Turonian, and [C] base of Upper Cretaceous [Albian].

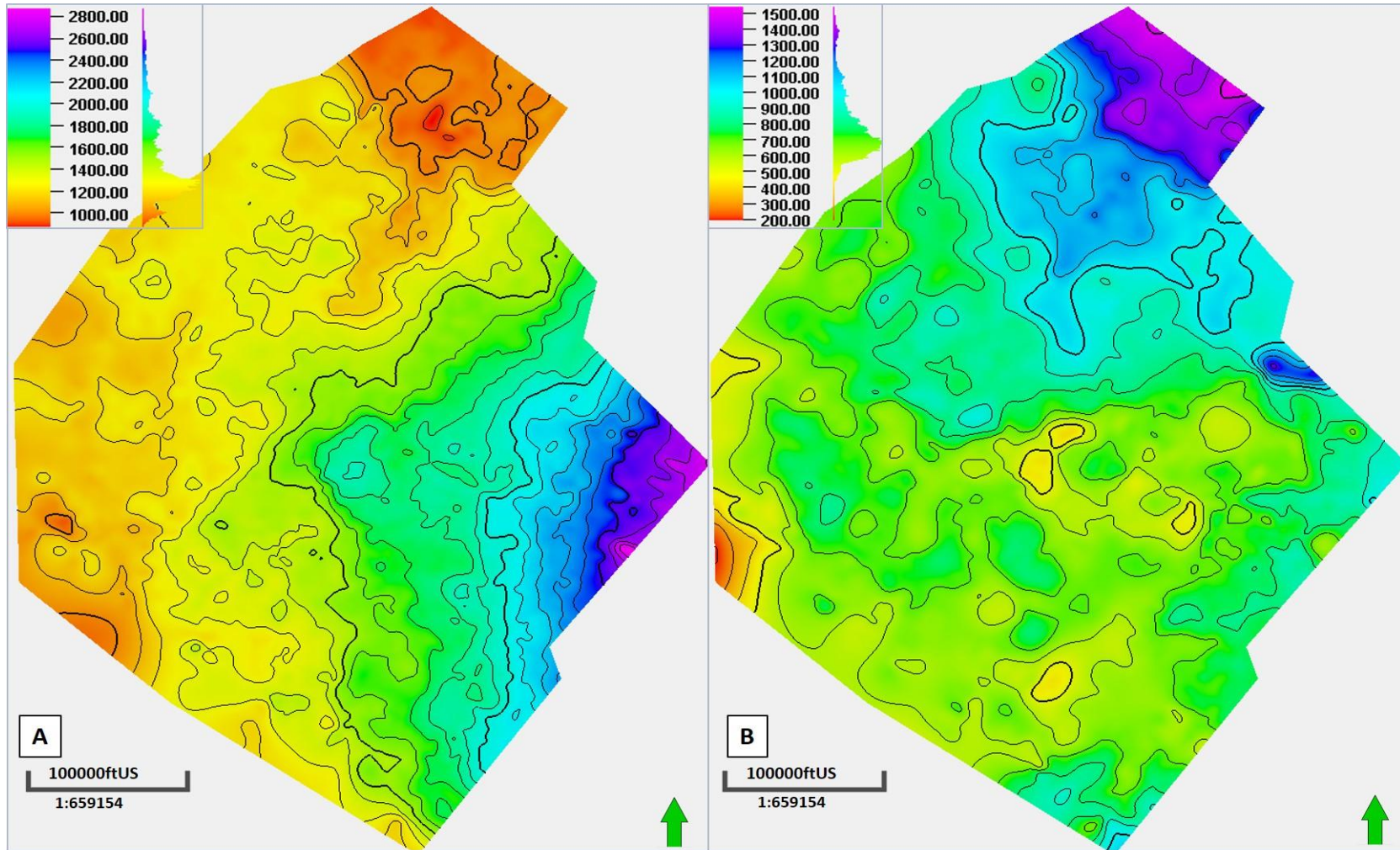


Figure 2.8: Thickness maps [isochore] in feet for [A] prospective seal and [B] potential reservoir within the offshore of Southeast Georgia Basin.

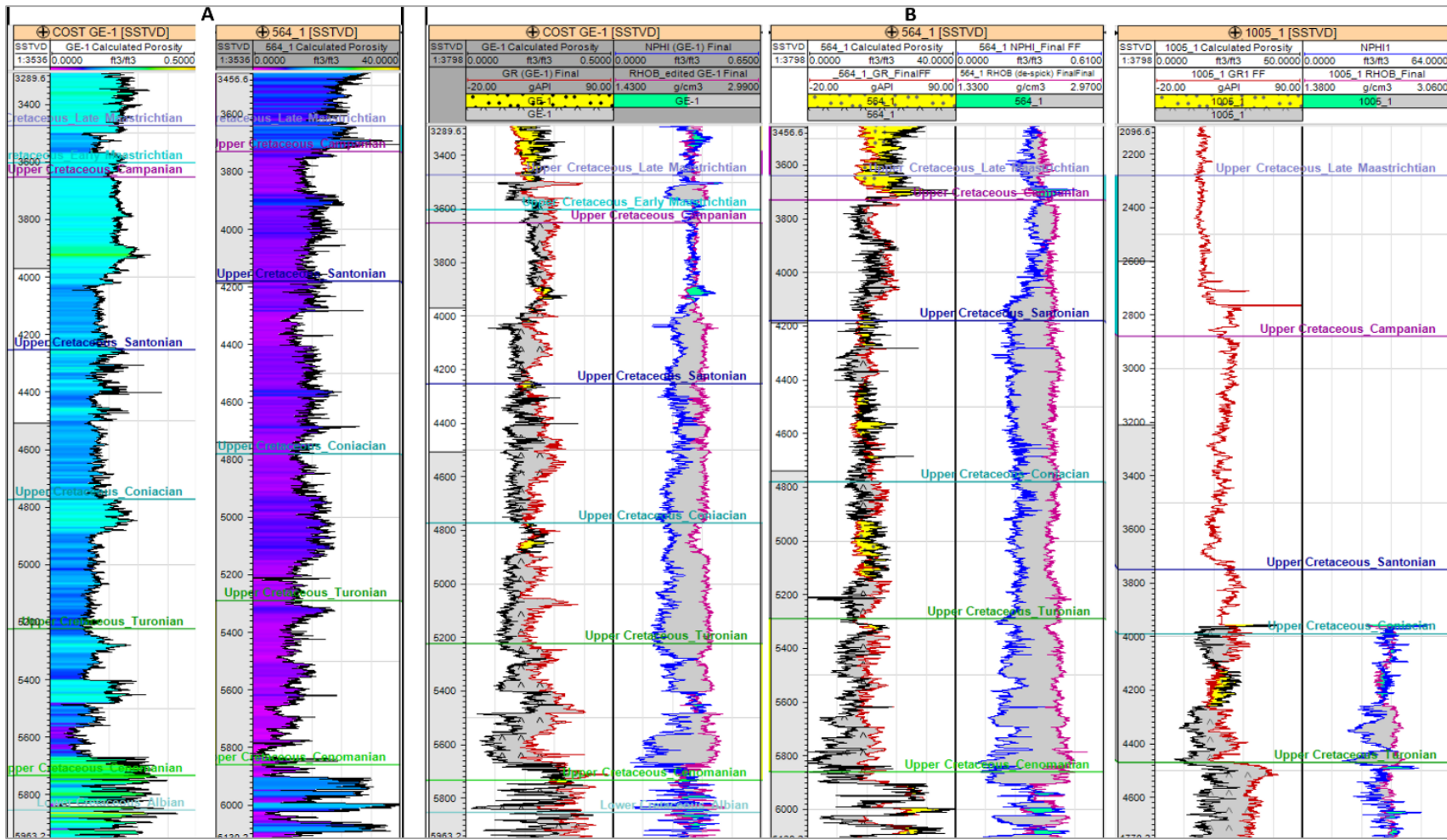


Figure 2.9: Logs for different wells: [A] calculated porosity logs at COST GE-1 and Exxon 564-1 wells, [B] gamma ray versus calculated porosity in one track to emphasize the sand and shale cutoffs, and in the next track density versus neutron log to emphasize the crossover which is indication to fluid-filled porosity which is a reflection to porous lithology.

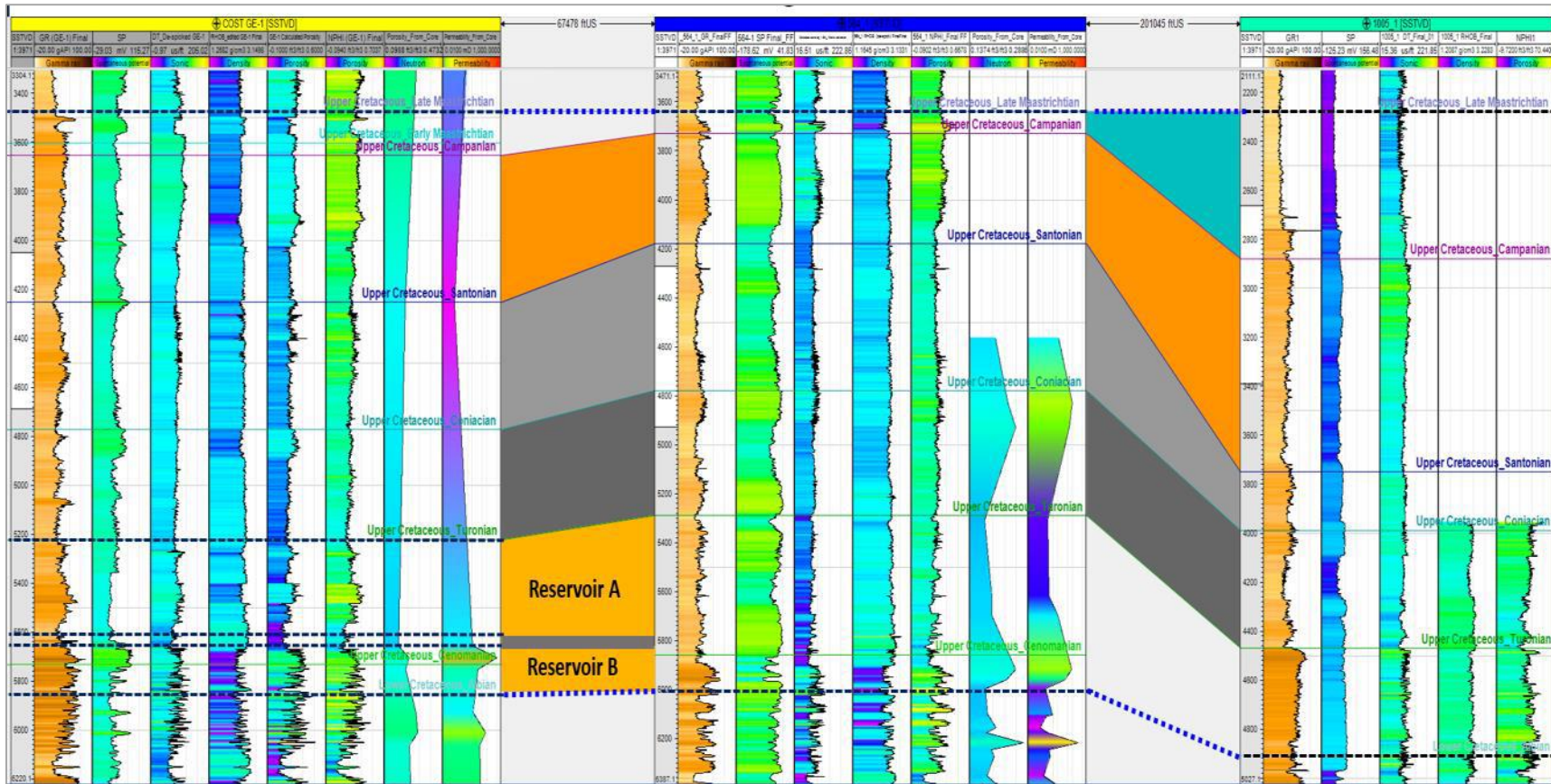


Figure 2.10: lithology logs (GR and SP) and the porosity logs (sonic, density, neutron) and porosity and permeability that calculated from core data, for the COST GE-1, Exxon 564-1 and Transco 1005-1 wells respectively.

However, shale has high radioactive elements which elevate the gamma-ray values as well as the Spontaneous Potential that also shows high voltage (Asquith, 2004). Density logs provide a continuous record of the formation's bulk density which is a function of formation porosity, fluid content in the pore spaces, and matrix density (Asquith, 2004). It is commonly used to calculate porosity. However, neutron log provides fluid-filled porosity and measures hydrogen concentration in a formation. The crossover between neutron and density logs is the most reliable indicator to a formation reservoir; (Figure 2.9). With the lower density and the higher neutron values, the two curves will crossover or touch each other. Therefore, greater crossover between the density and neutron logs indicates a better quality reservoir (Darling, 2005). This occurs at small intervals since most of the lithology is limestone and dolomite. In the lower part of upper Cretaceous, some intervals have crossover which in reality represent sandstone. Also, at small intervals, since the neutron porosity curve is to the right of the density porosity curve, it indicates a wet sand and / or porous medium. However, at most depth intervals, the neutron porosity curve is to the left of the density porosity curve; this is a good indicator of shale. Figure 2.10 shows stratigraphy correlation between wells after flattening the structure to the top of Upper Cretaceous [Early Maastrichtian surface]. Although porosity values (\emptyset) are available from core and side-wall cuts at specific intervals in the well COST GE-1, in this study, porosity was also calculated from the sonic logs using the Wyllie time average formula (Wyllie et al., 1956) at COST GE-1, Exxon 564-1 and Transco 1005-1 wells:

$$\emptyset = \left[\frac{\Delta t_{\log} - \Delta t_{\text{matrix}}}{\Delta t_f - \Delta t_{\text{matrix}}} \right]$$

where:

Δt_{\log} = acoustic transit time, in $\mu\text{sec}/\text{ft}$.

Δt_{matrix} = acoustic transit time of the formation matrix, in $\mu\text{sec}/\text{ft}$, and

Δt_f = acoustic transit time of interstitial fluids, in $\mu\text{sec}/\text{ft}$.

Acoustic transit times of 47.5 $\mu\text{sec}/\text{ft}$ and 89 $\mu\text{sec}/\text{ft}$ were obtained from the sonic log and used for the limestone matrix and the interstitial fluid (brine), respectively (Mavko et al., 2003). Log interpretations indicate a sequence of shale interbedded with limestone. In COST GE-1 well, the lithologic description indicates that the Coniacian could serve as a seal at a depth between 4,870 and 5,150 ft since it has poor to fair porosity, and consists of silt and calcareous. The intervals of depths from 5,500 to 5,575 ft and from 5,700 to 5,950 ft, which include Turonian and Cenomanian ages, have high porosity and permeability. These could serve as compartmentalized reservoirs; (Figures 2.10 and 2.12).

2.5 Results and Discussion

The porosity and permeability depth relationship for the upper 5,700 ft of the COST GE-1 well indicates that Upper Cretaceous section has a porosity range of 12 % to 23 % from 3,500 ft to about 5,500 ft; however, the approximate matrix permeability is in the range of 0.15 to 0.6 mD. Plots of porosities and permeabilities as a function of depth from conventional and sidewall cores from the COST GE-1 well (data from ((Amato and Bebout, 1978)). Figure 2.11 shows that very high porosities (25 to 40%) are encountered in the Cenozoic age chinks in the 1,000 to 3,000 ft depth interval, and the corresponding permeabilities for these fine-grained limestones are predictably low (Amato and Bebout, 1978).

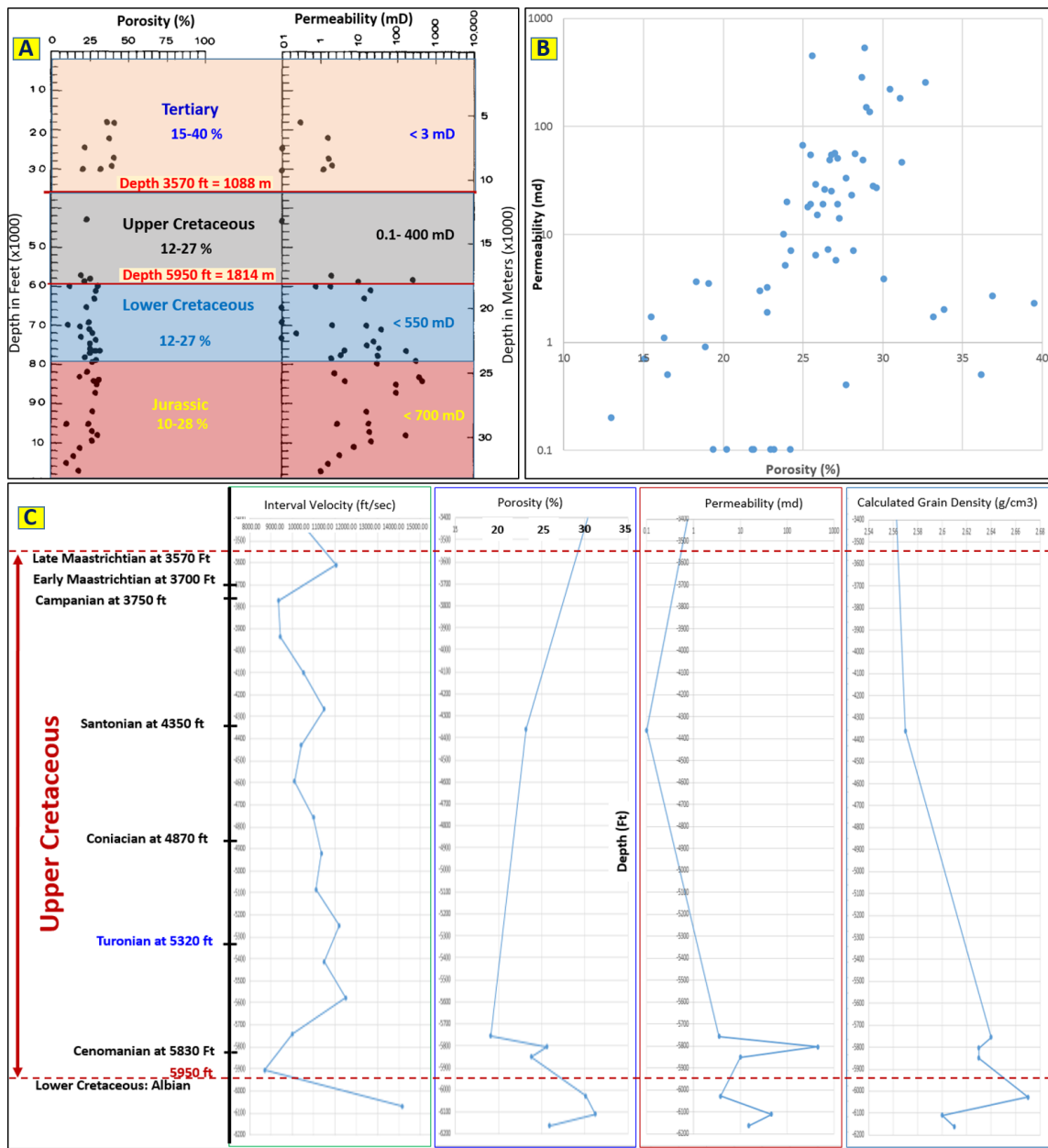


Figure 2.11: Relationship between porosities and permeabilities versus depth for the COST GE-1 well: [A] values measured on conventional and sidewall cores (data from (Amato, and Bebout, 1978)); [B] core porosities plotted against core permeabilities for the entire well, data from (Scholle, 1979); [C] plotting interval velocity, porosity, permeability, and densities that calculated from the cores, for Upper Cretaceous section (data from (Scholle, 1979)).

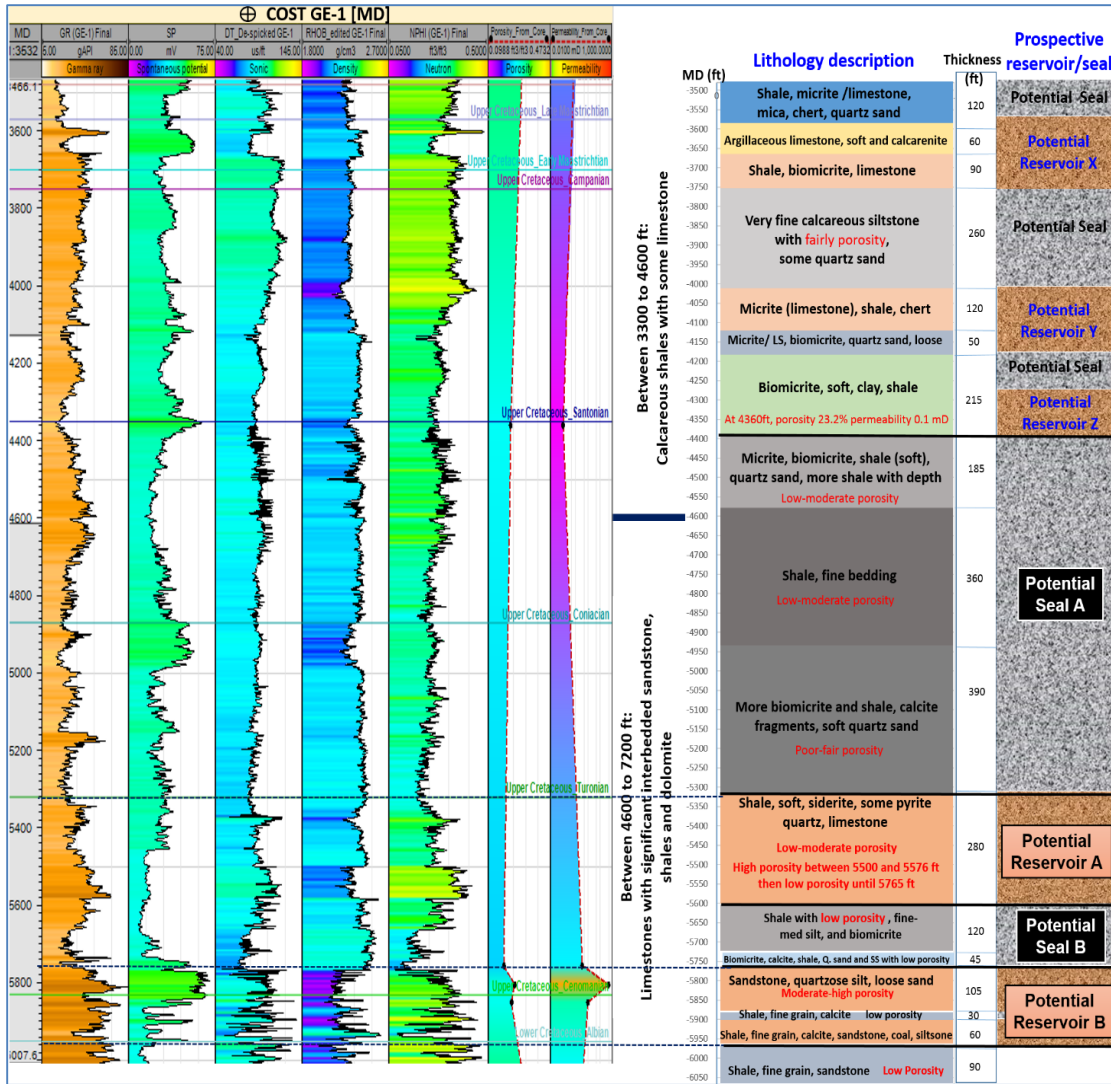


Figure 2.12: Logs of gamma ray, self-Potential, sonic, density, neutron as well as porosities and the permeabilities that calculated from the core data. Also, lithology description with a geological model for the main two potentials reservoirs and seals at the Upper Cretaceous section.

Five reservoirs and their associated seals were identified as potential sinks in the Upper Cretaceous section, (Figure 2.12 and Table 4.2). The two significant storage reservoirs for CO₂, which considered limestones with significant interbedded sandstone, shales and dolomite (Scholle, 1979), are sealed by thick sediments of mainly shale interbedded with limestone. These two reservoirs, named “A” and “B”, are illustrated in Figure 2.12. The trapping mechanism, an overlying caprock or seal, is stratigraphic trapping through lateral facies changes (Scholle, 1979):

- 1- Reservoir “A” is located between 5,320 to 5,600 ft, and sealed by about 725 ft. thick shale.
- 2- Reservoir “B” is located between 5,760 to 5,950 ft and sealed by 160 ft thick shale.

A significant potential for CO₂ storage occurs where high values of primary and secondary porosity account for much of the best permeability encountered in the Upper Cretaceous section at the well COST GE-1. This reservoir is interrupted at the middle by a thin layer of shale between depths 5,870 and 5,900 ft which could serve as an additional seal. In these intervals, the porosity range is from 20 to 30% especially after 5,500 ft, and the permeability range is 1 to 447 mD.

CHAPTER 3
ACOUSTIC IMPEDANCE INVERSIONS FOR OFFSHORE CO₂
STORAGE: SOUTH GEORGIA EMBAYMENT

3.1 Background and Objectives

The United States (U.S.) Environmental Protection Agency estimates that about 40 percent of the anthropogenic CO₂ emissions in the U.S. are generated in the southeastern U.S. This contribution is about 1,444 million metric tons of CO₂ (Litynski et al., 2008). Given that viable solutions are not yet available to reduce CO₂ emissions, the U.S. Department of Energy has been funding several efforts to study the feasibility of CO₂ storage as a long-term mitigation strategy. The Southeast Offshore Storage Resource Assessment (SOSRA) research project is funded by U.S. Department of Energy (DOE) and is tasked with assessing the offshore for CO₂ storage efficacy. Although the storage capacity of offshore reservoirs is expected to be substantial, and despite having a number of important advantages over onshore sites, no comprehensive assessment of the offshore storage capacity in the southeastern U.S. has been performed (Franklin, 2009). Smyth et al. (2008) considered that two potential CO₂ reservoirs are present in geologic strata below the Atlantic seafloor in Upper and Lower Cretaceous layers. The research and assessment for the South Eastern portion of the SOSRA project is divided based on the geologic age of the reservoir formation under study. Therefore, this chapter focuses on development of offshore prospective storage resource assessment of the Upper Cretaceous section at the

Southeast Georgia Embayment (SGE; Figure 3.1) where the storage capacity in the Upper Cretaceous strata is estimated at around 9 GT (Almutairi et al., 2017).

This chapter of the research has several objectives with the goal of providing an exhaustive subsurface evaluation for CO₂ geologic storage of the Upper Cretaceous section within the SGE. The main objectives are to (1) discriminate strata by lithology, (2) extract porosity from seismic data, (3) understand the porosity and permeability regimes for the Upper Cretaceous strata within the SGE by implementing acoustic impedance inversion techniques, and (4) identify strata and units containing potential reservoirs and seals with the areal extent in Upper Cretaceous age. Several hypotheses were proposed to achieve the research objectives. These are: (1) Upper Cretaceous formations at the SGE have potential for at least 9 GT of CO₂ storage capacity, (2) the Upper Cretaceous potential reservoir is overlain by a low-permeability seal layer with sufficient depth for CO₂ sequestration, (3) layers with significant porosity and permeability are present and widely distributed in the Upper Cretaceous section of the SGE, and (4) multiples and noises were taken in consideration when data were processed since the inversion interprets all reflections in the seismic as geologic changes.

Supercritical conditions are required for CO₂ storage which means that the CO₂ is at its thermodynamic critical point (temperature exceeding 88.3⁰F (31.1⁰C) and pressures exceeding of 72.9 atmospheres; NETL, 2015). At depths of 2,625 ft (800 m) or greater, CO₂ can be sequestered underground as a supercritical fluid which has properties of both a gas and liquid (NETL, 2015). Liquid at reservoir conditions, such as good porosity and permeability, occupies a much smaller volume than the gaseous state at atmospheric conditions thus providing a more effective exploitation of underground storage space and

improves storage security (IEA, 2007; 2008). At sufficient depths, 2,625 - 8,200 ft. (800 - 2,500 m), CO₂ is more like a liquid than a gas and its density is close to the density of some crude oils. In this case, since the CO₂ is less dense than saline water and the buoyant forces will drive CO₂ upwards within the geologic formations that accumulates within a porous reservoir when a cap seal is reached (NETL, 2013). In this study area, the CO₂ geological storage options within the Upper and Lower Cretaceous strata are deep saline formations. The Upper Cretaceous strata can be qualified for CO₂ storage based on geological criteria that include: (1) sufficient reservoir porosity (more than 20% is preferable, and not less than 10%), (2) sufficient reservoir permeability, i.e. ~200 millidarcy (mD), (3) reservoir properties (reservoir, seal, areal extent, depth greater than 2,625 ft, and net reservoir thickness of 164 ft; Chadwick et al., 2008) (4) temperature, pressure, salinity, uniform stratigraphy, and seal integrity, (5) a trapping mechanism, (overlying caprock or seal) is essential to prevent CO₂ vertical migration into overlying freshwater aquifers, (6) cap-rock efficacy including lateral continuity, no leaky faults, and capillary entry pressure, and (7) cap-rock thickness (328 ft is preferable, not less than 65 ft) (Chadwick et al., 2008; Eiken et al., 2011).

3.2 Geologic Setting of the South Georgia Embayment

The offshore area of the Southeastern United States has a complex geology (Poag, 1978). The latest collisional event of Laurentia and Gondwana occurred at the end of the Paleozoic (Alleghenian Mountains). The continental rifting then began in the Early Mesozoic as part of the breakup of the supercontinent Pangea. Locally, this involved tectonic subsidence in restricted extensional basins followed by thermal subsidence along the Eastern North American margin (Dillon and Popenoe, 1988). Generally, stratigraphic

sequences on this passive margin are characterized by extensive lateral continuity and relatively minor structural disruption (Poag, 1985a). There is a regional unconformity under the post-rift sediments known as the “post rift unconformity” that cuts the entire region after rifting between Africa and North America ceased and marks the transition to wide-spread sediment deposition during the “drift” stage (Poag, 1985a). The oldest post-rift sediments are in Jurassic age and the product of rapid clastic sedimentation from erosion followed through a period of evaporite deposition and subsequent initiation of widespread shallow water carbonate deposition with some terrigenous input (Dillon and Popenoe, 1988). Geophysical and stratigraphic studies suggest that the Jurassic section thickness is at least 24,600 ft in the basins and thickens seawards (Dillon et al., 1979). The Cretaceous section in the north is characterized by more clastic sedimentation whereas more carbonate deposition in the south, forming a large carbonate platform over the Blake Plateau and offshore Florida (Scholle, 1979). In Upper Cretaceous, the Suwanee Strait provided clastic sedimentation to the Blake Plateau creating a distinct facies province change to the neighboring offshore Florida and Bahamas carbonate platforms. Strong paleo-currents controlled the sedimentation in large portions of the offshore region from the Upper Cretaceous to the Cenozoic. The Gulf Stream provides strong erosive power that eroded most of the Paleogene sediments on the Blake Plateau and prevented deposition off the Florida-Hatteras slope where it continues to the north along the shelf edge (Pinet and Popenoe, 1985). The major sedimentary deposits from north to south (Figure 3.1A) include the Carolina Trough, the Southeast Georgia Embayment (SEG), and the Blake Plateau Basin which ranges in sediment column thicknesses from 9,850 to 23,000 ft (Maher and Applin, 1971).

This chapter of research focuses on the Southeast Georgia Embayment (SGE) which is a broad depression plunging eastward from the Atlantic Coastal Plain (Figure 3.1A). It is a major structural feature of the Florida-Hatteras Shelf, and is considered a minor sedimentary geologic unit compared to the other sedimentary basins in the region (Book, 1982). The SGE represents a transitional zone between a predominantly clastic depositional province north of Cape Hatteras and a carbonate province which includes Florida and the Bahamas. Based on cores recovered from the COST GE-1 well (Figure 3.1B; Amato, 1978), Paleozoic rocks sit in the embayment at a depth of ~10,560 ft and are overlain by probable Jurassic non-marine clasts (rocks fragments), dolomites, coal, and anhydrite (Edgar, 1981). This sedimentary sequence continued throughout the Mesozoic until carbonate sedimentation took over in the Cretaceous. Sedimentation in the SGE is still likely ongoing today (Dillon et al., 1975; Book, 1982). The lithology in the COST GE-1 well has two main intervals: (1) the interval from depth 3,300 ft to 4,600 ft, includes Upper Cretaceous, Paleocene, and lower Eocene and consists of limestone and calcareous shales, and (2) the depth interval from 4,600 to 7,200 ft consists of limestone and dolomites interbedded with sandstones. Existing Carbonate-cemented, feldspathic, and glauconitic sandstones at a depth of 5,800 ft, indicate a major regression between the shallow-water restricted-shelf carbonates and the overlying fine-grained open-marine limestones. In more details, the depth interval from about 5,700 ft to 7,200 ft contains a varied shallow marine sequence of generally medium grained calcarenites, dolomite, and anhydrite with significant amounts of quartz sandstone, pyrite, and glauconite. Common rock types include oolites, fossiliferous calcarenites, dolomite, micrite, and anhydrite (Scholle, 1979).

3.3 Geophysical Data

The geophysical data used for this analysis include two-dimensional (2D) multichannel seismic reflection data collected on the Atlantic Margin in the late 1970's as part of geophysical and geological exploration of oil and gas prospects on the U.S. Outer Continental Shelf. The seismic data ID is E08-76 which were acquired by the Bureau of Ocean Energy Management (BOEM). In addition, there are seven exploratory wells with a variety of geophysical logs in our study area; (Figure 3.2). Three wells have the digital logs necessary to implement acoustic impedance inversion and conduct integration with seismic data (Table 3.1); the others have reports. All the depth references in this research are based on Kelly Bushing (KB).

3.4 Methodology and Data Analysis

Acoustic impedance (AI), a product of rock density and compressional velocity, can be used as an indicator of lithology and porosity, which are important for CO₂ storage assessment (Alshuhail et al., 2009; Veeken, 2007). It gives sub-surface geology image in more detailed than the conventional seismic section, because the reflectivity coefficient (RC) on the conventional seismic section captures the layer interfaces while the AI, a layer-based property, focuses on the layers themselves and what is inside (Schlumberger, 2017). However, extracting acoustic impedance properties from seismic data requires seismic inversion which implies converting seismic reflection amplitudes into impedance profiles (Alshuhail et al., 2009; CGG, 2016). This process involves removing the band-pass filter (wavelet) imposed by seismic acquisition and processing.

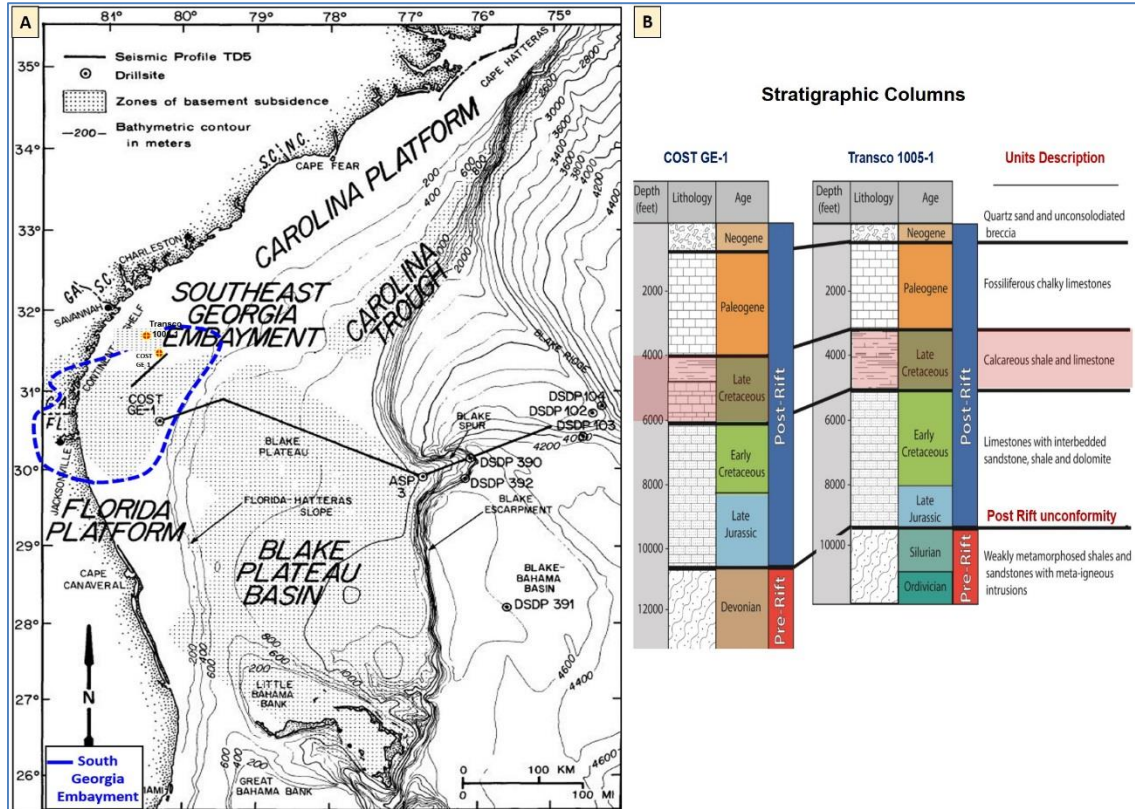


Figure 3.1: [A] Location map showing the main regional geologic provinces within the offshore areas considered for potential storage of CO₂, modified from (Smyth et al., 2008; Dillon, et al., 1976). [B] stratigraphic columns and lithology description at COST GE-1 and Transco 1005-1 wells, located at Southeast Georgia Embayment, modified from (Pollack, 2014).

Table 3.1: Wells used for acoustic impedance inversions and formation evaluations.

Well name	Long. X	Lat. Y	Water Depth (ft)	KB (ft)	TD (ft)	TVD (ft)
COST GE-1	-80.2997	30.619	136	99	13254	13254
Exxon 564-1	-80.25583	30.4397	145	81	12863	12863
Transco 1005-1	-80.2439	30.9928	134	101	11635	11635

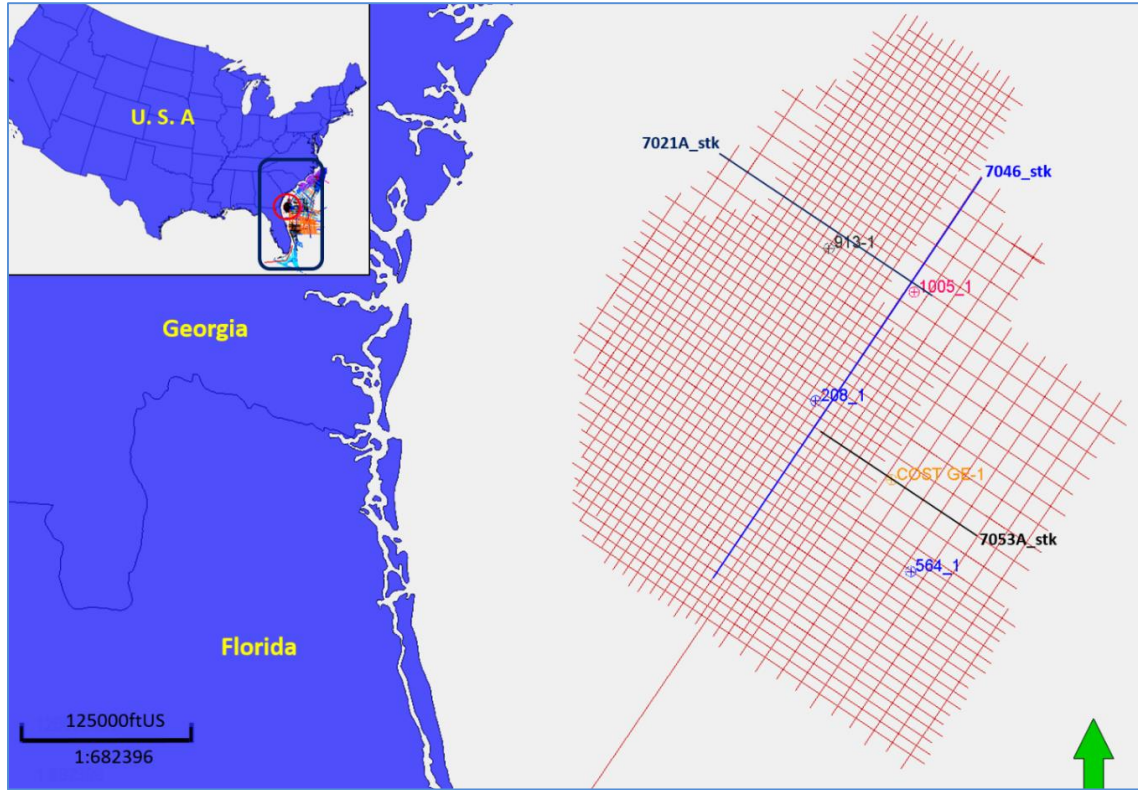


Figure 3.2: Location map of seismic survey and exploratory wells within the Southeast Georgia Embayment (SGE). Seismic lines used in the acoustic inversion analysis are bold.

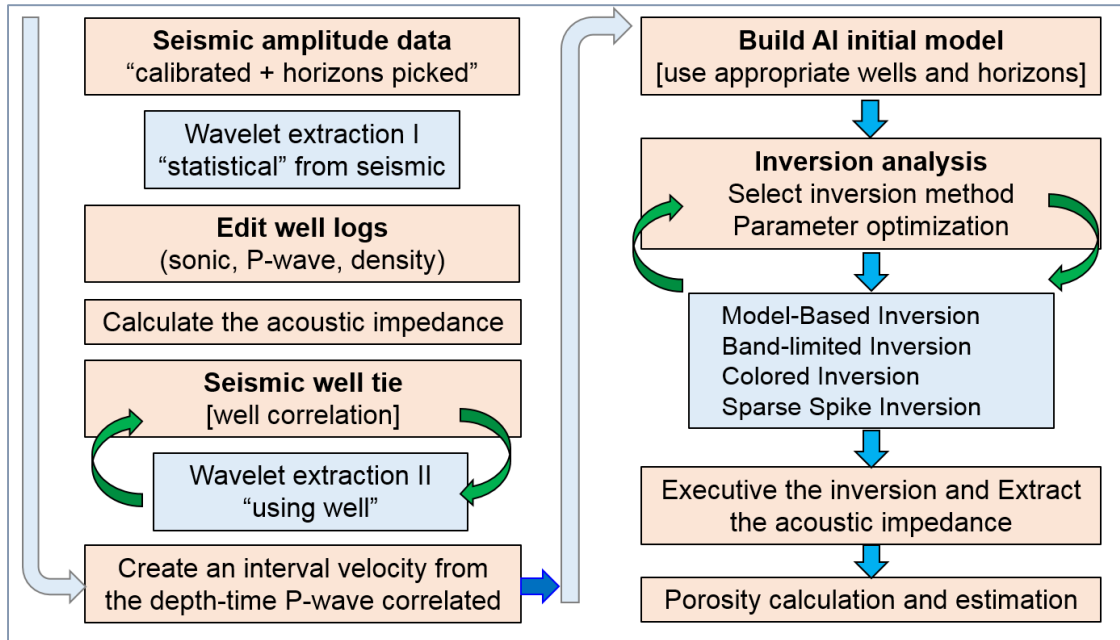


Figure 3.3: Flowchart outlining the seismic inversion workflow to extract the acoustic impedance.

In addition, it includes estimation of a background impedance model (low-frequency model), which incorporates well log data (P-wave and density) and interpreted horizons. Also, involves wavelet extraction and inversion analysis by synthetic seismogram and finally, seismic inversion (Vukadin and Brnada, 2015; CGG, 2016), (Figure 3.3). In this study, a series of post-stack inversions were applied to the data in order to provide a most accurate acoustic impedance model. They include Colored, Sparse-Spike, Band-Limited, and Model-Based Inversion Figure 3.7 shows a comparison of all different inversions results.

3.4.1 Model-Based Inversion

Model-Based Inversion (MBI) starts with the convolutional theory which states that the wavelet can be convolved with the Earth's reflectivity series to generate the seismic trace after addition of noise. MBI uses well control and seismic data (interpreted horizons) to build an initial low-frequency estimated model of the acoustic impedance distribution (Maurya and Sarkar, 2016). Using an estimate of the source wavelet, the model response in the form of synthetic seismograms is then compared to the actual seismic traces, usually by means of cross correlation. This process is iterated several times until the model response error falls within the acceptable range that is determined by the difference between the synthetic traces calculated from the inversion and the original seismic composite trace (Lee, 2013; CGG, 2016). The MBI is implemented through the following workflow: (1) select a proper seismic line and extract the input wavelet (a critical key for a successful post stack inversion result), (2) select and correlate the well using the interpreted horizons, (3) build the initial model and apply inversion analysis, and (4) apply the inversion result to the multi 2D seismic lines.

3.4.1.1 Extract Wavelets

Two main steps were used to extract the proper wavelet:

- a) Extract a Statistical Wavelet: statistical wavelet (zero phase) is extracted using a nearby seismic line (Figure 3.4 A). This involves correlating the initial synthetic seismogram with the seismic trace until getting a low correlation error percent. The algorithm extracts the wavelet amplitude spectrum by analyzing the autocorrelation of a group of traces within a selected time window that ranges from 400 to 1,500 ms. The required parameters for extracting the statistical wavelet were specified as: sample rate (4 ms), wavelet length (200 ms), phase type: constant (zero phase), Taper length (25 ms). After creating the depth-time relationship, the sonic and density logs were used to create the reflectivity series which was convolved with the wavelet to generate the seismic synthetic trace from the well logs (Lee, 2013; CGG, 2016; Maurya and Sarkar, 2016).
- b) Extract a Wavelet from Wells: both available wells and near seismic data are used to extract another wavelet to correct the phase (Figure 3.4 B). It extracts the wavelets by finding an operator which is convolved with reflectivity from the well. This extracts the actual wavelet phase from the data, but it is very sensitive to the correlation quality between well logs and seismic data (Lee, 2013; CGG, 2016).

3.4.1.2 Generate Synthetic Seismogram

The seismic forward modeling involves convolving the seismic reflectivity series $R(t)$ calculated from the P-wave velocity and density well logs with the wavelet $W(t)$ extracted from the seismic data at the well location (Figure 3.4 B) to generate a synthetic seismic trace $S(t)$ that is subsequently correlated with the real seismic trace (Figure 5).

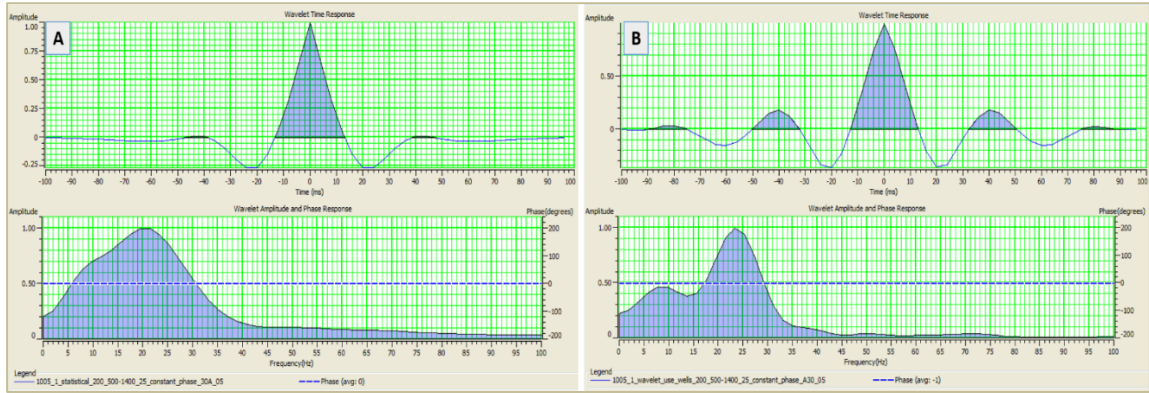


Figure 3.4: Extract statistical wavelets. [A] using seismic line # 7021A; and [B] using the 1005-1 well.

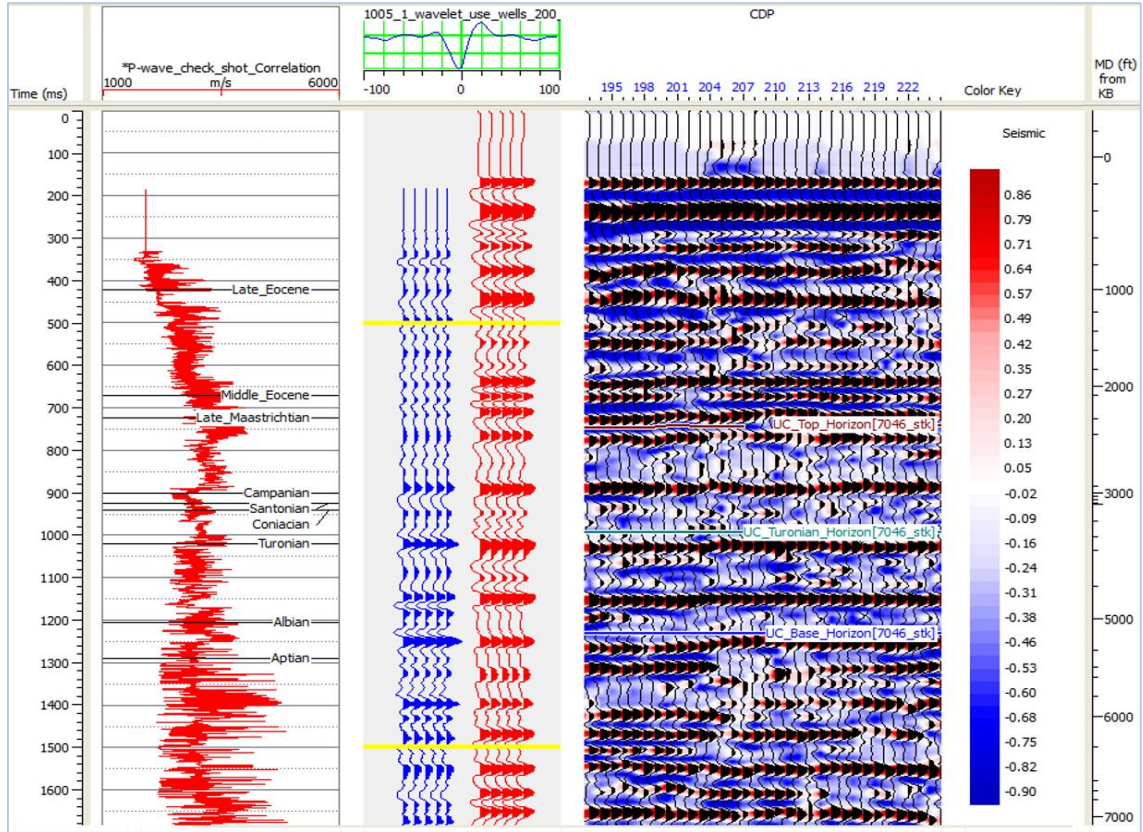


Figure 3.5: Seismic well correlation, achieved by matching events on the synthetic with the same events on seismic trace at the Transco 1005-1 well.

This procedure assumes that the well logs are accurate and the velocity varies only with depth. It is assumed that the geological structure is horizontal (Liner, 2004).

$$S(t) = R(t) * W(t)$$

3.4.1.3 Seismic-Well Correlation

It is important to relate horizon tops identified in the wells with specific reflectors on the seismic data in order to provide acoustic impedance values for the potential reservoir and seal intervals in order to estimate porosities. Therefore, seismic-well tie analysis has been conducted to compare well logs (measured in depth units), with seismic data (measured in time units), by creating a time depth relationship using the sonic log and the check shots to improve and adapt the depth-time conversion. The correlation applied included (1) using key well tops to match peak–peak or trough–trough, (2) using bulk shift to tie synthetic to seismic or variable time shift to move and stretch two or more horizons, and (3) using the alignment points to make small adjustments between the synthetic and real seismic data (Cubizolle, et al., 2015; Figure 3.5).

3.4.1.4 Build Initial Model and Inversion Analysis

In more detail, the initial model of impedance is generated by using the P-impedance logs calculated from the sonic and density logs from the well log with a low-pass filter. This filter passes all frequencies up to 10Hz, filters all frequencies above 15Hz, and interpolates the filter between those limits (Lee, 2013; CGG, 2016). Then, generate a 2D impedance model by interpolating the impedance at the well location using interpreted horizons to guide the interpolation (Figure 3.6 A). The extrapolation at the top and bottom of the well log curve depends on compaction trends in the well. The program uses a least square fit to determine a trend to use for the top and bottom of the well. However, MBI

analysis was performed initially at the location of the 1005-1 and COST GE-1 wells to QC the inversion results and optimize the inversion parameters properly. It runs on the target window that ranges from 400 to 1,600 ms and evaluates the efficacy of the inversion by comparing the impedance at the well with the impedance inverted from the seismic data for each initial model (Alshuhail, 2009; Lee, 2013; CGG, 2016; Maurya and Sarkar, 2016). Figure (3.6 B) shows a reasonable match between the inverted acoustic impedance (in red) and the computed impedance from the well (in blue). The black curve indicates the low frequency impedance extracted from the acoustic impedance log. The synthetic traces calculated from this inversion (in red) followed by the original seismic composite trace (in black, Figure 3.6 B). The last track represents the error traces or the difference between the two previous results (a low correlation error percent).

3.4.2 Porosity Analysis

Porosity and permeability distribution versus depth are critical factors to assess the Upper Cretaceous strata for CO₂ storage. Here, porosity is calculated at the wells, extrapolated with QC to the available core data and extracted from the acoustic impedance as discussed below.

3.4.2.1 Using Density and Neutron Logs

Density logs provide a continuous record of the formation's bulk density, which is a function of formation porosity, fluid content in the pore spaces, and matrix density (Asquith et al., 2004). It is commonly used to calculate porosity. However, the neutron log provides fluid-filled porosity and measures hydrogen concentration in a formation. Although sonic porosity logs are still used, the two predominant porosity measurements are density porosity and neutron porosity. Density tools emit medium-energy rays into a

borehole wall. The gamma rays collide with electrons in the formation, lose energy and scatter after successive collisions. The number of collisions is related to the number of electrons per unit volume, also called the electron density. The electron density for most minerals and fluids encountered in oil and gas wells is directly proportional to their bulk density, ρ_{bulk} . The bulk density measured by tools (ρ_{log}) result from the combined effects of the fluid (porosity) and the rock (matrix) and is used to compute density porosity ($\phi_{density}$) (Smithson, 2012). Using density and Neutron logs (CGG, 2016), total porosities were calculated at COST GE-1, Exxon 564-1 and Transco 1005-1 wells, (Figure 3.8), in two steps:

i. Using Density Porosity

$$\phi_{den} = \frac{\rho_{matrix} - \rho_{bulk}}{\rho_{matrix} - \rho_{fluid}} \quad (\text{Serra, 1984})$$

Here, formation bulk density (ρ_{bulk}) is a function of matrix density (ρ_{ma}), porosity, and formation fluid density (ρ_f). The estimated matrix density is 2.65 g/cc for sandstone, 2.71 g/cc for limestone, and 2.87 g/cc for dolomite, and the fluid density is 1.09 g/cc for brine (Smithson, 2012).

ii. Using Neutron and Density:

$$ND_{\phi} = \sqrt{\frac{(N_{\phi})^2 + (\phi_{den})^2}{2}} \quad (\text{Gaymard and Poupon, 1968})$$

Here ND_{ϕ} is neutron density porosity, N_{ϕ} is neutron porosity, and ϕ_{den} is density porosity.

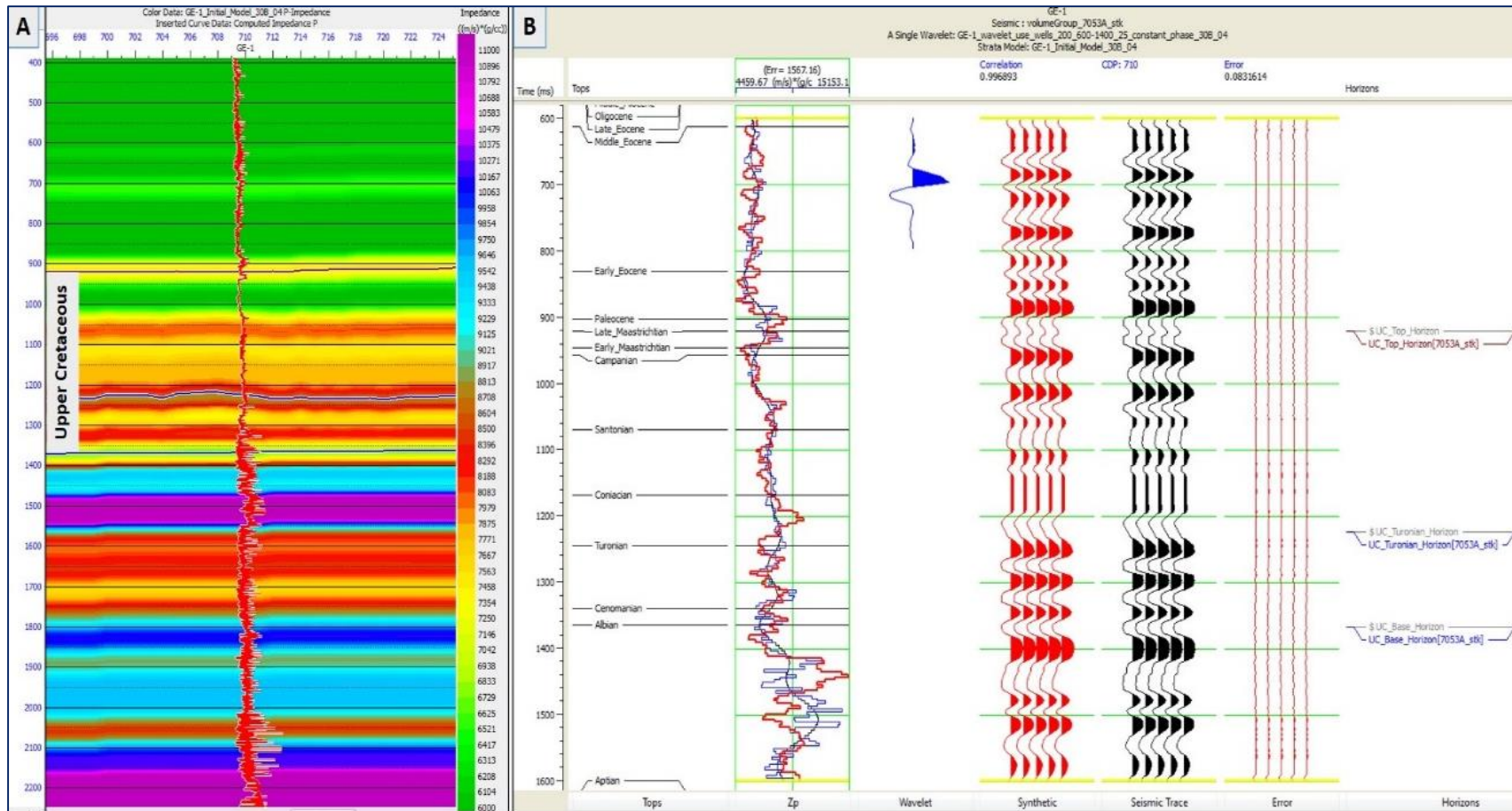


Figure 3.6: [A] Initial model for the acoustic impedance, and [B] post stack seismic inversion analysis results at the COST GE-1 well.

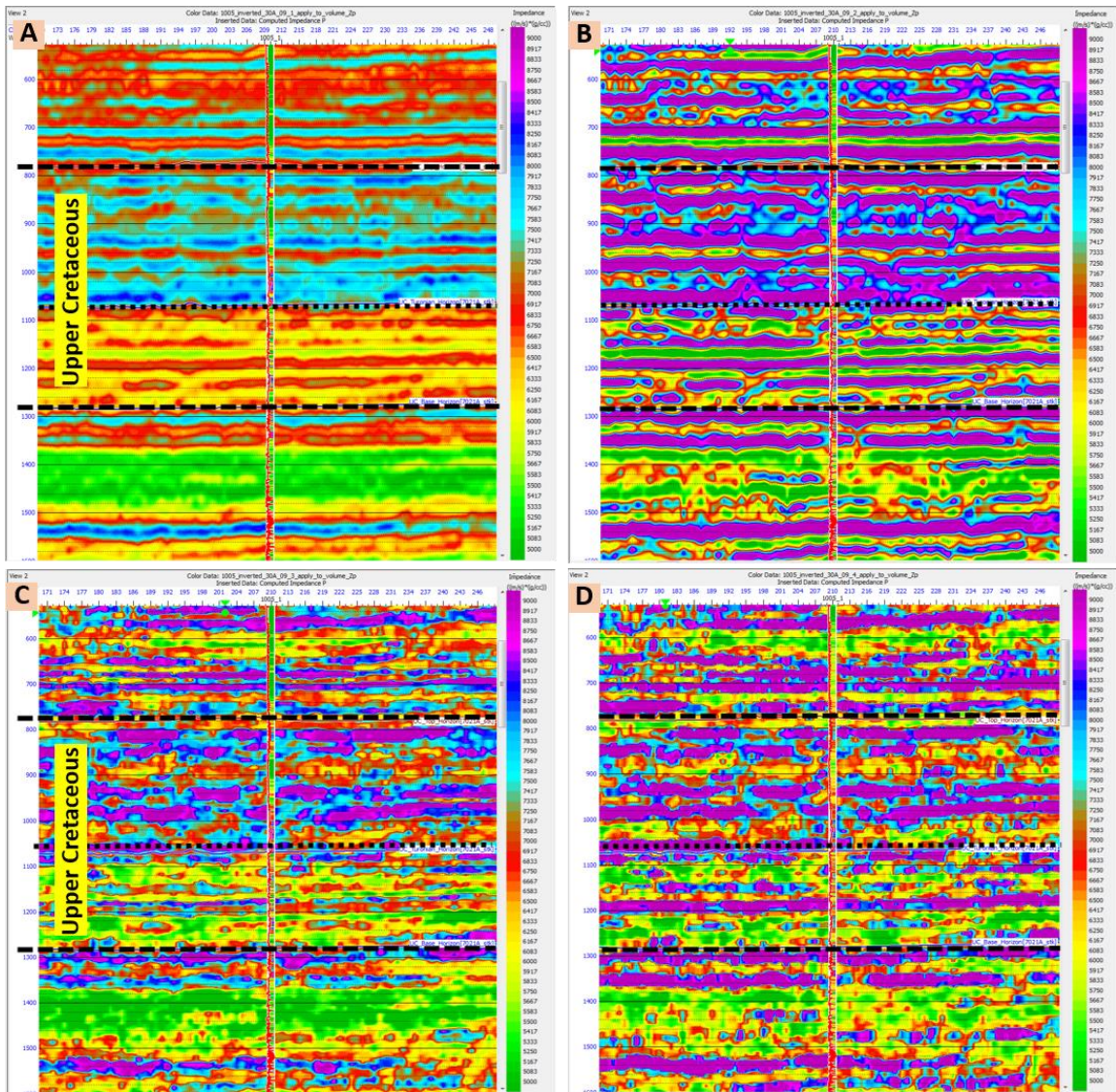


Figure 3.7: Comparison results of different post stack inversions that cover the Upper Cretaceous strata using seismic line # 7021A and the Transco 1005-1 well. [A] bandlimited inversion, [B] colored inversion, [C] linear programming sparse spike, and [D] maximum likelihood sparse spike.

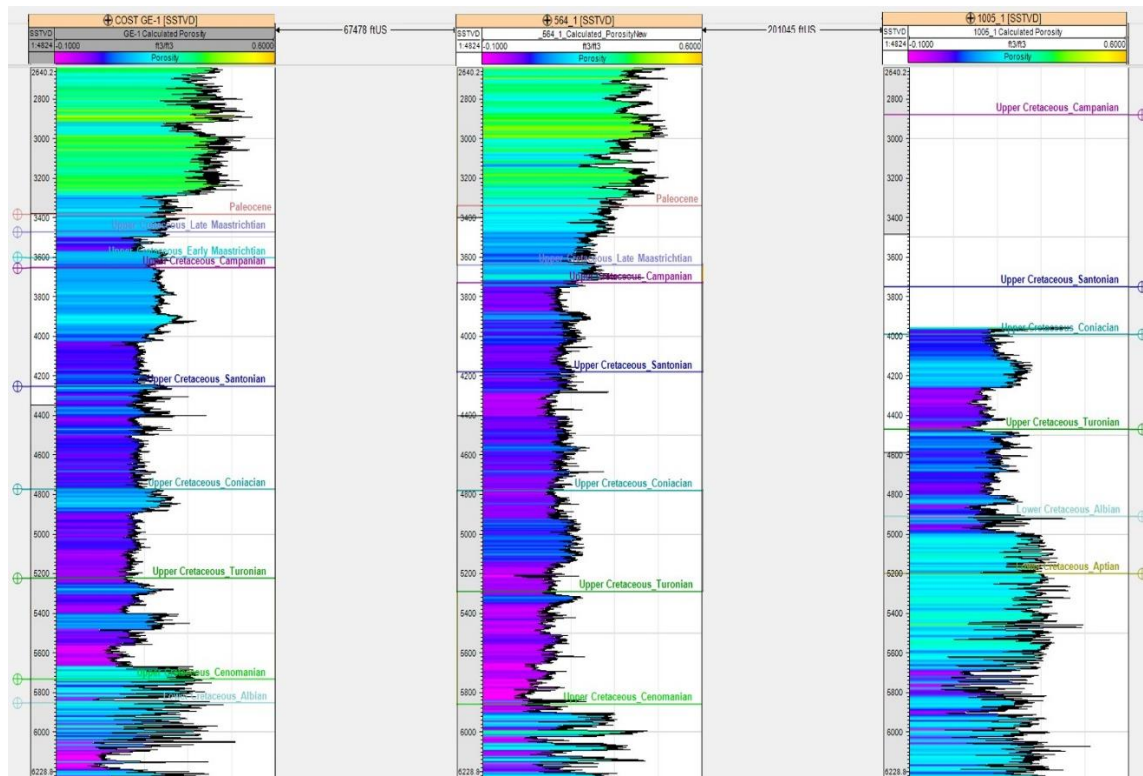


Figure 3.8: Calculated porosity logs at COST GE-1, Exxon 564-1 and Transco 1005-1 wells.

3.4.2.2 Porosity Extrapolation

Another way to estimate porosity distribution is the derivative from simultaneous inversion. In this process, inversion property builder tools were used to provide a porosity model, (Figure 3.9 A and B) by involving the porosity log, the top and the base of the horizons and the acoustic impedance as a guide model for geometry (Schlumberger, 2016; 2017). Since well logs provide critical information about geologic formations such as lithology discrimination and stratigraphy correlation, the gamma-ray (GR) log measures the natural radioactivity in different rocks and is overlaying the porosity section (Figure 3.9 A) (thick line) to determine the shale strata interval. Shale has high radioactive elements which elevate the gamma-ray values (Asquith, 2004). However, the porosity measured from the core at the GE-1 well is matching the inverted 2D porosity section (Figure 3.9 A and B) which is important for quality control.

3.4.3 Acoustic Impedance Inversion

Acoustic impedance (AI) inversion techniques were used to estimate porosity from seismic data. It indicates that the Upper Cretaceous strata at Southeast Georgia Embayment (SGE) has two intervals at the Transco 1005-1 well. First interval represents an impermeable seal which is the strata between the top of Upper Cretaceous and the Turonian surface that gives high impedance (low porosity).

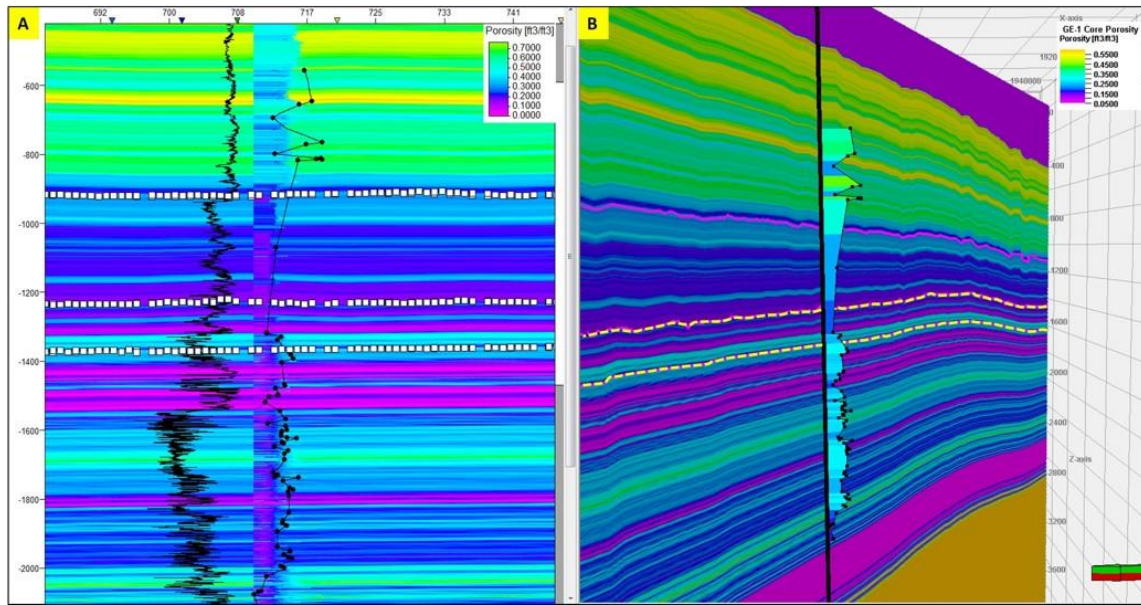


Figure 3.9: Extrapolated porosity using inversion property builder at the well GE-1.

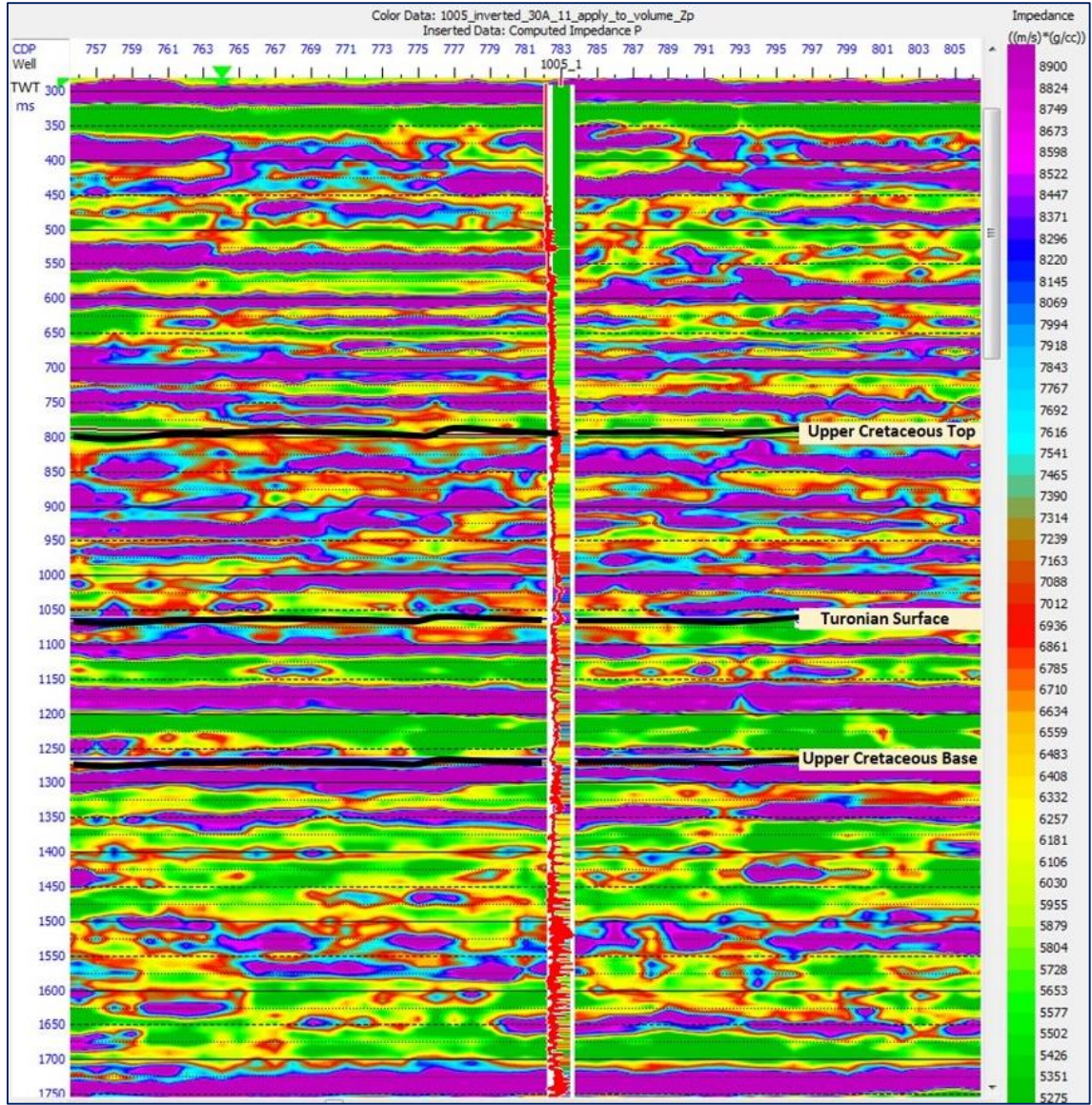


Figure 3.10: Acoustic impedance at the Transco 1005-1 well.

The second strata represent the interval between the Turonian surface and the base of the Upper Cretaceous (Figure 3.10). It is suggested to be the significant reservoirs for CO₂ storage (Almutairi et al., 2017), since it has two main intervals with low impedance values which is a reflection of high porosity. However, these results are similar to the impedance inversion values in a different well (COST GE-1) which has two strata intervals within the potential reservoir (Figures 3.11 and 3.12). In addition, the lowest impedance values are located where the highest porosity is and vice versa. It is correlated with the core's porosity at different wells for quality control. Therefore, the acoustic impedance inversion is a successful tool to discriminate lithology and estimate porosity when the proper workflow and analysis are implemented.

3.4.4 Porosity and Acoustic Impedance Relationship

Cross plotting is an effective method to link the acoustic impedance with porosities which were calculated from either density and neutron logs or measured from the well core (Kumar, 2016). Figures (3.13 and 3.14) show a linear regression between acoustic impedance and porosity at the COST GE-1 and Transco 1005-1 wells. This reasonable correlation between porosity and acoustic impedance from logs and core data in the Upper Cretaceous strata indicate a robust transform function for application to seismic inversion results. It helps to understand the porosity regimes which is a critical key for CO₂ storage assessment. Also, the inverted impedance is a good indicator for porosity changes and gives confidence when indicating porosities from impedance. In addition, it is a viability study to know whether porosity can be extracted from the impedance or not.

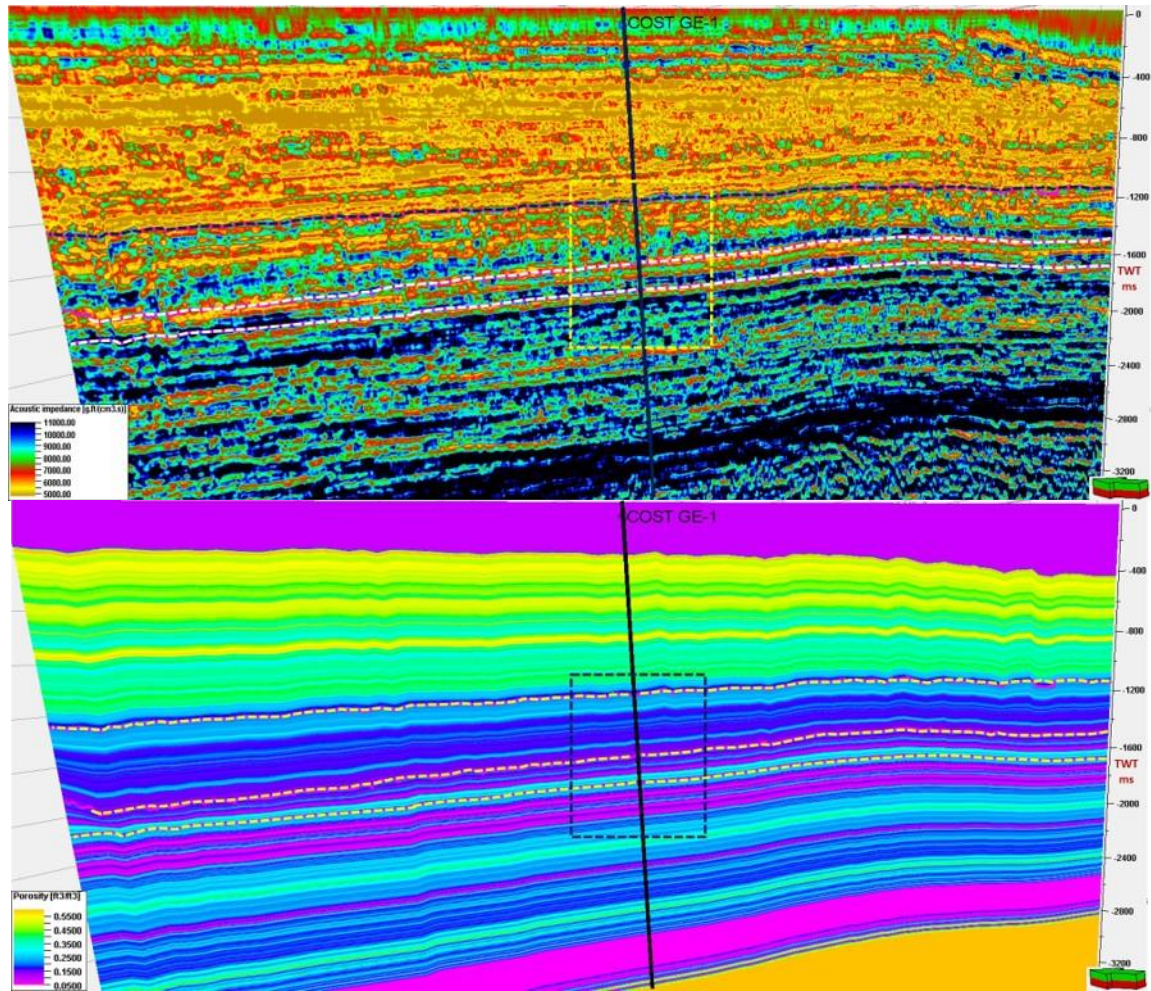


Figure 3.11: 3D view of the acoustic impedance (top) and the extrapolated porosity (bottom), using seismic lines # 7053A across the COST GE-1 well.

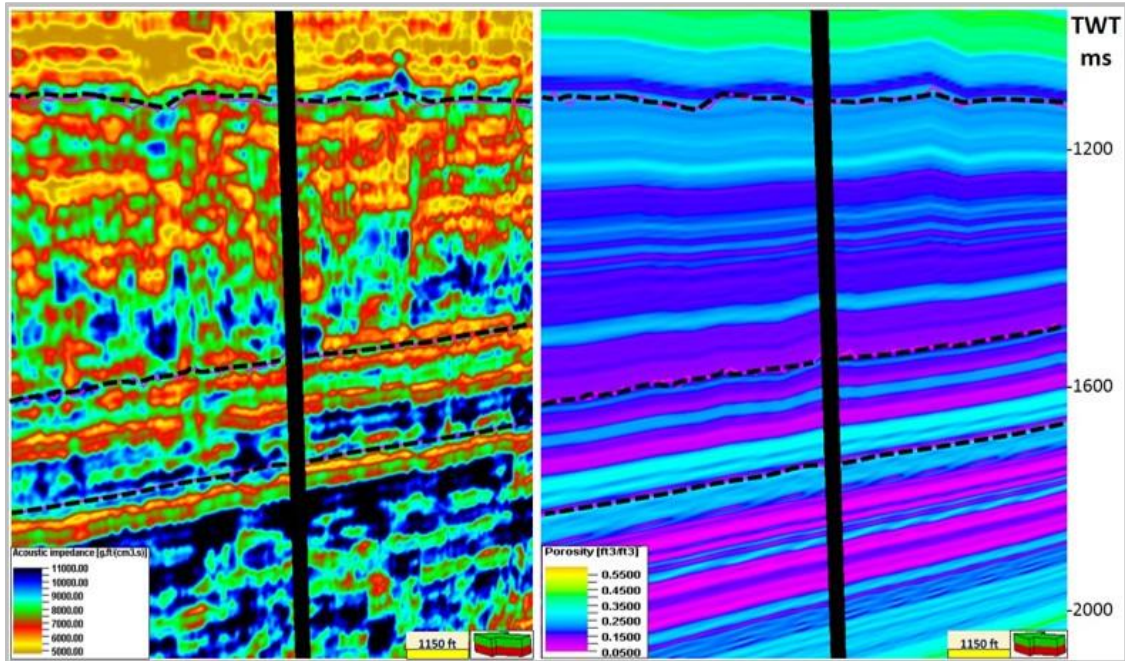


Figure 3.12: Zooming in for the acoustic impedance and the extrapolated porosity (see Fig. 3.11).

Figure (3.13 A) gives high porosities and low impedance in the lower strata of the Upper Cretaceous interval which is an indication of a potential porous reservoir overlaid by an impermeable seal interval which has high impedance values. Based on this relationship and the stratigraphic analysis, it appears that the most suitable reservoir strata for CO₂ storage are within restricted shelf carbonates with high primary and secondary porosity and good permeability occurring between 5,700 and 7,200 ft (Scholle, 1979). It has low to moderate acoustic impedance values which reflect high to moderate porosity values. In addition, it has the best permeability encountered below 1,000 ft in the COST GE-1 well (Scholle, 1979; Almutairi et al., 2017). This depth interval (5,700 and 7,200 ft), dominated by sandstone, shows porosities that vary widely and unsystematically with depth from 25% to 30% (probably due to variation in diagenesis), and the permeability is as high as 4,000 mD. Although characterized by good porosity and low impedance, the fine-grained limestone above 5,700 ft is likely too impermeable to make the strata interval a candidate for reservoir rocks, unless they are widely fractured or contain undetected permeable horizons. Data suggest that the rocks between 1,000 to 5,700 ft have a permeability of 3 mD or less (Scholle, 1979) which gives low acoustic impedance values (Figure 3.13 A). The porosity and acoustic impedance relationships for wells COST GE-1 and Transco 1005-1 are compatible with the core data where high porosities strata have low impedance values. At the Transco 1005-1 well, the acoustic impedance and porosity relationships were tested at different intervals to get the best correlation which is 0.68 at the interval between 4,046 to 6,000 ft. (Figure 3.14).

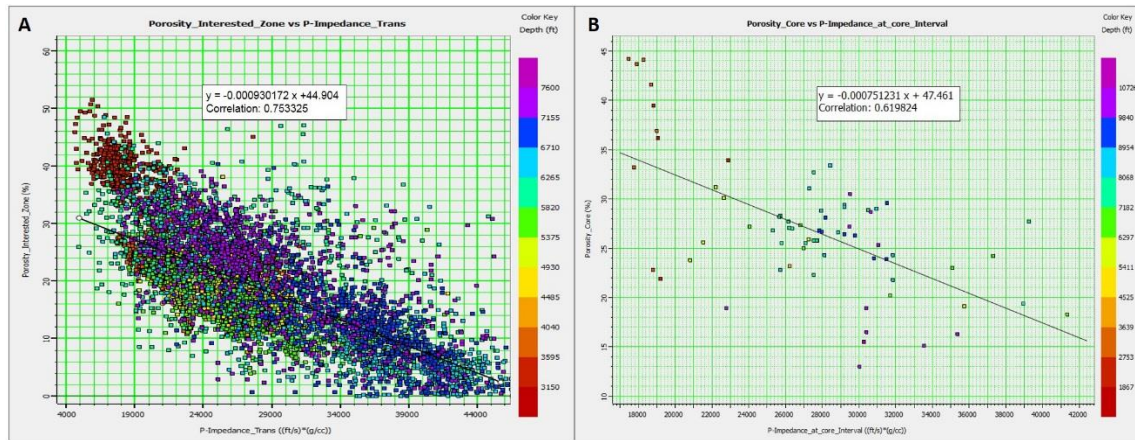


Figure 3.13: [A] Acoustic impedance relationship with calculated porosity at an interested zone [3,150-7,600] ft of the COST GE-1 well where the correlation coefficient is (0.75), however, [B] is the acoustic impedance and measured porosity relationship for the entire well, where the correlation coefficient is (0.62).

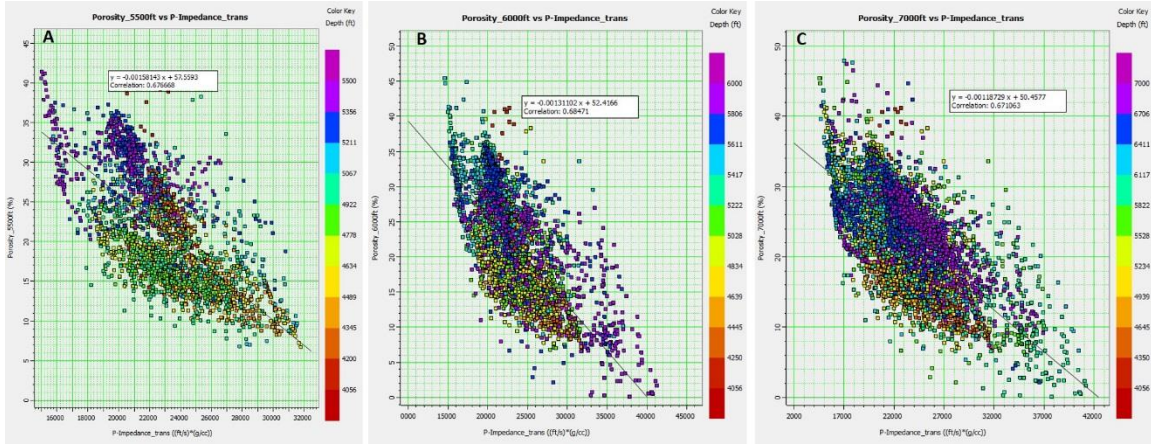


Figure 3.14: Acoustic impedance versus calculated porosities from density and neutron logs at three different depth intervals at the Transco 1005-1 well, where the best correlation coefficient achieved is 0.6847 at the interval between 4,046 to 6,000 ft.

3.4.5 Extract Porosity from Acoustic Impedance

Using the porosity and acoustic impedance relationship, the porosity distribution is extracted using linear regression with the better correlation (Dolberg and Helgesen, 2000). Therefore, seismic data predicts porosity with a maximum correlation (R) of (0.75). Figures (3.15) and (3.16) show the estimated porosity using the relationship between acoustic impedance and porosity at the GE-1 and Transco 1005-1 wells respectively.

3.4.6 Porosity and Permeability Relationship

Understanding porosity and permeability spatial distributions are critical for characterizing a potential CO₂ reservoir and its seal. Values calculated from well logs show an irregular pattern perhaps due to cementation and facies changes. COST GE-1 well data, for instance, shows a clear decrease of porosity with depth down to ~ 5,700 ft. Plotting the porosity versus depth for the upper portion of the COST GE-1 well, (Figure 3.17 A), shows that the fine-grained carbonates appear to behave similarly to chalks with respect to porosity modification with depth. Some of these carbonates are not strictly true chalks because of their argillaceous matrix. The porosity and permeability depth relationship for the upper 5,700 ft of the COST GE-1 well indicates that Upper Cretaceous section has a porosity range of 12 % to 23 % from 3,500 ft to about 5,500 ft; and the approximate matrix permeability is in the range of 0.15 to 0.6 mD. Porosities and permeabilities from conventional and sidewall cores at the COST GE-1 well show that very high porosities (25 to 40%) are encountered in the Cenozoic age chalks in the 1,000 to 3,000 ft depth interval, and the corresponding permeabilities for these fine-grained limestones are predictably low (Amato and Bebout, 1978).

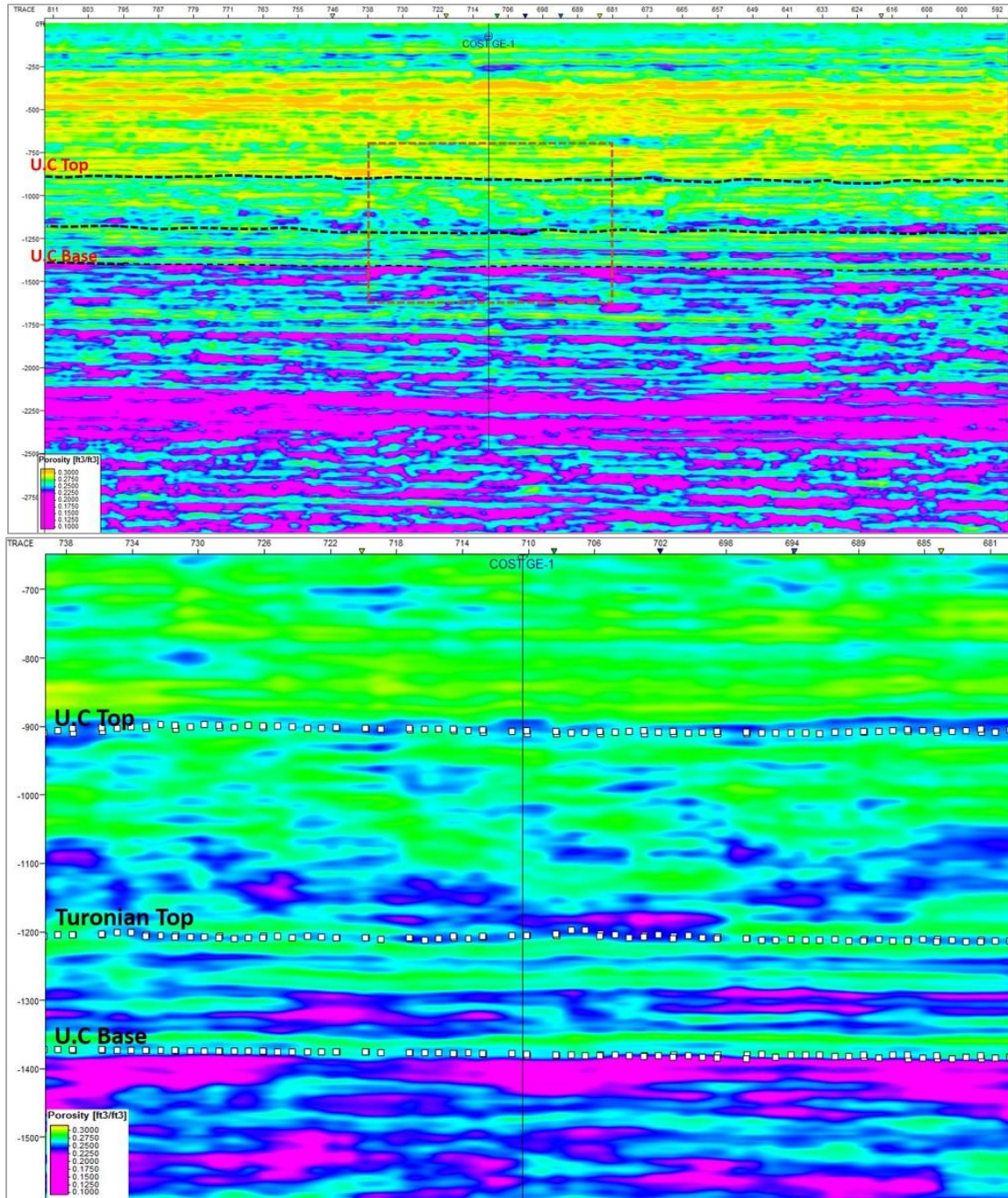


Figure 3.15: Extracted Porosity from the acoustic impedance at the GE-1 well using the linear regression relationship of: $[\text{Porosity} = (-0.0018164 \cdot \text{AI}) + 73.137]$, where the correlation coefficient is 0.75.

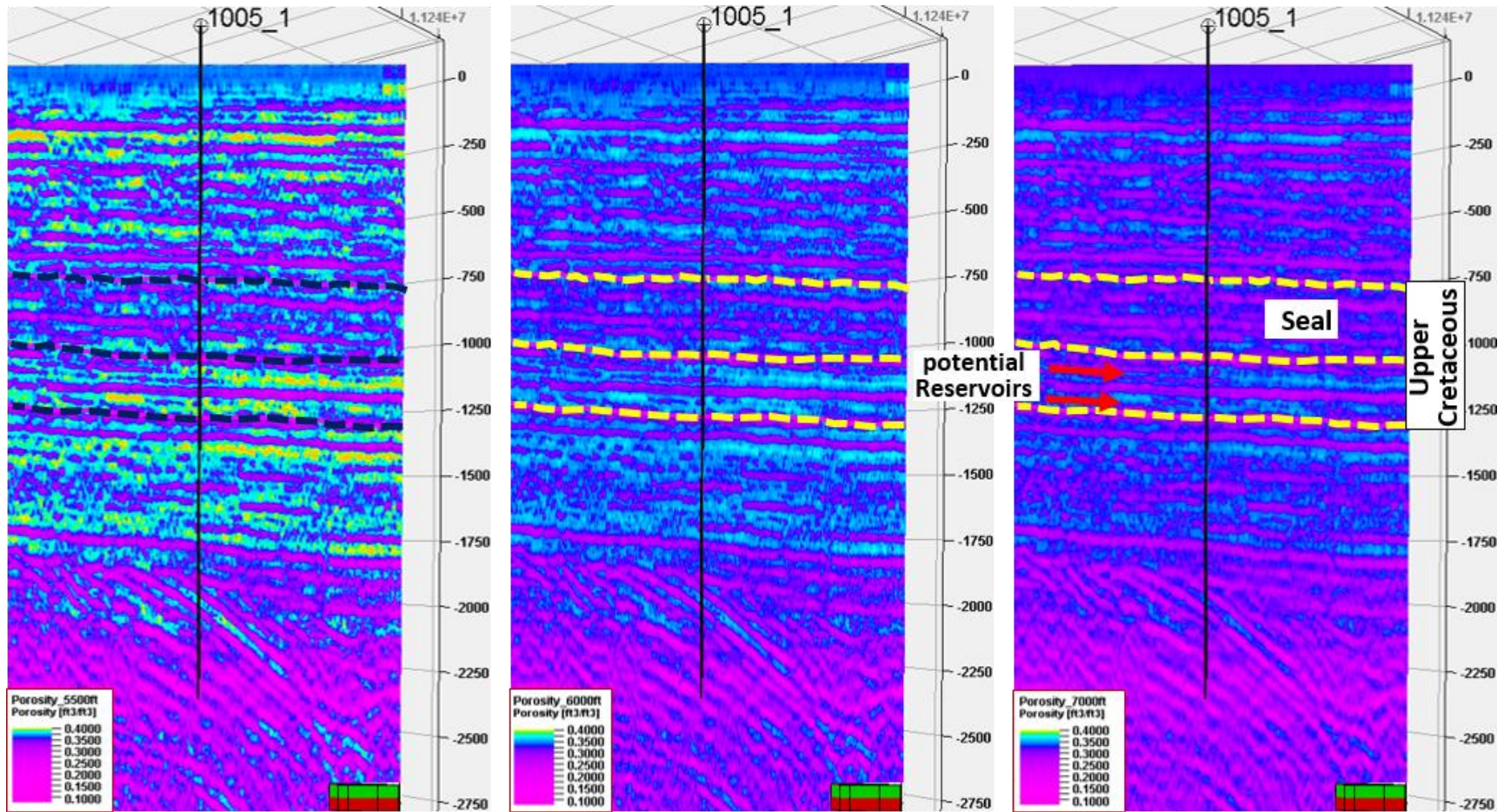


Figure 3.16: Extracted porosity from the acoustic impedance at three different intervals at the Transco 1005-1 well which discriminates two strata within the potential reservoir intervals at Upper Cretaceous.

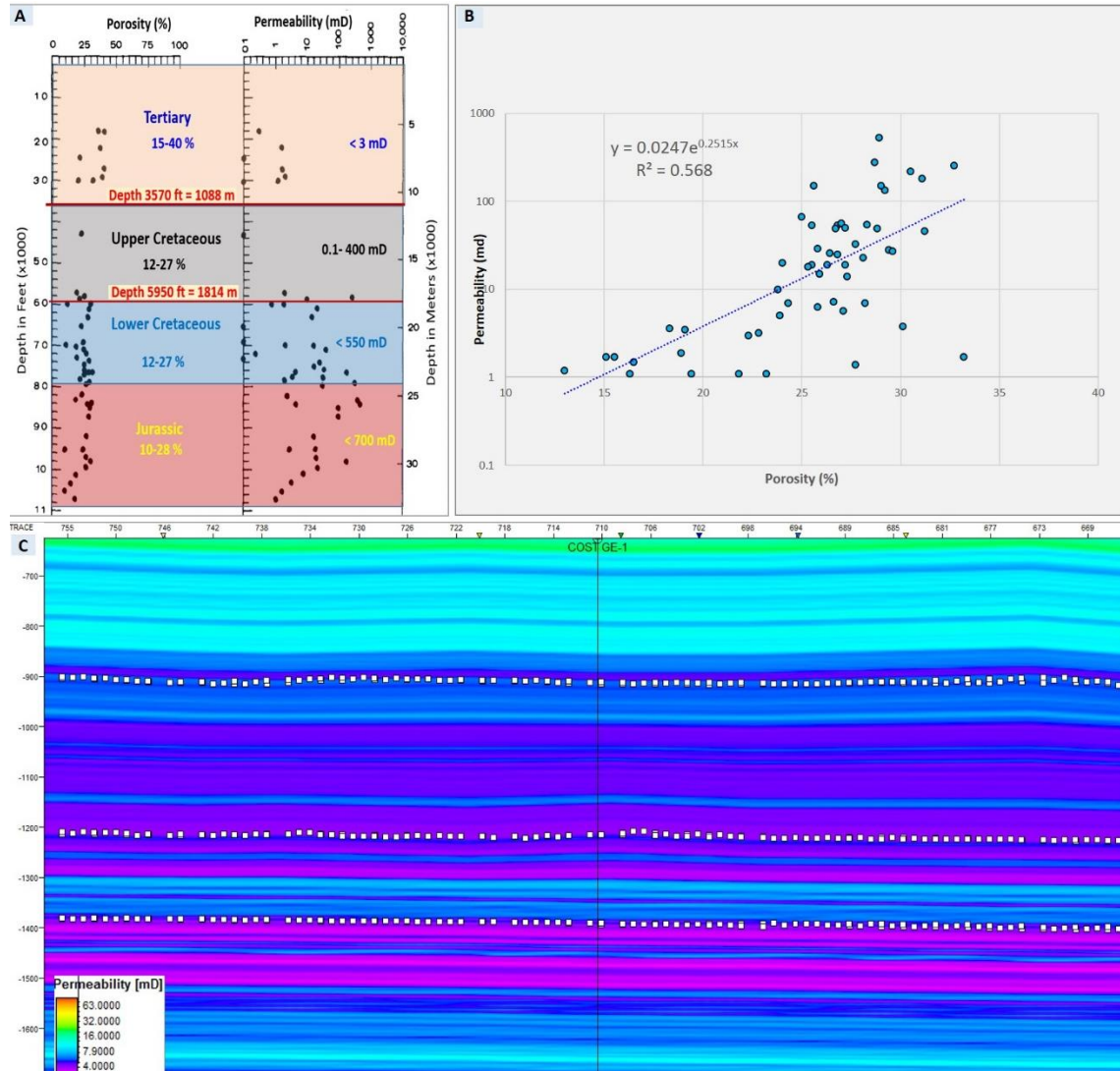


Figure 3.17: Porosity and permeability relationship at the COST GE-1 well: [A] values measured on conventional and sidewall cores as a function of depth (Amato and Bebout, 1978; Almutairi et al., 2017); [B] cross plotting core porosities versus core permeabilities for the entire well, data (from Scholle, 1979). [C] permeability distribution using the core's porosities and permeability relationship.

However, the lower part of the Upper Cretaceous interval (5,500 ft) has porosity of 20-35% and high permeability (450 mD) which makes it a candidate for a reservoir rock since it is capped by thick low permeability strata. Figure 3.17 (B) shows the core's porosity and permeability relationship as a function of depth. This relationship supports the previous study conducted by Almutairi et al. (2017) proposed that the Upper Cretaceous strata has two significant potential storage reservoirs for CO₂ including limestones with significant interbedded sandstone, shale and dolomite (Scholle, 1979). These strata are sealed by thick sediments of mainly shale interbedded with limestone (Figure 3.18 C).

The cross plotting relationship of porosity against permeability and acoustic impedance provides more evidence that the best two potential reservoirs are located in the lower part of the Upper Cretaceous section with high values of primary and secondary porosity, low acoustic impedance, and best permeability. The first potential reservoir is between 5,320 to 5,600 ft, which is sealed by about 725 ft. thick shale. The second between 5,760 to 5,950 ft, which is sealed by 160 ft thick shale. However, permeability distribution is estimated using the regression relationship between the core's porosity and permeability (Nelson, 1996; Gilles, 2000). The equation of the least square exponential fit was used to predict the permeability distribution as a function of porosity that was extracted previously from the acoustic impedance. Figure 3.17 (C) shows the estimated permeability using the estimated porosity from the acoustic impedance of seismic line # 7053A and the COST GE-1 well data, as an example.

$$\text{Permeability} = 0.0247e^{0.2515 x}$$

where the correlation coefficient $R^2 = 0.568$, and x is the estimated porosity.

3.5 Structure Maps and Properties

Significant markers in the Upper Cretaceous section were identified for potential reservoirs and seals within the SGE. The main potential units were selected based on paleontological data, depths versus geologic series or stage. These units are (1) Maastrichtian, representing the top of Upper Cretaceous (Figure 2.7 A), (2) Turonian, (Figure 2.7 B) and (3) top Albian, representing the base of Upper Cretaceous, (Figure 2.7 C) (Amato and Bebout, 1978; Almutairi et al., 2017). Since SGE has conformable deposition, lateral facies changes may be of greater interest in this study area than in other basins along the Atlantic offshore margin (Scholle, 1979). Therefore, acoustic impedance inversion conducted for providing more detail on the critical properties such porosity and permeability, leads to more clear lithology discrimination for the potential reservoir and seal. However, CO₂ sequestration requires reservoir and associated seal with minimum depth and thickness (NETL, 2015; IEA, 2007; 2008). The depth to the top of Upper Cretaceous strata varies approximately from 3,000 ft to 4,500 ft at the SGE. The prospective reservoir, strata interval between the Turonian strata and the base of Upper Cretaceous, has a depth range from 4,000 ft to 7,000 ft and a thickness from approximately 250 ft to 1,200 ft (Figure 2.8 A). Nevertheless, the sediment column between the top of the Upper Cretaceous and the Turonian strata, mostly shales with low permeability, would serve as a thick (800 to 2,600 ft) seal (Almutairi et al., 2017; Figure 2.8 B). Therefore, such depths and thicknesses are suitable for CO₂ sequestration. Since geologic CO₂ sequestration requires suitable porosities and permeabilities for the reservoir and the seal, the relationship between acoustic impedance and porosity cross-plotted with permeability indicates two main reservoirs capped by impermeable strata (Figure 3.18):

The first potential reservoir, located at depths between 5,400 to 5,580 ft, and composed of siderite, some pyrite quartz, limestone, with high porosity (17-23%) and high permeability (3.5 to 447 mD) are encountered. It is overlain by thick seal layers, located at depths between 4,400 to 5,400 ft, composed of shale, fine bedding, and has porosity of 23.5% and low permeability (0.1 mD).

The second potential reservoir which is composed of sandstone, quartzose silt, dolomite loose sand, coal, siltsone, located at depth 5720 to 5950 ft. The estimated porosity is (19 to 30.1%) and the permeability is between 3.5 to 447 mD, (Scholle, 1979; Almutairi et al., 2017). However, it capped by seal strata, composed of calcareous shale, fine-med silt, and biomicrite, and located at depth range of 5,580 to 5,720 ft. Its porosity is 12% and has less permeable clayey sequence.

3.6 Discussions

This study allowed us to distinguish lithology strata, extract porosity from seismic data, and understand porosity and permeability regimes for the potential reservoirs and seals within Upper Cretaceous strata at the SGE by employing different acoustic impedance inversion techniques and providing the reliable workflow of seismic inversion. This workflow can be applied to future CO₂ storage resource assessments at the U.S. Outer Continental Shelf.

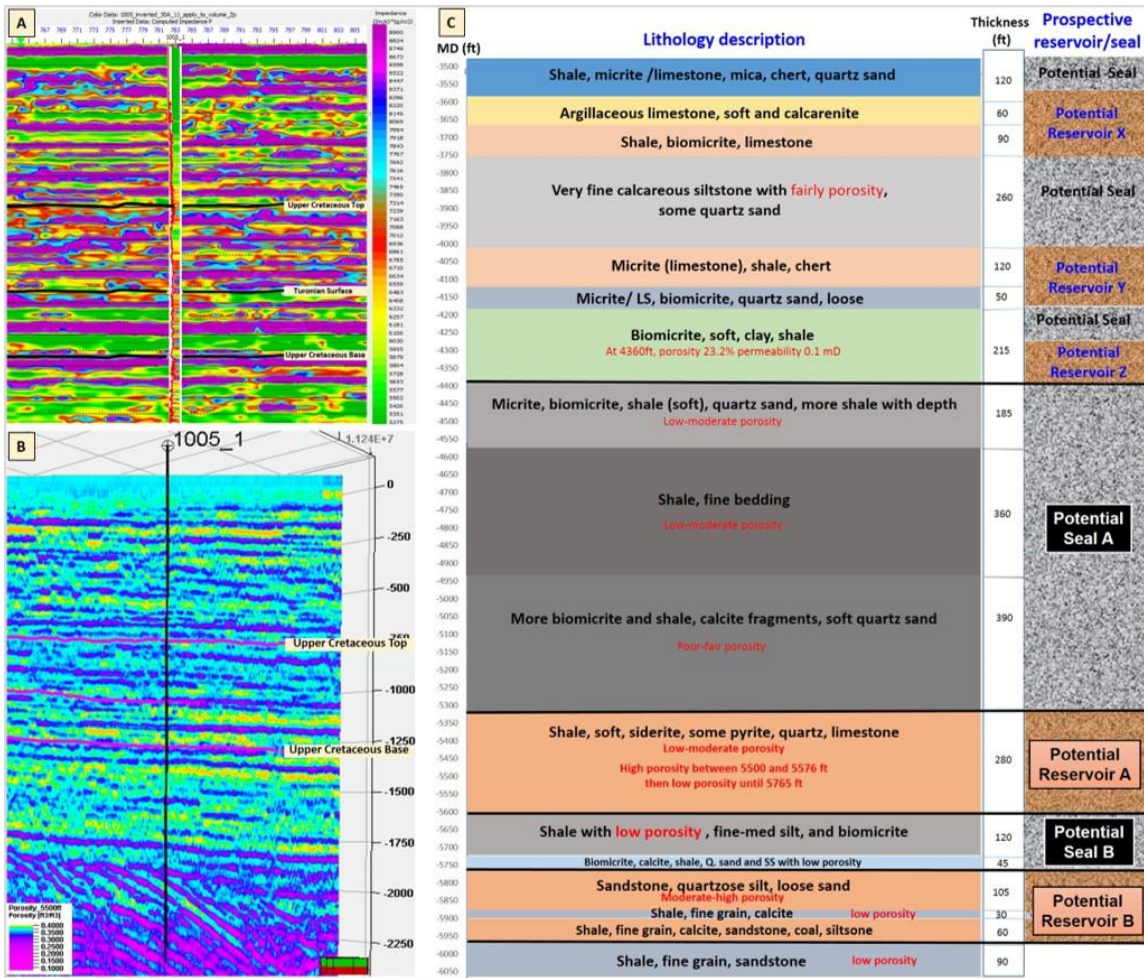


Figure 3.18: [A] Acoustic impedance, [B] extracted porosity and [C] lithology description with a geological model for the main two potentials reservoirs and seals at the Upper Cretaceous strata at South Georgia Embayment, modified after Almutairi et al. (2017); data from (Scholle, 1979).

Physical properties such as impedance contrast, calculated porosity from either density or neutron logs, measured porosity and permeability from the well's core, and well logs interpretation were integrated to determine the potential reservoir and seal strata. The acoustic inversion results identified strata and units containing potential reservoirs and seals with the areal extent in the Upper Cretaceous strata. In addition, the inversion results indicate that distinct porosity and permeability regimes are present and distributed in the Upper Cretaceous strata within the SGE. This result supports the previous study by (Almutairi, et al., 2017) and provides more details about the areal extent of potential reservoirs and seals as well as porosity and permeability distributions.

The regressions analysis between the acoustic impedance and porosity show a good relationship within the interested zone, Upper Cretaceous strata. This reasonable correlation indicates a robust transform for application to seismic inversion results. Since the porosity distribution is estimated using different methods, the porosity follows the trends of seismic signature and structures of Upper Cretaceous strata. The acoustic impedance (AI) and porosity relationship is defined by:

$$\text{Porosity} = (-0.0018164 * \text{AI}) + 73.137$$

where the correlation coefficient is $R^2 = 0.75$.

However, the relationship between porosity and permeability is defined by:

$$[\text{Permeability} = 0.0247e^{0.2515 x}],$$

where the correlation coefficient is $R^2 = 0.568$.

The extracted values of porosity and permeability are close to the measured values from the well cores at the Upper Cretaceous strata interval. Correlation coefficients in the linear regressions between the acoustic impedance, the porosity and the permeability are within the range of similar studies that related to CO₂ sequestration and porosity prediction such as Alshuhail (2011), Patricia (2014), and Hills and Pashin (2010). The high impedance zones observed in the seismic section of Upper Cretaceous have low porosity. Since Almutairi et al. (2017) proposed two significant storage reservoirs for CO₂ at the Upper Cretaceous strata, the seismic inversion and the regression between the acoustic impedance and porosity fairly closely agreed with those results. The potential reservoir zones give low impedance, and high porosity. Comparing the low impedance zone with the well lithology description, the reservoir is comprised of limestone with significant interbedded sandstone, shale and dolomite (Scholle, 1979). It is sealed by thick sediments, mainly shale interbedded with limestone, which have high impedance and low porosity values (Almutairi et al., 2017).

From the acoustic inversion analysis and physical property relationships, the Upper Cretaceous strata have two main potential reservoirs which extend within the South Georgia Embayment (SGE).

The shallow potential reservoir, located at depths between 5,400 to 5,580 ft, and composed of siderite, some pyrite quartz, limestone, with high porosity (17-23%) and high permeability (3.5 to 447 mD) are encountered. However, it is overlain by thick seal layers, located at depths between 4,400 to 5,400 ft, composed of shale, fine bedding, and has porosity of 23.5 % and low permeability (0.1 mD). Nevertheless, the deep potential reservoir which is composed of sandstone, quartzose silt, dolomite loose sand, coal,

siltstone, located at depth 5,720 to 5,950 ft. The porosity is (19 to 30.1%) and the permeability is between 3.5 to 447 mD, (Scholle, 1979; Almutairi et al., 2017). However, it capped by a seal interval, composed of calcareous shale, fine-med silt, and biomicrite, located at a depth range of 5,580 to 5,720 ft. Its porosity is 12% and has less permeable clayey sequence at the GE-1 well.

3.7 Conclusions

This study provides a more detailed evaluation of certain physical parameters of the Upper Cretaceous strata restricted to SGE. Ultimately, this study provides a quantitative estimate of porosity and permeability regimes distributed across the SGE. Furthermore, it demonstrates the value of using multiple seismic inversion techniques to define reservoir and seal properties. In addition, this study provides the reliable workflow for Model-Based inversion which provides a better method to discriminate lithology and predict porosity. In addition, it optimizes parameters for assessing geologic CO₂ storage resources. The impedance inversion workflow may be applied to future CO₂ storage resource assessments. Results of the acoustic impedance inversion indicate that the Upper Cretaceous strata at SGE contain porous intervals which have low acoustic impedance (relatively high porosity) overlain by a thick impermeable interval, mostly shale, with high impedance (low porosity) and low permeability. It supports the results from the previous study (Almutairi et al., 2017). However, stratigraphic trapping through lateral facies changes may be of greater interest in SGE than in other basins along the Atlantic offshore margin (Scholle, 1979). Suggestions for future work include conducting a 3D seismic survey to obtain a more complete assessment of formation evaluation and geologic characterization for CO₂ storage resources for Upper Cretaceous strata at SGE.

CHAPTER 4

DISCUSSIONS AND CONCLUSIONS

4.1 Discussions

The lithological section of the COST GE-1 well has two main intervals (Scholle, 1979): 1) the depth interval from 3,300 to 4,600 ft, includes Upper Cretaceous, Paleocene, and lower Eocene, consists of limestone and calcareous shales, and 2) the depth interval from 4,600 to 7,200 ft, consists of limestone and dolomites interbedded with sandstones. Figure 2.10 shows the lithologic description versus depth and thickness from the COST GE-1 well based on core cuts and geophysical logs. In addition, it provides a geological model of the potential CO₂ storage reservoirs and seals.

Loss of fluid circulation in the chalk and calcareous shale interval from 2,800 to 4,900 ft during the drilling of the COST GE-1 well, may indicate significant fracturing (Scholle, 1979). At the COST GE-1 well, reports indicate that the presence of impermeable beds could serve as seals for CO₂ entrapment. The thick shales and calcareous shales between 3,600 and 5,700 ft, as well as thinner shales and anhydrite beds in the deeper parts of the section, are the best potential seals (Figure 2.10). However, no sandstones above the depth of 5,700 ft were recovered in either the conventional or sidewall cores. The carbonate rocks in this section are highly porous chinks, but their permeability is very low. Nevertheless, chinks with low permeability values are highly productive in the North Sea

(Scholle, 1979). Carbonate-cemented, feldspathic, glauconitic sandstones at a depth of 5,800 ft, suggest a major regression, if not a hiatus, between the shallow-water restricted-shelf carbonates and the overlying fine-grained open-marine limestones. This observation is supported by bio-stratigraphic data (Scholle, 1979). The depth interval from about 5,700 to 7,200 ft in the COST GE-1 well contains a varied shallow marine sequence of generally medium grained calcarenites, dolomite, and anhydrite, with significant amounts of quartz sandstone, pyrite, and glauconite. Common rock types include oolites, fossiliferous calcarenites, dolomite, micrite, and anhydrite.

Based on this stratigraphic analysis, it appears that the most suitable reservoir rocks for CO₂ sequestration are within restricted shelf carbonates with high primary and secondary porosity and good permeability occurring between 5,700 and 7,200 ft. It has the best permeability encountered below 1,000 ft in the COST GE-1 well. This depth interval (5,700 and 7,200 ft), dominated by sandstone, shows porosities that vary widely and unsystematically with depth from 25 % to 30 % (perhaps due to variation in diagenesis), and the permeability is as high as 4,000 mD. Although characterized by good porosity, the fine-grained limestones above 5,700 ft are likely too impermeable to make them candidates for reservoir rocks unless they are widely fractured or contain undetected permeable horizons. Data suggest that the rocks between 1,000 to 5,700 ft have a permeability of 3 mD or less (Scholle, 1979). Porosity values calculated from well logs shows an irregular pattern perhaps due to cementation and facies changes. However, COST GE-1 well shows a clear decrease of porosity with depth down to about 5,700 ft; Figure (2.8 A). Plotting the porosity versus depth for the upper portion of the COST GE-1 well, see Figure 2.9 (A and C), shows that the fine-grained carbonates appear to behave similarly to chalks with respect

to porosity modification. Some of these carbonates are not strictly true chalks because of their argillaceous matrix.

For estimation of CO₂ storage capacity, a theoretical approach based on the DOE-NETL equation (DOE, 2008) was used to estimate the saline reservoir storage capacity. It estimates CO₂ storage capacity (GCO₂) based on the following expression:

$$GCO_2 = A \times h \times \emptyset \times \rho \times E, \text{ where:}$$

A: total area covered by target reservoir and seal,

h: Reservoir thickness

\emptyset : Reservoir porosity

ρ : Density of supercritical CO₂

E: CO₂ Storage efficiency factor

Regional CO₂ storage capacity is estimated using the interpolated surfaces with geographical total area of $19 \times 10^{10} \text{ m}^2$. The average reservoir thickness is about 263 ft (80 m). This estimate depends on the regional thickness map for the prospective reservoir. The average porosity values, from the core, within the reservoir interval is 15%. A density of 700 kg/m^3 was used for supercritical CO₂ (NETL, 2015). The storage efficiency factor E is an important source of uncertainty for capacity assessment. It reflects a fraction of the total pore volume that will be occupied by the injected CO₂. For saline formations, their storage efficiency coefficients range between 1.41 and 6.0 % over the P10 and P90 percent probability range. Comparing with different methods, efficiency factors ranging between 1.2 and 4.1% over the P10 and P90 percent probability range. Therefore, storage efficiency

value is 2.0%, which represents the probability level P50, in the limestone lithology, using Monte Carlo method (Goodman et al., 2001).

Locally, within the SGE, CO₂ storage capacity is estimated with high confidence for the offshore Southeast Georgia Embayment, which is reasonably covered by seismic lines and wells data. The geographical total area that covers the two significant potential reservoir, named A and B, is 15.9x10⁹ m², (Figure 2.10). The total net thickness of the two significant reservoirs is about 470 ft (143.3 m) determined from the well logs. The average porosity value, from the core data, within the two reservoirs is 25.83%. Therefore, the CO₂ storage capacity is approximately 31.92 GT regionally. The local storage capacity for the two significant reservoirs in the Southeast Georgia Embayment provides 8.79 GT of that amount.

Table 4.1 shows CO₂ storage capacity estimations in GT using different storage efficiency factor for the saline reservoir which are (in percent): P₁₀ = 0.51, P₅₀ = 2.0, and P₉₀ = 5.4 (NETL, 2015; Peck et al., 2014).

4.2 Conclusions

To summarize, this research is the first assessment of Upper Cretaceous strata for offshore CO₂ storage resource capacity in the southeastern United States outer continental shelf. It provides an integrated description and reliable subsurface evaluation of the top and base of Upper Cretaceous section and predict some potential reservoirs for CO₂ geologic storage regionally and locally within the offshore of Southeast Georgia Embayment. Also, seismic reflectors and stratigraphic units, containing reservoirs or sinks that might be suitable for effective CO₂ storage, were identified. To get accurate interpolation, the

structure and thickness maps were created for the top and base of Upper Cretaceous section and the top of reservoirs using specific boundaries (polygons). The study identified five potential reservoirs and seals (Table 4.2). Two of them, discussed in detail, are considered to be the significant compartmented storage in the study area for CO₂ with high quality and integrity. These two main prospects are located at depths between 5,320 to 5,600 ft and 5,660 to 5,950 ft at the COST GE-1 well. All CO₂ storage criteria are met in these intervals, most notably high porosity and permeable stratigraphic traps that are capped by thick seals. Since there is lack of 4-way closure on trap and the regional structure map indicates to general up dip seal, the associated risks are migration up dip and trap limitation. However, stratigraphic trapping through lateral facies changes may be of greater interest in SGE than in other basins along the Atlantic offshore margin (Scholle, 1979). SGE has a potential for 4-way closure seal.

Because the Southeast Georgia Embayment has been extensively covered with seismic surveys and wells, the structure maps of the lateral extent of the main reservoir and sealing rock were created locally with high confidence. Therefore, Southeast Georgia Embayment is a strong candidate for CO₂ sequestration in the Atlantic offshore and the existing deep exploratory wells can be exploited in developing CO₂ sequestration. However, this assessment is the first application of multiple seismic inversion techniques of the Upper Cretaceous strata in the SGE. It provides a reliable and repeatable workflow of Model-Based inversion which gives an improved image to discriminate lithology and predict porosity. This workflow can be applied to future CO₂ storage resource assessment studies elsewhere. This assessment (1) provides a quantitative estimate of porosity and permeability regimes distributed across the SGE; (2) demonstrates the value of using

multiple seismic inversion techniques to define reservoir and seal properties; (3) provides a reliable and repeatable workflow for Model-Based inversion which provides a better method to discriminate lithology and predict porosity; and (4) optimizes parameters for assessing geologic CO₂ storage resources. In addition, the impedance inversion workflow may be applied to future CO₂ storage resource assessments. Results of the acoustic impedance inversion indicate that the Upper Cretaceous strata at SGE contain porous intervals which have low acoustic impedance (relatively high porosity) overlain by a thick impermeable interval, mostly shale, with high impedance (low porosity) and low permeability. Suggestions for future work include conducting a 3D seismic survey to obtain a more complete assessment of formation evaluation and geologic characterization for CO₂ storage resources for Upper Cretaceous strata at SGE.

This research investigates the hypotheses and answers the research questions that are mentioned in the introduction. Smyth et al. (2008) estimated that the Upper Cretaceous strata at the Carolinas offshore has storage capacity of 16 GT, but this study indicates that the Upper Cretaceous formations have an even greater CO₂ storage capacity than that. It is estimated to be 31.92 GT regionally, and 8.79 GT of that amount represents the local storage capacity for the two significant reservoirs in the Southeast Georgia Embayment. This is the first time CO₂ storage capacities have been quantified in the study areas. The potential sinks are overlain by low-permeability seal layers. There are distinct porosity and permeability regimes that are widely distributed, especially in the lower part of the Upper Cretaceous section, and are influenced by depositional environments and lithologic composition. Also, the results indicate that the Upper Cretaceous units consist of moderate to highly compartmented stratigraphic systems. This helps increase the storage capacity.

The research hypotheses were suitable for CO₂ sequestration assessment of the Upper Cretaceous section at the study areas. The limitations of this study are due to the sparsity and asymmetric distribution of the well data regionally. This caused an uncertainty with the regional extent and the integrity of the seal and reservoir.

The results are an important step for further studies in the future. The research integrates the available data to provide an assessment of the Upper Cretaceous section. Two main reservoirs were introduced with regional and local estimates for the significant storage capacity. Since the offshore South Georgia Embayment has a significant storage capacity and is covered reasonably by seismic surveys and exploratory well data, it is qualified as a candidate for CO₂ injection. The study suggests directions for future work to include:

- 1) Conduct 3D seismic survey.
- 2) Resample 2D seismic lines to create a volume within SGE.
- 3) Digitize the exploratory wells data professionally.
- 4) Build a unified database of the wells of the Atlantic offshore.
- 5) More investigation to the lateral changes in porosity and permeability due to facies changes in the potential reservoir rocks. This could be explored with a pseudo 3D or 3D seismic mapping of porosity from seismic, and
- 6) Create a regional velocity model (to provide the correct depths for the structures as well as the potential reservoirs and seals).

This will lead to a more complete assessment of formation evaluation and geologic characterization for CO₂ storage resources.

Table 4.1: CO₂ storage capacity estimation in GT using different storage efficiency factor for the saline reservoir which are (in percent): P₁₀ = 0.51, P₅₀ = 2.0, and P₉₀ = 5.4 (NETL, 2015; Peck et al., 2014).

Storage efficiency factor E		CO ₂ storage capacity in MT	
		At (South Georgia Embayment)	At a regional Scale (South Georgia Embayment, Carolina Trough and Blake Plateau basins)
P ₁₀	0.0051	2.25	8.97
P ₅₀	0.02	8.79	31.92
P ₉₀	0.055	24.2	96.76

Table 4.2: Summary of prospective reservoirs and seals for CO₂ sequestration in Upper Cretaceous strata of the Southeast Georgia Embayment, (data from (Scholle, 1979)).

Potential CO ₂ Storage	Lithology	Depth (ft)	Porosity in percent or level	Permeability (mD)	Priority
Seal X	Shale, micrite /limestone, mica, chert	3500 to 3570 ft	moderate	1.7	Low
Reservoir X	Argillaceous limestone, soft and calcarenite, biomicrite, limestone	3570 to 3750 ft	19.1 %	3.5	Low
Seal Y	Very fine calcareous Siltstone	3750 to 4000 ft	fairly porosity	3	Low
Reservoir Y	Micrite (limestone), chert, biomicrite, quartz sand, loose	4020 to 4170 ft	19.1 %	3.5	Medium
Seal Z	Clay, shale	4170 to 4250 ft	fairly porosity	0.1	High
Reservoir Z	Micrite/ LS, dolomite, biomicrite	At 4360 ft	23.2 %	0.1	Low
Seal A	Shale, fine bedding	4400 to 5500 ft at 4906 ft	23.5 %	0.1	High
Reservoir A	Siderite, some pyrite quartz, limestone	5400 to 5580 ft	High porosity 17-23%	3.5 to 447 mD	High
Seal B	Calcareous shale, fine-med silt, and biomicrite	5580 to 5720 ft	Poor-fair porosity 12%	Less permeable, clayey sequence	High
Reservoir B	Sandstone, quartzose silt, dolomite loose sand, coal, siltstone	5720 to 5950 ft	Moderate-high porosity 19-30.1 %	3.5 to 447 mD	High

REFERENCES

- Almutairi, K., Knapp, C., Knapp, J., and Terry D., (2017) “Assessment of Upper Cretaceous Strata for Offshore CO₂ Storage, Southeastern United States.” *Modern Environmental Science and Engineering*, vol. 03, no. 08, 3 Aug. 2017, pp. 532–552.
- Alshuhail, A., Lawton D., Isaac H., (2009), “Acoustic impedance inversion of vintage seismic data over a proposed CO₂ sequestration site in the Lake Wabamun Area, Alberta”, *CREWES Research Report*, Volume 21.
- Alshuhail, A., (2011). *CO₂ Sequestration Site Characterization and Time-lapse Monitoring, Using Reflection Seismic Methods*: PhD. Thesis, Univ. of Calgary.
- Amato, V., and Bebout, W., eds., (1978). *Geological and Operational Summary COST No. GE-1 well, Southeast Georgia Embayment Area, South Atlantic OCS*: United States Geological Survey.
- Asquith, B., Krygowski, D., and Gibson, C. R. (2004). *Basic well log analysis* (Vol. 16). Tulsa: American Association of Petroleum Geologists.
- CGG, (2016), Hampson Russell Software materials, “Post-stack Inversion in STRATA”.
- Chadwick, A., Arts, R., Bernstone, C., May, F., Thibeau, S., & Zweigel, P. (2008). *Best practice for the storage of CO₂ in saline aquifers - observations and guidelines from the SACS and CO₂ STORE projects*, Nottingham, UK, (British Geological Survey Occasional Publication, 14).
- Cubizolle F., Valding T., Lacaze L., Pauget F., Eliis, (2015), “Global method for seismic-well tie based on real time synthetic model”, *SEG New Orleans Annual Meeting*.
- Darling, T. (2005). *Well logging and formation evaluation*. Elsevier.
- Dillon, P., Girard, W., Weed, A., Sheridan, E., Dolton, G., Sable, E., Krivoy, L., Grim, M., Robbins, E., Rhodehamel, C., Amato, R., Foley, N. (1975). *Sediments, structural framework, petroleum potential, environmental considerations and operational considerations of the United States South Atlantic outer continental shelf*. U.S. Geological Survey Open-File Report 75-411, 262 pp.

- Dillon, P., Sheridan, E., and Fail, P., (1976), Structure of the western Blake- Bahama Basin as shown by 24 channel CDP pro-filing: *Geology*, v. 4, no. 7, p. 459-462.
- Dillon, P., Paull, K., Buffler, T., and Fail, P., (1979), Structure and development of the Southeast Georgia embayment and northern Blake Plateau: Preliminary analysis, in Watkins, J.S., Montadert, Lucien, and Dickerson, P.W., eds., *Geological and geophysical investigations of continental margins: American Association of Petroleum Geologists Memoir 29*, p. 27-41.
- Dillon, P., and Popenoe, P., (1988), The Blake Plateau Basin and Carolina Trough, in Sheridan, R.E., and Grow, J.A., eds., *The Atlantic continental margin, U.S.*, v. I-2 of *The geology of North America: Boulder, Colo., Geological Society of America*, p. 291-328.
- Dolberg D., Helgesen J., Hanssen T., Magnus I., Saigal G., and Pedersen B., (2000). Porosity prediction from seismic inversion, Lavrans Field, Halten Terrace, Norway. *The Leading Edge*, 19(4), 392-399.
- Edgar, T., (1981), Oil and GAS Resources of the U.S. Continental Margin-South Atlantic Area. Report prepared for the Conference of the Future of Gas and Oil from the sea, Univ. of Delaware.
- Eiken O., Ringrose P., Hermanrud C., Nazarian B., Torp T., and Høier L., (2011). Lessons Learned from 14 years of CCS Operations: Sleipner, In Salah and Snøhvit, *Statoil ASA, Technology and New Energy*, Trondheim, N-7005, Norway.
- Franklin Jr., (2009), Onshore Geologic Storage of CO₂, *Science* vol. 325, 1656; DOI: 10.1126/science.1175677.
- Gaymard, R., and A. Poupon, A., (1968), Response of neutron and formation density logs in hydrocarbon bearing formations: *The Log Analyst*, 9, 3–12.
- Gilles, G., 2000. Acoustic and Thermal Characterization of Oil Migration, Gas Hydrates Formation and Silica Diagenesis, PhD. Thesis, Columbia University.
- Goodman, A., Hakala A., Bromhal G., Deel D., Rodosta, T., Frailey, T., Small, M., Allen, D., Romanova, V., Fazio, J., Huerta, N., McIntyre, D., Kutchko, D., Guthrie, G., 2011, “U.S. DOE methodology for the development of geologic storage potential for carbon dioxide at the national and regional scale, *International Journal of Greenhouse Gas Control*, 5 (2011), pp. 952-965.
- Hathaway, C, Schlee, J., Poag, W., Valentine, C., Weed, A., Bothner, H., Kohout, A., Manheim, T., Schoen, R., Miller, E., and Schultz, M., 1976. Preliminary study of the 1976 Atlantic Margin Coring Project of the U.S. Geological Survey. *Open-File Rep.—U.S. Geol. Surv.*, 76-844.


- Hills D. & Pashin J. (2010), Preliminary of offshore transport and storage of CO₂: Southeastern Regional Carbon Sequestration Partnership Final Report, prepared for Southern States Energy Board, Geological Survey of Alabama, 11 p.
- IEA (International Energy Agency), (2007). Legal Aspects of Storing CO₂: update and Recommendations.
- IEA (International Energy Agency), (2008). CO₂ Capture and Storage: A Key Carbon Abatement Option, OECD/IEA, Paris.
- Johnston S., and Goncharov A., (2012). Velocity Analysis and Depth Conversion in the Offshore Northern Perth Basin, Australia, 34th International Geological Congress Australia.
- Kumar R., Das B., Chatterjee R., Sain K., (2016). A methodology of porosity estimation from inversion of post-stack seismic data” *Journal of Natural Gas Science and Engineering* 28 (2016) 356e364.
- Lee, K., Yoo G., McMechan G., Hwang N., and Lee G., (2013). A two-dimensional post-stack seismic inversion for acoustic impedance of gas and hydrate bearing deep-water sediments within the continental slope of the Ulleung Basin, East Sea, Korea. *Terr. Atmos. Ocean. Sci.*, 24, 295-310, doi: 10.3319/TAO.2013.01.10.01T.
- Liner, L. (2004), Elements of 3D Seismology (2nd edition): PennWell Corporation, 608 p.
- Litynski, J. T., S. Plasynski, H. G. McIlvried, C. Mahoney, and R. K. Srivastava, (2008). The United States Department of Energy’s Regional Carbon Sequestration Partnerships Program Validation Phase: Environment International, v. 34, p. 127-138.
- Maher C., Applin R., (1971). Geologic framework and petroleum potential of the Atlantic coastal plain and continental shelf. U.S. Geol. Surv. Prof. Pap. No. 659. 98 pp.
- Maurya S., and Sarkar P., (2016), “Comparison of Post stack Seismic Inversion Methods: A-case study from Blackfoot Field, Canada”, *International Journal of Scientific & Engineering Research*, Volume 7, Issue 8.
- Mavko, G., T. Mukerji, and J. Dvorkin, (2003), The rock physics handbook: Cambridge University Press.
- Nelson, P. H. (1996). Permeability-porosity relationships in sedimentary rocks, *The Log Analyst*, 35, 3, 38-62.
- NETL, (2013), Best Practices for: “Site Screening, Site Selection, and Initial Characterization for Storage of CO₂ in Deep Geologic Formations”, by National Energy Technology Laboratory, Revised Edition.

- NETL, (2015) Carbon Storage Atlas, 5th Edition, National Energy Technology Laboratory.
- Patricia G., (2014), Model-based inversion of broadband seismic data: MSc. Thesis, Department of Geoscience, University of Calgary.
- Peck W., Glazewski K., Klenner R., Gorecki C., Steadman E., and Harju J., (2014). A Workflow to Determine CO2 Storage Potential in Deep Saline Formations. *Energy Procedia*, Volume 63, p. 5231-5238, ISSN 1876-6102.
- Pinet, P. R., and Popenoe, Peter, (1985). Shallow seismic stratigraphy and post- Albian geologic history of the northern and central Blake Plateau: Geological Society of America Bull. v. 96, no. 5, p. 627-638.
- Poag W., (1978), Stratigraphy of the Atlantic Continental Shelf and Slope of the United States, Paleontology and Stratigraphy Branch, U.S. Geological Survey, Woods Hole, Massachusetts 02543.
- Poag, W., (1985a). Depositional history and stratigraphic reference section for central Baltimore Canyon trough, in Poag, C.W., ed., Geologic Evolution of the United States Atlantic margin: New York, Van Nostrand Reinhold Co., p. 217-264.
- Poppe, J., Popenoe, P., Poag, W. and Swift A., 1995. Stratigraphic and paleo-environmental summary of the south-east Georgia embayment: a correlation of exploratory wells”, *Marine and Petroleum Geology*, Vol. 12, No. 6, pp. 677-690, 1995, Elsevier Science Ltd.
- Pollack, A. (2014). Tectonic Studies of the Atlantic Margin in the Southeastern United States. (Master's thesis). Retrieved from <https://scholarcommons.sc.edu/etd/2871>
- Schlumberger, (2016), Petrel Geophysics Training Course Manual: *Module 14: Depth Conversion*, October 2016, Houston U.S.A.
- Schlumberger, (2017), Practical AVO and Seismic Inversion with Petrel, Training Course Manual, November 2017, Houston, Tx. U.S.A.
- Scholle P. A., eds., (1979), Geological Studies of the COST GE-1 Well, United States South Atlantic Outer Continental Shelf Area. GEOLOGICAL SURVEY CIRCULAR 800.
- Semere S., Bellona R., “Carbon Dioxide Storage: Geological Security and Environmental Issues, Case Study on the Sleipner Gas field in Norway”, May 2007.
- Serra, O., (1984). *Fundamentals of Well-Log Interpretation* (Vol. 1): *The Acquisition of Logging Data*: Dev. Pet. Sci., 15A: Amsterdam (Elsevier).

- Smithson T., “How Porosity is Measured”, Oilfield Review Autumn, (2012): 24, no.3 Schlumberger.
- Smyth, R., Hovorka, S., Meckel, T., Breton, C., Paine, J., Hill, G., Herzog, H., Zhang, H., and Li, W., (2008), “Potential Sinks for Geologic Storage of Carbon Dioxide Generated by Power Plants in North and South Carolina”, 57 pages, Final Carolinas report.
- United States. Book, (1982), Minerals Management Service. Atlantic OCS Region. New York Office. Proposed 1983 Outer Continental Shelf Oil and Gas Lease Sale Offshore the South-Atlantic States: OCS Sale No. 78: Draft Environmental Impact Statement. [New York].
- Veeken, H. (2007), Seismic stratigraphy, basin analysis and reservoir characteristics, in Helberg, K., and Treitel, S., eds., Handbook of Geophysical Exploration, Seismic Exploration Vol. 37, 509 p.
- Vidas, H., B. Hugman, A. Chikkatur, B. Venkatesh. (2012). Analysis of the Costs and Benefits of CO₂ Sequestration on the U.S. Outer Continental Shelf. U.S. Department of the Interior, Bureau of Ocean Energy Management. Herndon, Virginia. OCS Study BOEM 2012-100.
- Vukadin D., Brnada S., “Acoustic impedance inversion analysis: Croatia offshore and onshore case studies”, SPE conference, 2015.
- Wyllie, M.R.J., Gregory, A.R., and Gardner, L.W., 1956, Elastic wave velocities in heterogeneous and porous media: Geophysics, 21, 41-70.

APPENDIX A

COPYRIGHT PERMISSION

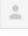
 **Khaled Almutairi** <kalmutairi@geol.sc.edu> May 24
to environment ▾

Hi Penny,

I may need a permission (by email is enough) to reproduce my manuscript to use it since it is a part of my dissertation.

Thank you

...

 **environment@academicstar.us** <environment@academicstar.us> May 24
to me ▾

Dear Khaled F. Almutairi,
Thanks for your kind email.

Yes, you can use your paper "**Assessment of Upper Cretaceous Strata for Offshore CO2 Storage, Southeastern United States**" as a part of your dissertation.
Our colleagues will mail you two journals from China.

Keep in touch!

Best regards,

Penny
Editorial office
Modern Environmental Science and Engineering, USA
Academic Star Publishing Company,
[257 Grand Street #1147, Brooklyn NY 11211](#)
Tel: 347-566-2153, Fax: 646-619-4168
E-mail: environment@academicstar.us, mese@academicstar.us